OPS MCC
Level B/C
Formulation Requirements

Area Targets and Space Volumes Processor

Mission Planning and Analysis Division

July 1979

National Aeronautics and Space Administration

Lyndon B. Johnson Space Center
Houston, Texas

79-FM-26

JSC-16029

SHUTTLE PROGRAM

OPS MCC LEVEL B/C FORMULATION REQUIREMENTS

AREA TARGETS AND SPACE VOLUMES PROCESSOR

By Mack J. Bishop, Jr.
Computer Science Corporation

JSC Task Monitor: Alfred A. Menchaca
Flight Planning Branch

Approved: _____
Edgar C. Lineberry, Chief
Mission Planning and Analysis Division

Approved: _____
Ronald L. Berry, Chief
Mission Planning and Analysis Division

Mission Planning and Analysis Division

National Aeronautics and Space Administration

Lyndon B. Johnson Space Center

Houston, Texas

July 1979

ACKNOWLEDGMENTS

The author wishes to gratefully acknowledge the technical inspiration and guidance provided by A. A. Menchaca of JSC and Messieurs R. Rich and H. Norman of IBM. Their patience and ideas contributed greatly to the contents of this document.

CONTENTS

FIGURES

ACRONYMS AND SYMBOLS

AOS	Acquisition-of-signal
ATSVP	Area Targets and Space Volumes Processor
LOS	Loss-of-signal
MCC	Mission Control Center
M50	Mean-of-1950
RNP	Rotation, nutation, and precession
S/C	Spacecraft
TCA	Time of closest approach
TEI	True-of-epoch inertial

Symbols:

a	Semimajor axis
a_F	"Adjustment factor" for computing altitude above the Fischer ellipsoid
$\vec{C}$	Vector along the centerline of a polyhedron
d	Perpendicular distance to the side of a polyhedron
e	Eccentricity
E	Eccentric anomaly
F	Flattening coefficient
f	True anomaly
h	Altitude
i	Inclination
M	Mean anolmaly
n	Number of sides
$\hat{N}$	Unit outward normal vector

r_c	Radius of the Earth-referenced circle
R_{em}	Mean equatorial radius
$\vec{R}_{sc}$	Spacecraft position vector
$[RNP]^{TEI}_{M50}$	RNP matrix from the mean-of-1950 coordinate system to the true-of-epoch inertial system
t	Time
t_e	Epoch time corresponding to the RNP matrix
u	Argument of latitude
α	Right ascension
δ	Declination
ϕ	Geodetic latitude
ϕ_c	Geocentric latitude
γ	Central angle
λ	Longitude
μ	Earth gravitational constant
$\vec{\rho}$	Slant range vector
τ	Time of perigee passage
ω	Argument of perigee
ω_e	Earth rotation rate
Ω	Right ascension of ascending node
$\hat{\Omega}$	Ascending node vector

Subscripts:

AOS	Denotes a parameter associated with the AOS point
B	Denotes a vector measured from the lower boundary (i.e., base) of a polyhedron
CA	Denotes a parameter associated with the closest approach point
i	Denotes the i^{th} vertex or side of a polygon or polyhedron. Also denotes the i^{th} occurrence of an event
LOS	Denotes a parameter associated with the LOS point

Superscripts:

G	Denotes a parameter in the rotating geocentric coordinate system
TEI	Denotes a parameter in the true-of-epoch inertial coordinate system
blank	Denotes a parameter in the mean-of-1950 coordinate system
	Denotes a unit vector
	Denotes a vector

1.0 INTRODUCTION

This document provides the level B/C mathematical specifications for the Area Targets and Space Volumes Processor (ATSVP). Pursuant to the requirements of reference 1, this processor is designed to compute the acquisition-of-signal (AOS) and loss-of-signal (LOS) times for the following:

a. Area targets
   (1) Earth-referenced circles which are specified by a latitude, longitude, altitude, and radius.
   (2) Celestial circles which are specified by a right ascension, declination, and angular radius.
   (3) Earth-referenced polygons which are an arbitrary Earth-fixed figure having up to five sides with the "corner points" defined by latitude, longitude, and altitude.
   (4) Celestial polygons which are an arbitrary, inertially fixed figure having up to five sides with the corner points defined by right ascension and declination on the celestial sphere.

b. Space volumes
   (1) Earth-referenced space volumes which are an arbitrary, Earth-fixed, five-sided polyhedron. These volumes are defined by a lower-limit polygon at an altitude, h_1, and the projection of this polygon to an altitude, h_2. The corner points of the polygon are defined by latitudes and longitudes and rotate with the Earth. . .
   (2) Celestial-fixed space volumes which are an arbitrary, inertially fixed, five-sided polyhedron. These volumes are defined by a lower-limit polygon at an altitude, h_1, and the projection of this polygon to an altitude, h_2. The corner points of the polygon are defined by right ascension and declination on the celestial sphere.

The AOS and LOS times for these targets are defined (ref. 1) as follows:

a. Ground circles and polygons
   AOS - the time corresponding to the first subsatellite point to lie just inside the area.
   LOS - the time corresponding to the last subsatellite point just prior to exiting the area.
b. Celestial circles and polygons
   AOS - the time corresponding to the first zenith point to lie just inside the area.
   LOS - the time corresponding to the last zenith point just prior to exiting the area.
c. Earth-referenced and celestial-fixed space volumes
   AOS - the time at which the spacecraft (S/C) is just entering the volume.
   LOS - the time just prior to the S/C exiting the volume.

Six data tables will contain the information necessary to completely describe the area targets and space volumes. These tables (ref. 1) are as follows:

a. Ground targets table containing 10 targets in 1 block of data.
b. Celestial circles table containing 10 targets in 1 block of data.
c. Ground polygons table containing 20 targets in 2 blocks of data.
d. Celestial polygons table containing 10 targets in 1 block of data
e. Earth-referenced space volumes table containing 10 targets in 1 block of data.
f. Celestial-fixed volumes table containing 10 targets in 1 block of data.

Section 2 of this document describes the characteristics of the area targets and space volumes and provides the mathematical equations necessary to determine whether the S/C lies within the area target or space volume. These equations provide a detailed model of the target geometry and will be used during the precise numerical search.

Section 3 discusses a semianalytical technique for predicting the AOS and LOS time periods. This technique is designed to bound the actual visibility period using a simplified target geometry model and unperturbed orbital motion. Its principal purpose is to reduce the burden on the precise numerical search by eliminating regions of the S/C orbit where AOS and LOS times are physically impossible. Section 4 provides a functional overview of the ATSVP. This section outlines the overall process required to determine precise AOS and LOS times.

Section 5 presents the detailed logic flow for the ATSVP. This section integrates the functional overview presented in section 4 with the equations and approach presented in sections 2 and 3 and the appendixes. Appendix A discusses the procedure for subdividing complex concave polygons into two or more simpler convex segments. The purpose of this subdivision process is to permit the equations in section 2 to be used on a segment-by-segment basis to test for containment. Appendix B provides a solution to the conic intersection equations used in section 3 for celestial-fixed targets.

2.0 AREA TARGETS AND SPACE VOLUMES CHARACTERISTICS AND CONTAINMENT CRITERIA

The following subsections discuss the characteristics of each of the area targets and space volumes presented in section 1. The mathematical equations necessary to determine whether the S/C lies within the area target or space volume are also developed and discussed.

Two reference coordinate systems will be used. The inertial Aries mean-of-1950 (M50) coordinate system (fig. 2-1) will be the reference system when dealing with area targets and space volumes which remain inertially fixed. The rotating geocentric coordinate system (fig. 2-2) will be used when dealing with area targets and space volumes which rotate with the Earth.

Each of the following six subsections is further subdivided into three topics:

a. Procedure - a brief description of the steps to be performed.
b. Equations - a statement of the input parameter requirements and development of the mathematical equations.
c. Assumptions and limitations - a description of any simplifying assumptions and/or mathematical restrictions.

For convenience, section 2.7 summarizes the equations for all of the area targets and space volumes.

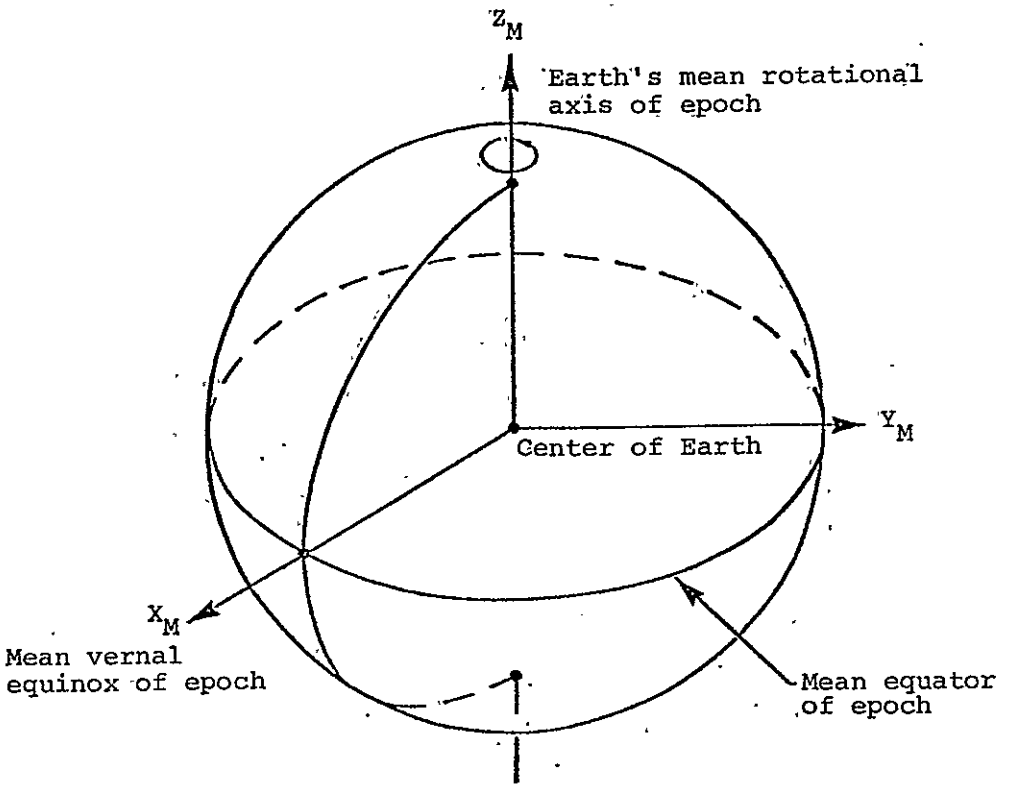

NAME: Aries mean-of-1950, Cartesian, coordinate system.

ORIGIN: The center of the Earth.

ORIENTATION: The epoch is the beginning of Besselian year 1950 or Julian ephemeris date 2433282.423357.

The X_M-Y_M plane is the mean Earth's equator of epoch.

The X_M axis is directed towards the mean vernal equinox of epoch

The Z_M axis is directed along the Earth's mean rotational axis of epoch and is positive north.

The Y_M axis completes a right-handed system.

CHARACTERISTICS: Inertial, right-handed, Cartesian system.

Figure 2-1.- Aries mean-of-1950 coordinate system.

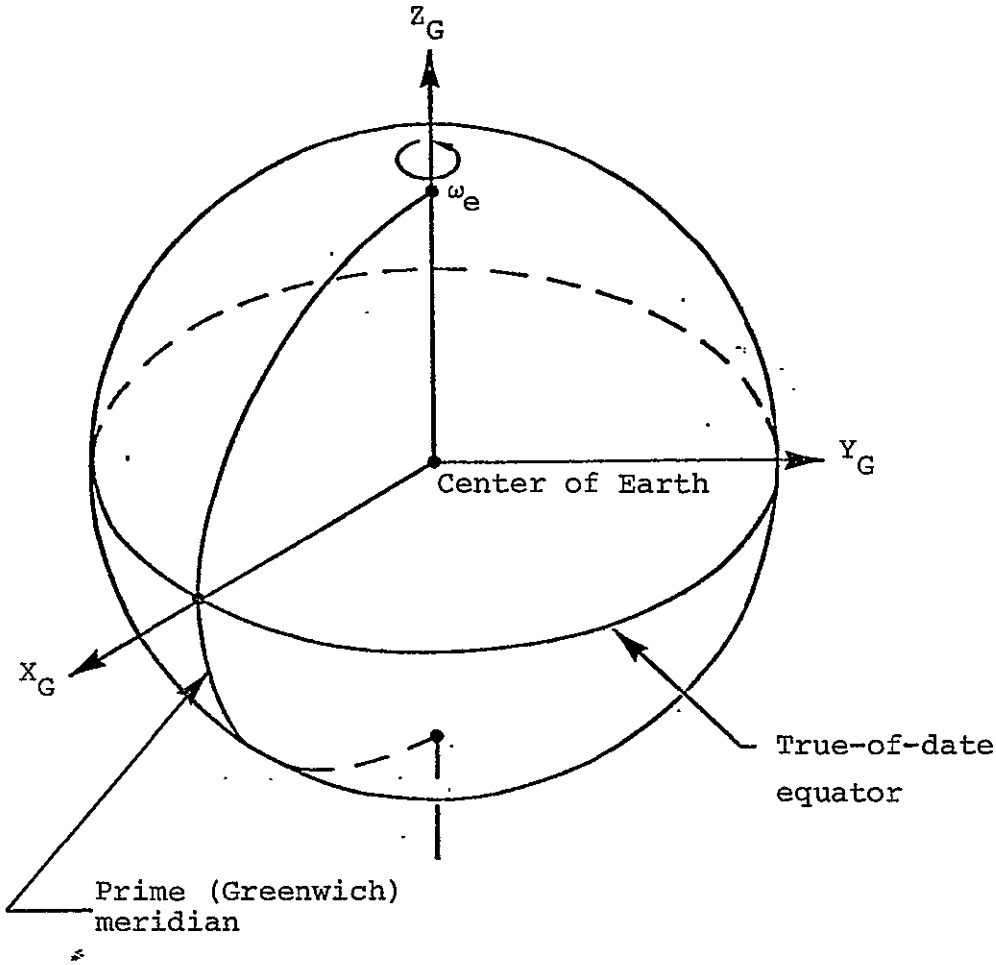

NAME:	Geocentric coordinate system
ORIGIN:	Center of the Earth
ORIENTATION:	X_G - Y_G plane is the Earth's true-of-date equator
	X_G passes through the Greenwich meridian
	Z_G is along the Earth's rotational axis
	Y_G completes the right-handed system
CHARACTERISTICS:	Rotating, right-handed, Earth-fixed

Figure 2-2.- Rotating geocentric coordinate system.

2.1 EARTH-REFERENCED CIRCLES

Earth-referenced circles are defined to be circular ground target areas whose centers are defined by geodetic latitude, longitude, and altitude (fig. 2-3). The S/C lies within this ground target area if its subsatellite point lies within the perimeter of the circular area.

2.1.1 Procedure

The following procedure will be used to determine whether the S/C lies within the ground target area:

a. The geodetic coordinates of the ground target area will be transformed to the geocentric system.
b. The S/C position vector will be transformed from the M50 system to the geocentric system.
c. A test will be performed to determine whether the S/C subsatellite point lies within the perimeter of the ground target area.

2.1.2 Equations

The following parameters are required:

ϕ and λ - geodetic latitude and longitude, respectively, of the center of the Earth-referenced circle (fig. 2-4)

h - altitude of the Earth-referenced circle, measured with respect to the Fischer ellipsoid of 1960 (fig. 2-4)

r_c - radius of the Earth-referenced circle (fig. 2-3)

$\vec{R}_{sc}$ - S/C position vector in the M50 system (fig. 2-3)

t - time corresponding to $\vec{R}_{sc}$

$[RNP]^{TEI}_{M50}$ - Rotation, nutation, and precession (RNP) matrix which is used to transform vectors from the M50 system to the true-of-epoch inertial (TEI) coordinate system

t_e - epoch time corresponding to the RNP matrix

R_{em} - mean equatorial radius for the Fischer ellipsoid of 1960

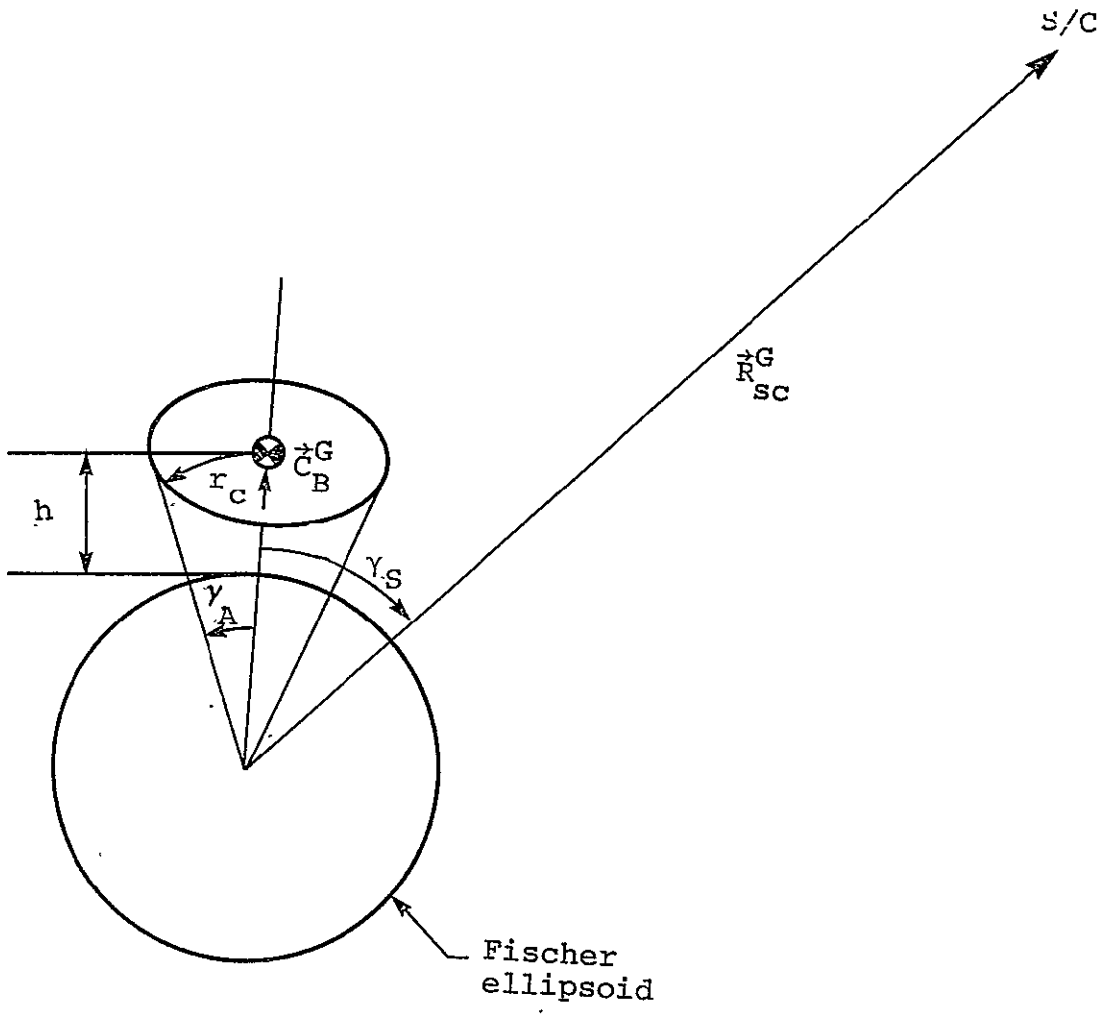

Figure 2-3.- Earth-referenced circle.

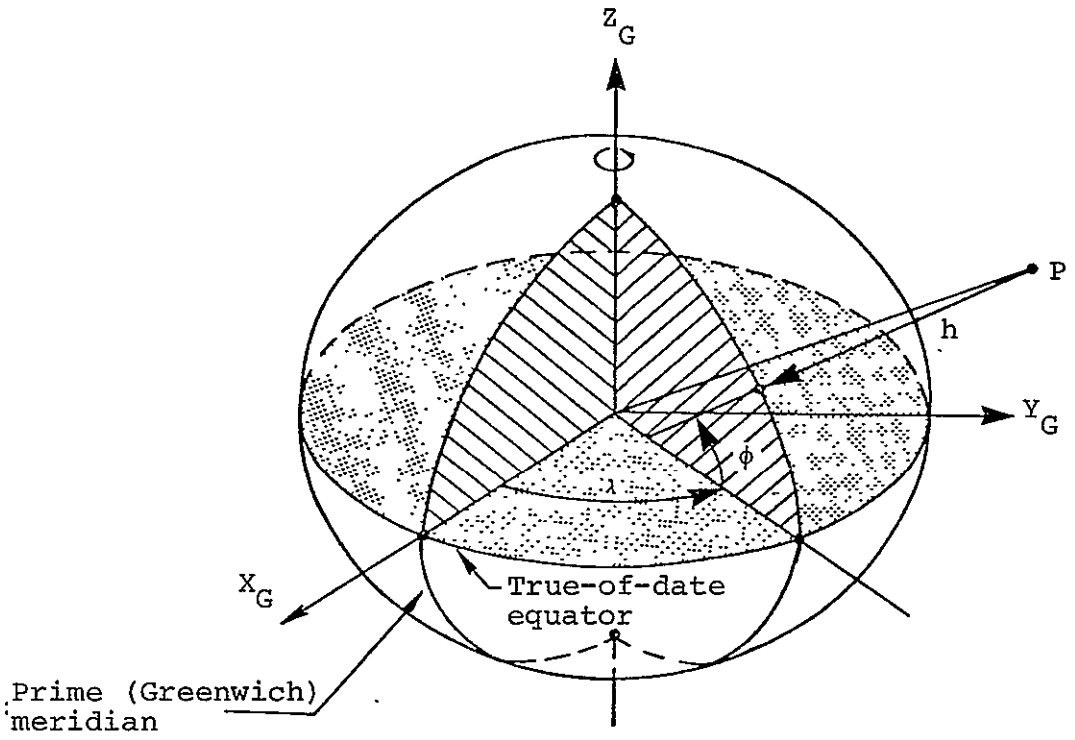

NAME: Geodetic coordinate system.

ORIGIN: This system consists of a set of parameters rather than a coordinate system; therefore, no origin is specified.

ORIENTATION: This system of parameters is based on an ellipsoidal model of the Earth (e.g., the Fischer ellipse of 1960). For any point of interest we define a line, known as the geodetic local vertical, which is perpendicular to the ellipsoid and which contains the point of interest.

h, geodetic altitude, is the distance from the point of interest to the reference ellipsoid, measured along the geodetic local vertical, and is positive for points outside the ellipsoid.

λ is the longitude measured in the plane of the Earth's true equator from the prime (Greenwich) meridian to the local meridian, measured positive eastward.

ϕ is the geodetic latitude, measured in the plane of the local meridian from the Earth's true equator to the geodetic local vertical, measured positive north from the equator.

NOTE: A detailed explanation of declination, geodetic latitude, and geocentric latitude is provided on figure 2-4(b).

CHARACTERISTICS: Rotating polar coordinate parameters. Only position vectors are expressed in this coordinate system. Velocity vectors should be expressed in the Aries mean-of-1950, or the Aries true-of-date, polar for inertial or quasi-inertial representations, respectively. The Fischer ellipsoid model should be used with this system.

(a) Basic definitions.

Figure 2-4.- Geodetic coordinate system.

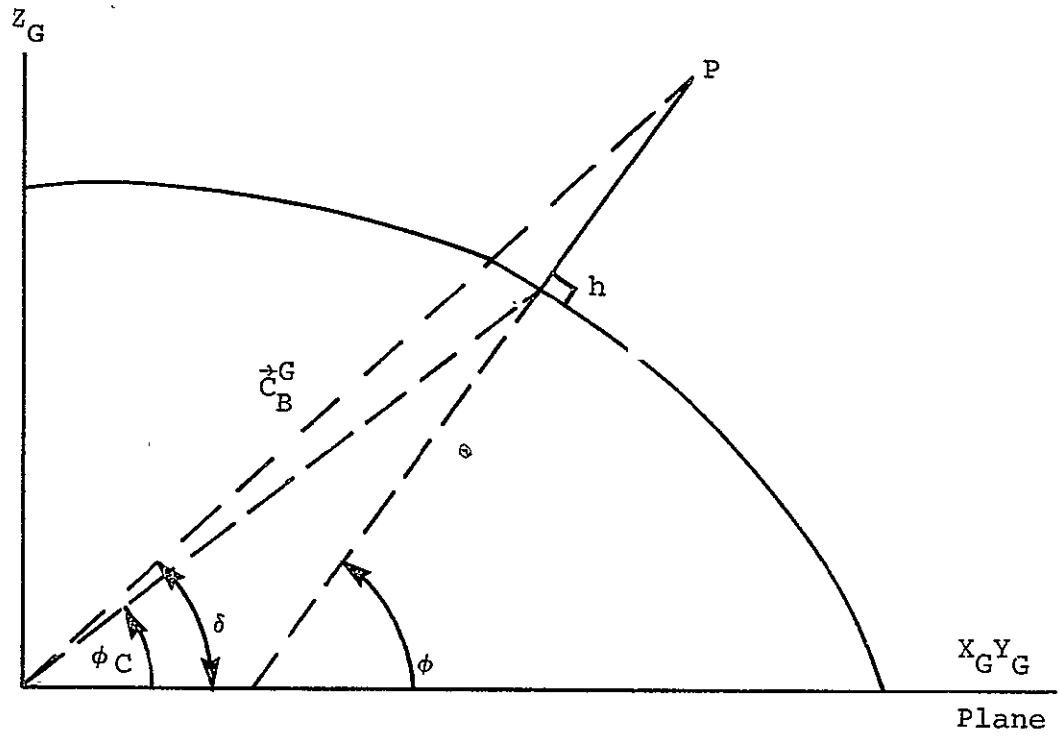

NAME: Geodetic coordinate system of point P.

DEFINITIONS: h is the altitude of point P measured perpendicular from the surface of the referenced ellipsoid.

ϕ is the geodetic latitude of point P.

ϕ_C is the geocentric latitude of point P.

δ is the angle between radius vector and equatorial plane (declination).

λ is the longitude of point P. Angle (+ east) between plane of the figure and the plane formed by the Greenwich meridian.

(b) Detailed explanation.

Figure 2-4.- Concluded.

F - flattening coefficient for the Fischer ellipsoid of 1960

ω_e - Earth rotation rate

The first step is to transform the ground target area from the geodetic system to the geocentric system. The vector from the center of the Earth to the center of the ground target area can be expressed in the rotating geocentric system by

$$\vec{C}^{G}_{B} = \begin{Bmatrix} (h + a_F) \cos\lambda \cos\phi \\ (h + a_F) \sin\lambda \cos\phi \\ \left[h + (1 - F)^2 a_F\right] \sin\phi \end{Bmatrix} \tag{2-1}$$

where

$$a_F = \frac{R_{em}}{\sqrt{\cos^2\phi + (1 - F)^2 \sin^2\phi}} \tag{2-2}$$

The second step is to transform the S/C position vector from the M50 system to the geocentric system. This is accomplished by

a. Transforming the vector from the M50 system to the TEI system using the RNP matrix.
b. Transforming the resultant vector from the TEI system to the geocentric system.

The S/C position vector in the TEI system is given by

$$\vec{R}^{TEI}_{sc} = [RNP]^{TEI}_{M50} \vec{R}_{sc} \tag{2-3}$$

The S/C position vector in the geocentric system (fig. 2-5) is given by

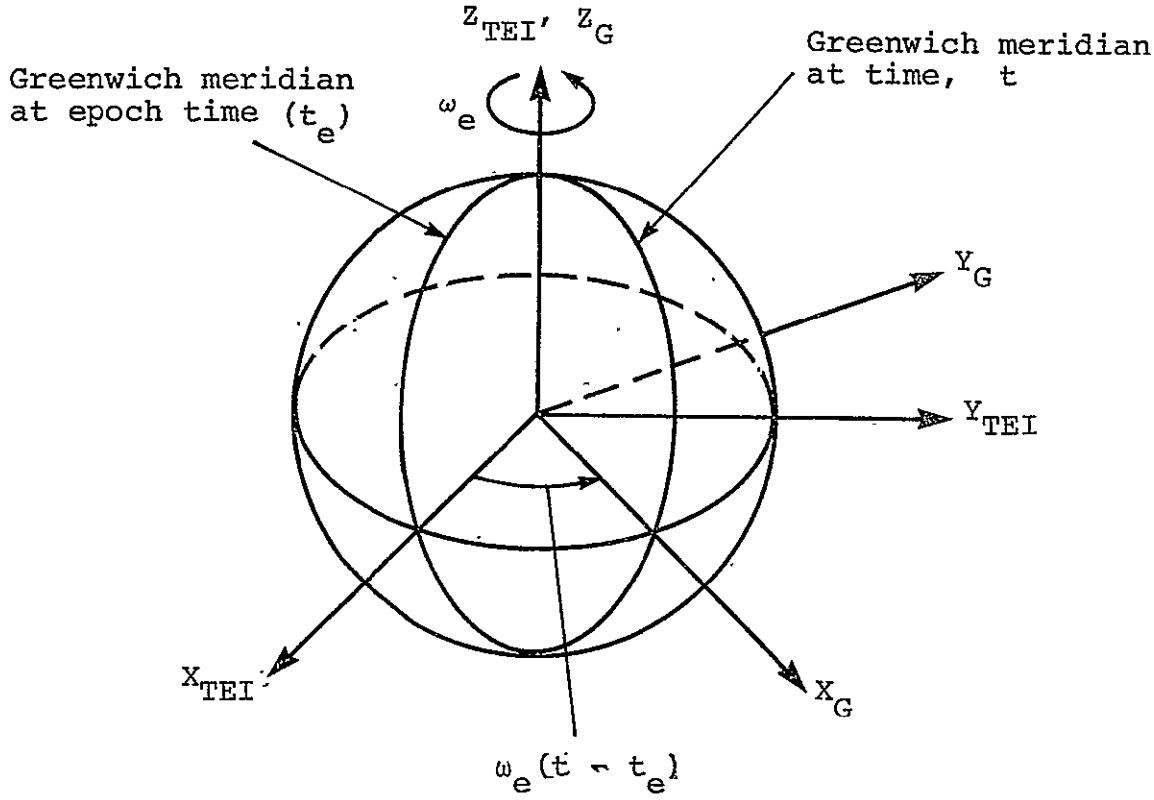

Figure 2-5.- Relationship between TEI and rotating geocentric systems.

$$\vec{R}^{G}_{sc} = \begin{bmatrix} \cos \Delta\lambda & \sin \Delta\lambda & 0 \\ -\sin \Delta\lambda & \cos \Delta\lambda & 0 \\ 0 & 0 & 1 \end{bmatrix}_{TEI}^{G} \vec{R}^{TEI}_{sc} \tag{2-4}$$

where

$$\Delta\lambda = \omega_e \, (t - t_e) \tag{2-5}$$

The final step is to determine whether the S/C subsatellite point lies within the ground target area (fig. 2-3). The angle from $\vec{C}^{G}_{B}$ to the perimeter of the circular ground target area, γ_A, is given (in degrees) by

$$\gamma_A = \left(\frac{r_c}{\left| \vec{C}^{G}_{B} \right|} \right) \frac{180}{\pi} \tag{2-6}$$

The angle from $\vec{C}^{G}_{B}$ to the S/C, γ_S, is given by

$$\gamma_S = \cos^{-1} \left\{ \frac{\vec{R}^{G}_{sc} \cdot \vec{C}^{G}_{B}}{\left| \vec{R}^{G}_{sc} \right| \left| \vec{C}^{G}_{B} \right|} \right\} \tag{2-7}$$

The S/C lies within the ground target area if

$$\gamma_S \leq \gamma_A \tag{2-8}$$

2.1.3 Assumptions and Limitations

The following assumptions are implicit in the equations presented in section 2.1.2:

a. The S/C geocentric subsatellite point is used to compute entry into the ground target area.

b. The effects of polar nutation and precession from time t_e to time t can be neglected.

c. The radius of the Earth-referenced circle, r_c, is a segment of arc.

2.2 CELESTIAL CIRCLES

Celestial circles are defined to be circular areas on the celestial sphere (fig. 2-6). The center of this area target is defined by right ascension and declination. The criterion for a S/C to lie within this area is for the S/C zenith point to lie within the perimeter of the celestial circle.

2.2.1 Procedure

The following procedure will be used to determine whether the S/C lies within the celestial circle:

a. The unit vector along the centerline of the celestial circle will be computed in the M50 system.
b. The dot product between this vector and the S/C position vector will be formed to determine whether the S/C lies within the celestial circle.

2.2.2 Equations

The following parameters are required:

α_A and δ_A - the right ascension and declination, respectively, of the centerline of the celestial circle expressed in the M50 system (fig. 2-6).

γ_A - the celestial circle angular radius (fig. 2-6).

$\vec{R}_{sc}$ - S/C position vector in the M50 system.

The unit vector from the center of the Earth to the center of the celestial circle, $\hat{C}_B$, is given by

$$\hat{C}_B = \begin{Bmatrix} \cos \alpha_A \cos \delta_A \\ \sin \alpha_A \cos \delta_A \\ \sin \delta_A \end{Bmatrix} \tag{2-9}$$

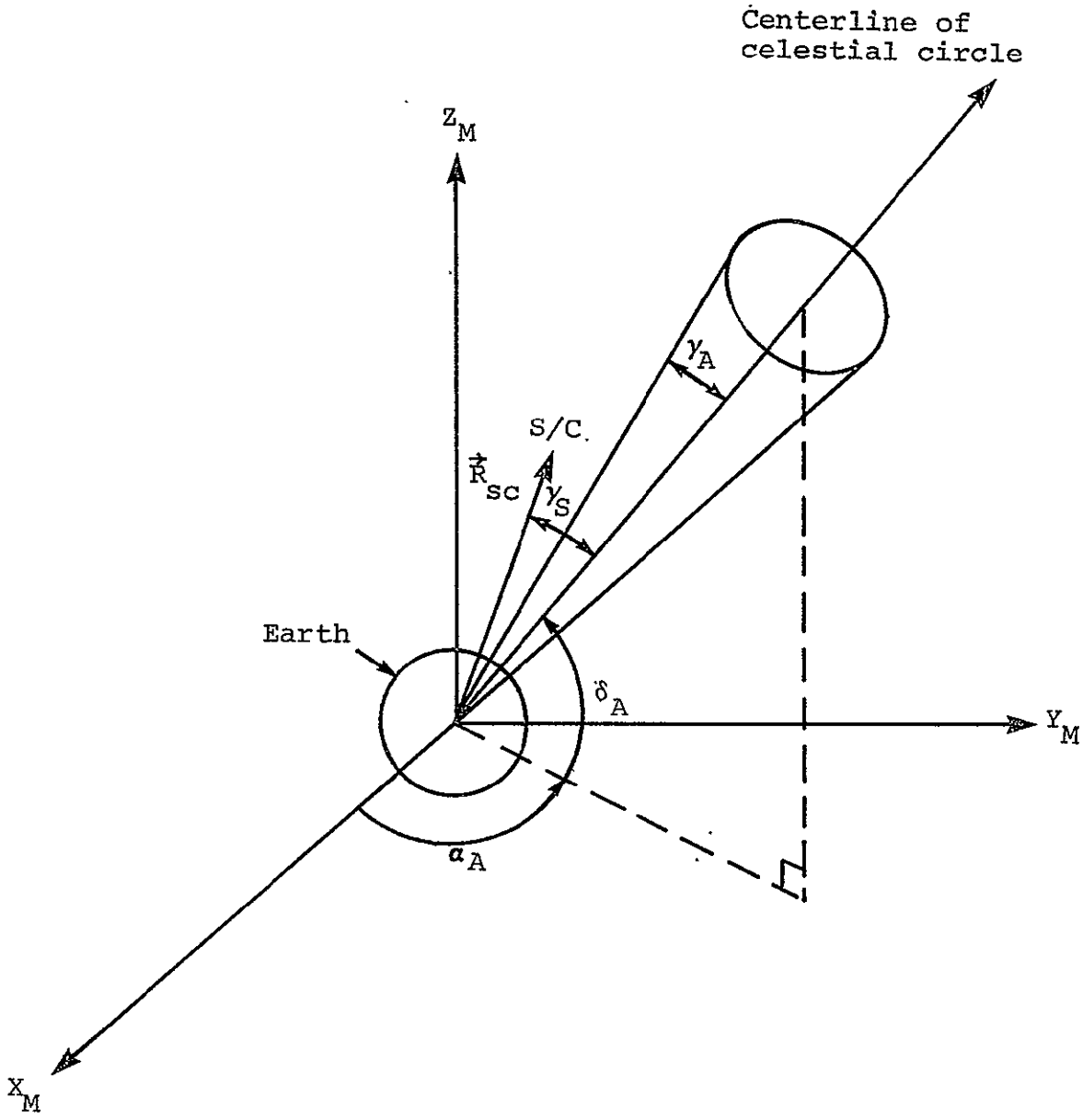

Figure 2-6.- Containment test for celestial circles.

The angle between this vector and the S/C, γ_S, is

$$\gamma_S = \cos^{-1}\left\{\hat{C}_B \cdot \frac{\vec{R}_{sc}}{|\vec{R}_{sc}|}\right\} \qquad (2\text{-}10)$$

The S/C lies within the celestial circle if

$$\gamma_S \leq \gamma_A \qquad (2\text{-}11)$$

2.2.3 Assumptions and Limitations

None.

2.3 EARTH-REFERENCED POLYGONS

The Earth-referenced polygon is defined to be an arbitrary planar figure having up to five sides (fig. 2-7). This figure is fixed with respect to the rotating Earth. The corner points (i.e., vertices) of this polygon are defined by geodetic latitude, longitude, and altitude. The basic criterion for penetration is to ensure that the S/C subsatellite point lies within the perimeter of the ground target area.

2.3.1 Procedure

The basic procedure for this ground target area is similar to the procedure presented in section 2.1.1. It consists of

a. Transforming the geodetic coordinates of each polygon vertex to the geocentric system.
b. Transforming the S/C position vector from the M50 system to the geocentric system.
c. Testing to determine whether the S/C is interior to all planes defined by the sides of the polygon.

2.3.2 Equations

The following parameters are required:

- n - number of sides
- ϕ_i and λ_i - geodetic latitude and longitude, respectively, of each vertex (fig. 2-7)
- h_i - geodetic altitude of each vertex (fig. 2-7)
- $\vec{R}_{sc}$ - S/C position vector in the M50 system
- t - time corresponding to $\vec{R}_{sc}$
- $[RNP]_{M50}^{TEI}$ - RNP matrix to transform from the M50 system to the TEI system
- t_e - epoch time corresponding to the RNP matrix
- R_{em} - mean equatorial radius for the Fischer ellipsoid of 1960
- F - flattening coefficient for the Fischer ellipsoid of 1960
- ω_e - Earth rotation rate

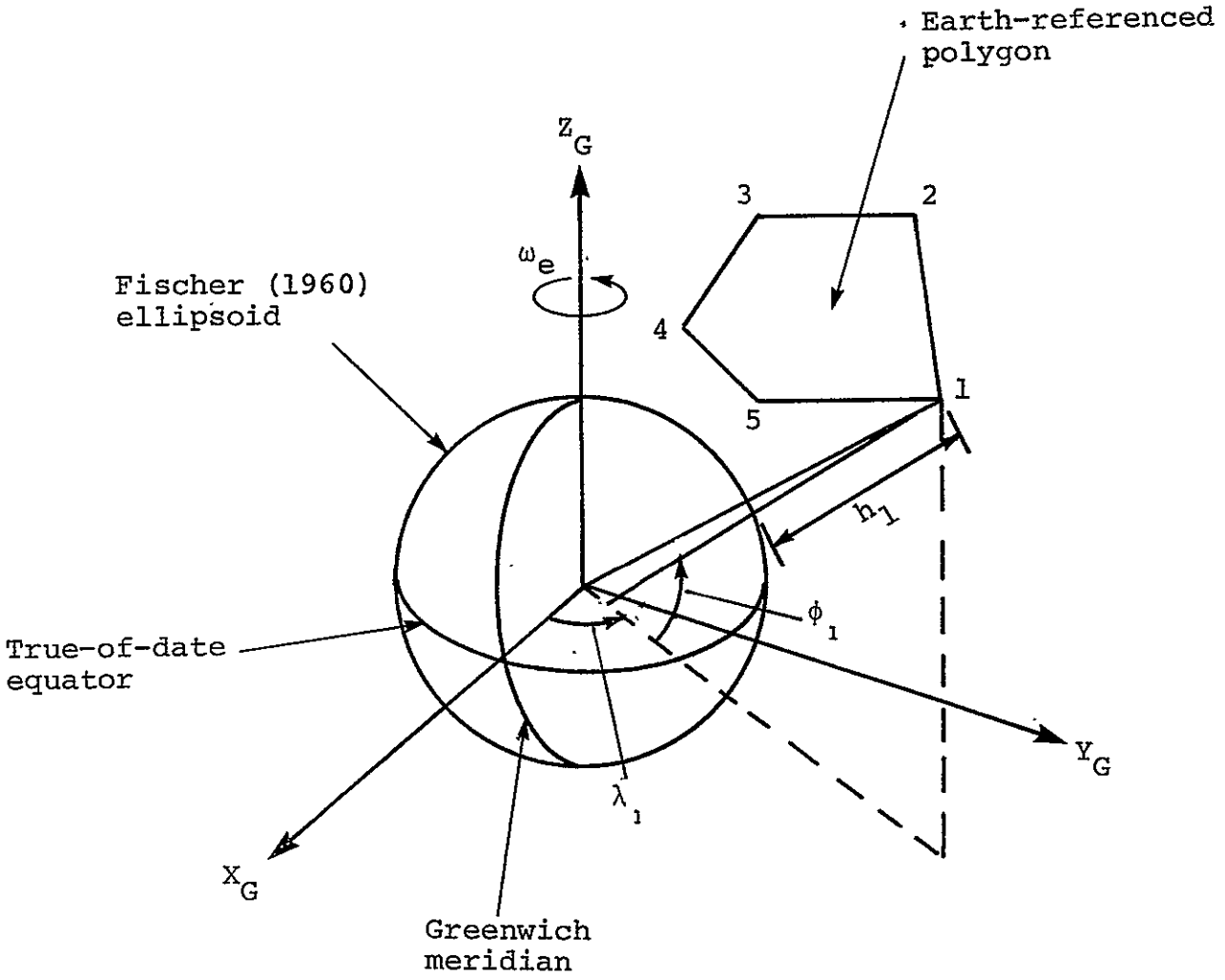

Figure 2-7.- Earth-referenced polygon.

The first step is to transform the parameters defining each vertex of the polygon from the geodetic system to the rotating geocentric system. These vectors are given by

$$\vec{R}_i^G = \begin{Bmatrix} (h_i + a_F) \cos \lambda_i \cos \phi_i \\ (h_i + a_F) \sin \lambda_i \cos \phi_i \\ \left[h_i + (1 - F)^2 a_F\right] \sin \phi_i \end{Bmatrix} i = 1,2,3,\ldots n \qquad (2\text{-}12)$$

where

a_F is defined by equation 2-2 with ϕ_i replacing ϕ.

The S/C position vector in the geocentric system, $\vec{R}_{sc}^G$, is then obtained by using equations 2-3 through 2-5.

The next step in the procedure is to determine whether the S/C lies interior to all planes defined by the sides of the polygon. Figures 2-8 and 2-9 illustrate the geometry. All vectors in these figures are with respect to the geocentric system. The centroid of the ground target area, $\vec{C}_B^G$, (fig. 2-8) is defined as

$$\vec{C}_B^G = \frac{\sum_{i=1}^{n} \vec{R}_i^G}{n} \qquad (2\text{-}13)$$

The unit normal vectors to each side of the polygon (fig. 2-9) are given by

$$\hat{N}_i^G = \frac{\vec{R}_{i+1}^G \times \vec{R}_i^G}{\left|\vec{R}_{i+1}^G \times \vec{R}_i^G\right|} \quad i = 1,2,3,\ldots n-1 \qquad (2\text{-}14a)$$

$$\hat{N}_n^G = \frac{\vec{R}_1^G \times \vec{R}_n^G}{\left|\vec{R}_1^G \times \vec{R}_n^G\right|} \qquad (2\text{-}14b)$$

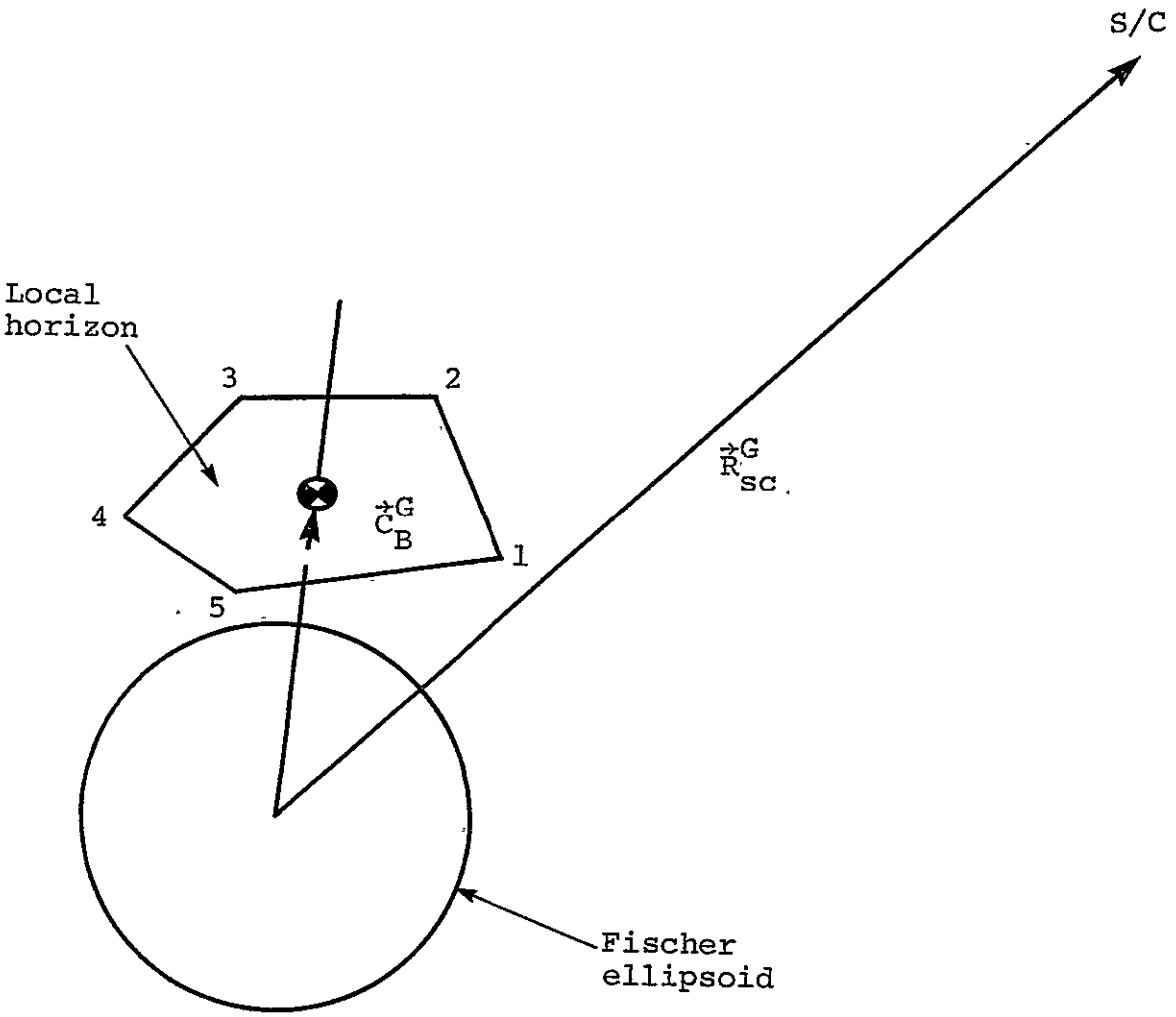

Figure 2-8.- Centroid of Earth-referenced polygons.

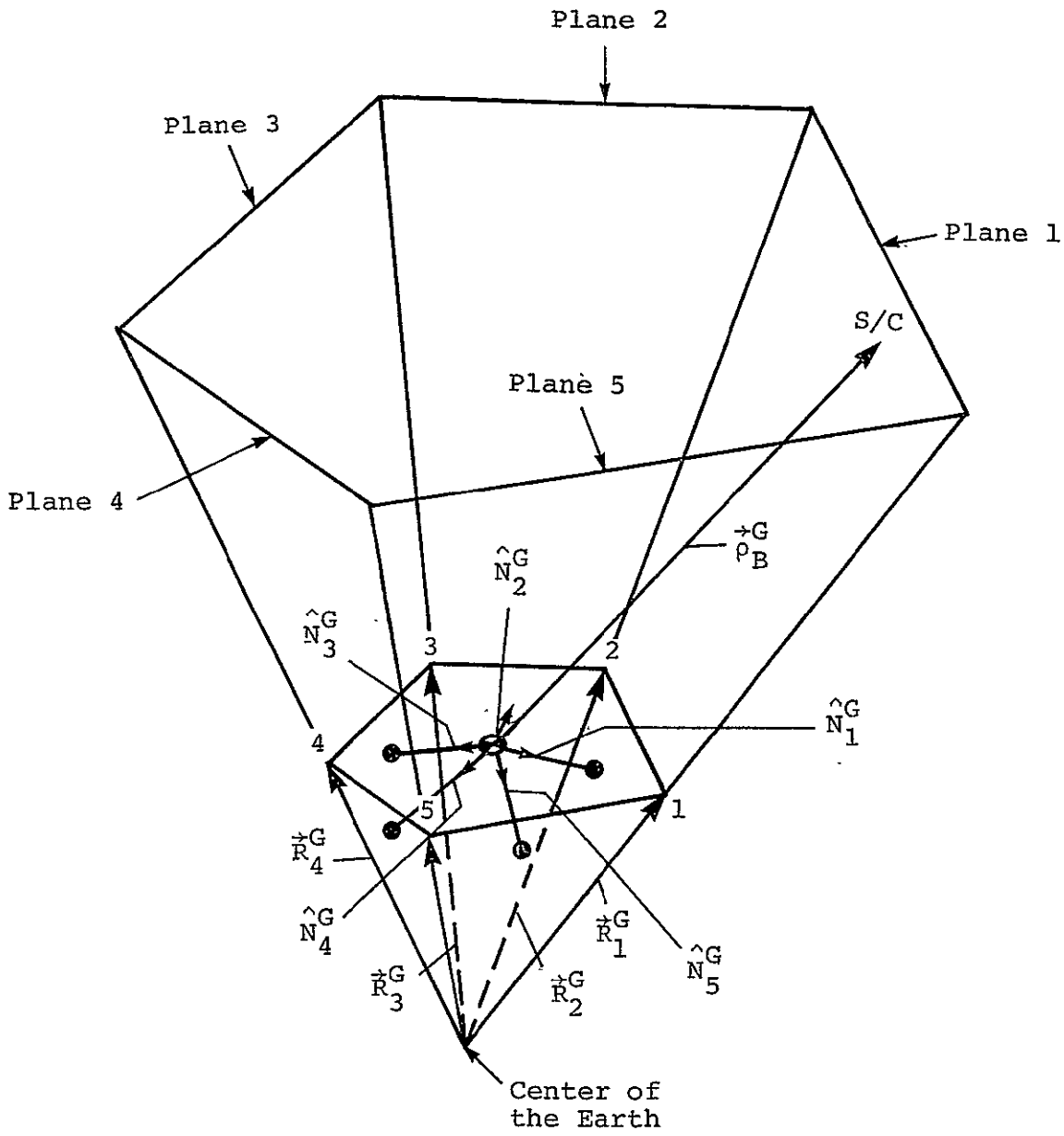

Figure 2-9.- Containment test for Earth-referenced polygons.

The perpendicular distance from $\vec{C}_B^G$ to each polygon side is

$$d_i = \hat{N}_i^G \cdot \left(\vec{R}_i^G - \vec{C}_B^G \right) \qquad i = 1,2,3,\ldots n \qquad (2\text{-}15)$$

The S/C must lie interior to the i^{th} plane if

$$\hat{N}_i^G \cdot \vec{\rho}_B^G \leq d_i \qquad (2\text{-}16)$$

where

$$\vec{\rho}_B^G = \vec{R}_{sc}^G - \vec{C}_B^G \qquad (2\text{-}17)$$

If equation 2-16 is satisfied for all sides, then the S/C subsatellite point lies within the perimeter of the polygon.

2.3.3 Assumptions and Limitations

The following assumptions and limitations are implicit in the equations presented in section 2.3.2:

a. The S/C geocentric subsatellite point is used to determine entry into the ground target area.
b. The effects of polar nutation and precession from time t_e to t can be neglected.
c. The vertices of the polygon are specified in a counterclockwise order as viewed from the top.
d. The polygon is convex; i.e., the interior angles between the sides defining the vertices are less than 180 degrees.[1]
e. The angular separation between two consecutive vertices is sufficient to permit a nonzero cross product (eq. 2-14).
f. The S/C and the ground target area lie in the same hemisphere. The procedure discussed in section 3 will assure this condition.

---

[1] Concave polygons can be accommodated by subdividing them into two or more convex polygons. Appendix A discusses this procedure.

2.4 CELESTIAL POLYGONS

Celestial polygons are defined to be arbitrary figures having up to five sides with the corner points (i.e., vertices) defined by right ascension and declination on the celestial sphere. The criterion for penetration into this area is to ensure that the S/C zenith point lies within the confines of the polygon. Figure 2-10 illustrates the celestial polygon. It is noted that this polygon also represents a variable area polyhedron which remains inertially fixed.

2.4.1 Procedure

The basic procedure for this area target is similar to the procedure presented in section 2.3.1, i.e.,:

a. The unit vector along the "centroid" of the polyhedron will be computed in the M50 system.
b. Tests will be made to determine whether the S/C is interior to all planes defined by the sides of the polyhedron.

2.4.2. Equations

The following parameters are required:

n - number of sides

α_i and δ_i - right ascension and declination, respectively, of each vertex in the M50 system ($i = 1,2,3,\ldots n$)

$\vec{R}_{sc}$ - S/C position vector in the M50 system

The first step is to determine the unit vector along the centroid of the polyhedron. The unit vectors from the center of the Earth to each vertex in the M50 system are given by

$$\hat{R}_i = \begin{Bmatrix} \cos \alpha_i \cos \delta_i \\ \sin \alpha_i \cos \delta_i \\ \sin \delta_i \end{Bmatrix} \quad i = 1,2,3,\ldots n \qquad (2\text{-}18)$$

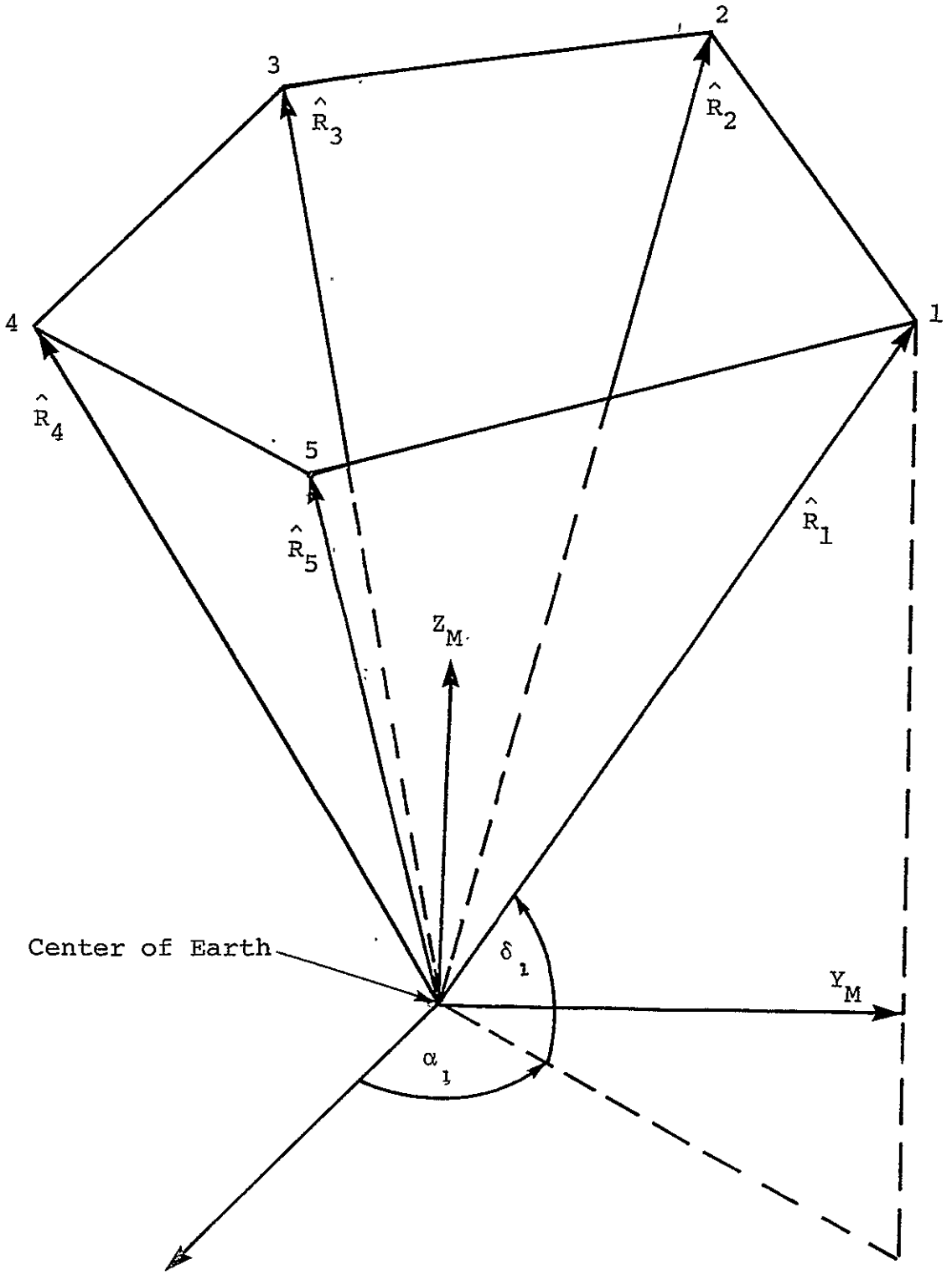

Figure 2-10.- Celestial polygon.

The unit vector along the centroid of the polyhedron is

$$\hat{C} = \frac{\vec{C}}{|\vec{C}|} \tag{2-19}$$

where

$$\vec{C} = \frac{\sum_{i=1}^{n} \hat{R}_i}{n} \tag{2-20}$$

The final step is to determine whether the S/C lies interior to all planes defined by the sides of the polyhedron. Figure 2-11 illustrates the geometry. The slant range from $\hat{C}$ to the S/C is

$$\vec{\rho}_B = \vec{R}_{sc} - \hat{C} \tag{2-21}$$

Equations 2-14 through 2-16 (with $\vec{R}^G_i$, $\vec{C}^G_B$, and $\vec{\rho}^G_B$ replaced by $\hat{R}_i$, $\hat{C}$, and $\vec{\rho}_B$, respectively) are then used to determine whether the S/C is interior to all polyhedron planes.

2.4.3 Assumptions and Limitations

The following assumptions and limitations are implicit in the equations presented in section 2.4.2:

a. The vertices of the polygon are specified in a counterclockwise order as viewed from the top.
b. The polygon is convex; i.e., the interior angles between the sides defining the vertices are less than 180 degrees.[1]
c. The angular separation between two consecutive vertices is sufficient to permit a nonzero cross product (eq. 2-14).
d. The S/C and the area target lie within the same hemisphere. The procedure outlined in section 3 will assure this condition.

[1] Concave polygons can be accommodated by subdividing them into two or more convex polygons as discussed in appendix A.

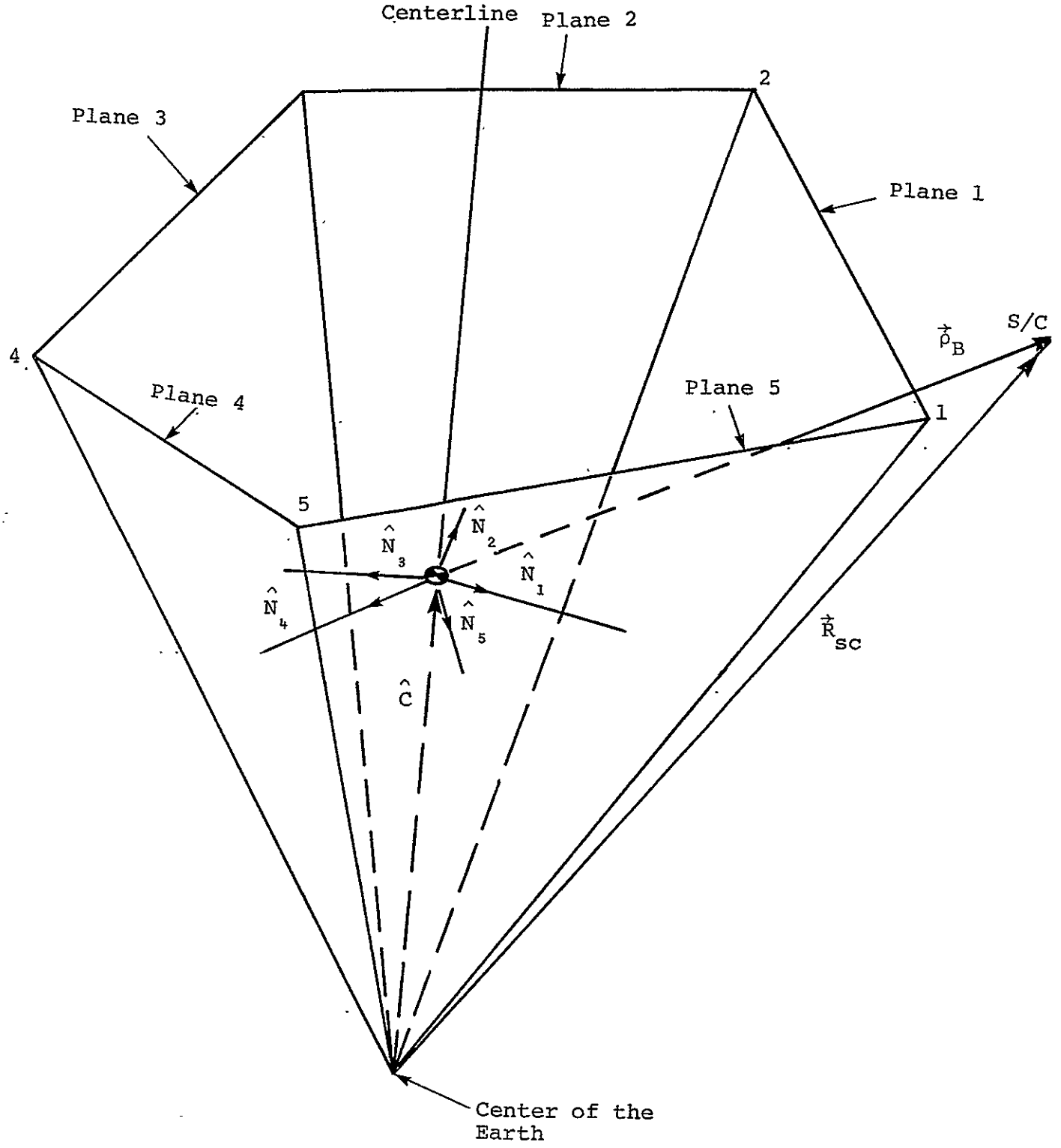

Figure 2-11.- Containment test for celestial polygons.

2.5 EARTH-REFERENCED SPACE VOLUMES

The Earth-referenced space volumes are arbitrary five-sided polyhedrons which are defined by a lower-limit polygon at an altitude, h_1, and the projection of this polygon to an altitude, h_2. The vertices of this polygon are defined by geodetic latitude and longitude and rotate with the Earth. Figure 2-12 illustrates this type of space volume. As shown, the planar cross sectional area of this polyhedron remains constant with respect to altitude.

2.5.1 Procedure

The following procedure will be used to determine whether the S/C lies within the space volume:

a. The geodetic parameters defining each vertex of the lower boundary will be transformed to geocentric position vectors.
b. The centroid vector to the lower boundary will be computed in the geocentric system.
c. The S/C position vector will be transformed from the M50 system to the geocentric system.
d. Tests will be performed to ensure that the S/C lies above the lower boundary and below the upper boundary. If either of these tests fails, then no further computations are required.
e. Assuming the previous step is passed, tests will be performed to determine whether the S/C is interior to all planes defined by the sides of the polyhedron.

2.5.2 Equations

The following parameters are required:

ϕ_i and λ_i - geodetic latitude and longitude, respectively, of each vertex of the lower boundary ($i = 1,2,3,4,5$)

h_1 - geodetic altitude of the lower boundary

h_2 - geodetic altitude of the upper boundary

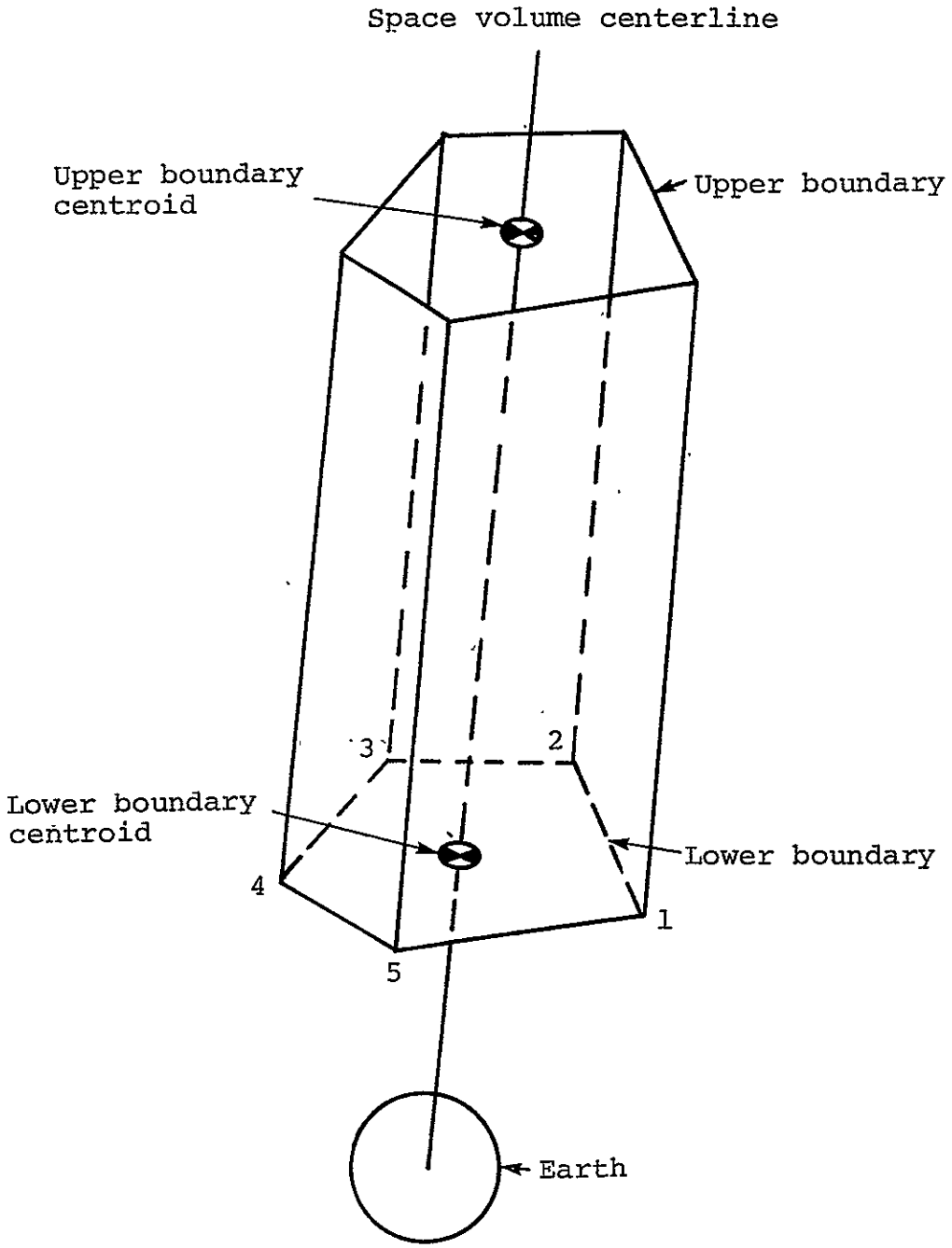

Figure 2-12.- Constant area polyhedron.

$\vec{R}_{sc}$ - S/C position vector in the M50 system

t - time corresponding to $\vec{R}_{sc}$

$[RNP]^{TEI}_{M50}$ - RNP matrix to transform from the M50 to TEI system

t_e - epoch time corresponding to the RNP matrix

R_{em} - mean equatorial radius for the Fischer ellipsoid of 1960

F - flattening coefficient for the Fischer ellipsoid of 1960

ω_e - Earth rotation rate

The first step is to transform the parameters defining each vertex of the lower boundary to geocentric position vectors. Equation 2-12 (with $h_i = 0$) provides the necessary transformation.

The centroid of these vectors is given by

$$\vec{C}^G = \frac{\sum_{i=1}^{n} \vec{R}_i^G}{n} \qquad (2\text{-}22)$$

The geocentric vector to the centroid of the lower boundary (fig. 2-13) is given by

$$\vec{C}_B^G = \vec{C}^G + h_1 \frac{\vec{C}^G}{|\vec{C}^G|} \qquad (2\text{-}23)$$

Next, the S/C position vector in the geocentric system, $\vec{R}_{sc}^G$, is computed using equations 2-3 through 2-5.

The fourth step in the procedure is to ensure that the S/C lies between the upper and lower boundaries. Figure 2-13 illustrates the geometry. All vectors in this figure are with respect to the geocentric system. The slant range from $\vec{C}_B^G$ to the S/C, $\vec{\rho}_B^G$,

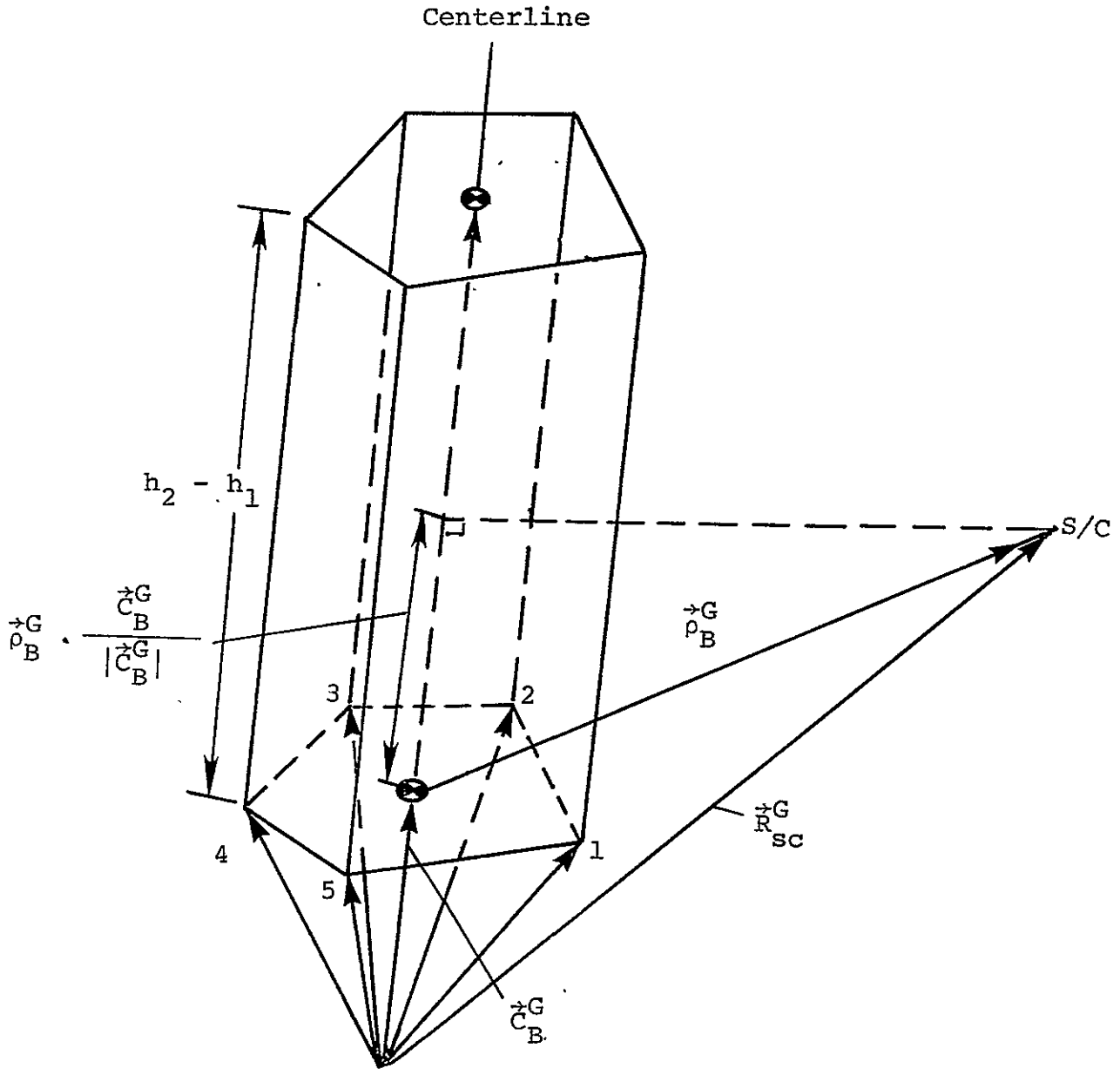

Figure 2-13.- Boundary tests for constant area polyhedrons.

is given by

$$\vec{\rho}_B^G = \vec{R}_{sc}^G - \vec{C}_B^G \qquad (2\text{-}24)$$

The S/C lies above the lower boundary and below the upper boundary if

$$h_2 - h_1 \geq \vec{\rho}_B^G \cdot \frac{\vec{C}_B^G}{|\vec{C}_B^G|} \geq 0 \qquad (2\text{-}25)$$

Assuming that equation 2-25 is satisfied, the final step is to determine whether the S/C lies interior to the side planes of the polyhedron. Figure 2-14 illustrates the geometry. The unit normal vectors from $\vec{C}_B^G$ to each side of the polygon are given by

$$\hat{N}_i^G = \frac{\vec{C}_B^G \times \left(\vec{R}_i^G - \vec{R}_{i+1}^G\right)}{\left|\vec{C}_B^G \times \left(\vec{R}_i^G - \vec{R}_{i+1}^G\right)\right|} \quad i = 1,2,3,4 \qquad (2\text{-}26a)$$

$$\hat{N}_5^G = \frac{\vec{C}_B^G \times \left(\vec{R}_5^G - \vec{R}_1^G\right)}{\left|\vec{C}_B^G \times \left(\vec{R}_5^G - \vec{R}_1^G\right)\right|} \qquad (2\text{-}26b)$$

Equations 2-15 and 2-16 are then used to determine whether the S/C is contained within the polyhedron.

2.5.3 Assumptions and Limitations

The following assumptions and limitations are implicit in the equations presented in section 2.5.2:

a. The altitude of the lower boundary, h_1, is measured with respect to the centroid of the vertices which lie on the Fischer ellipsoid.

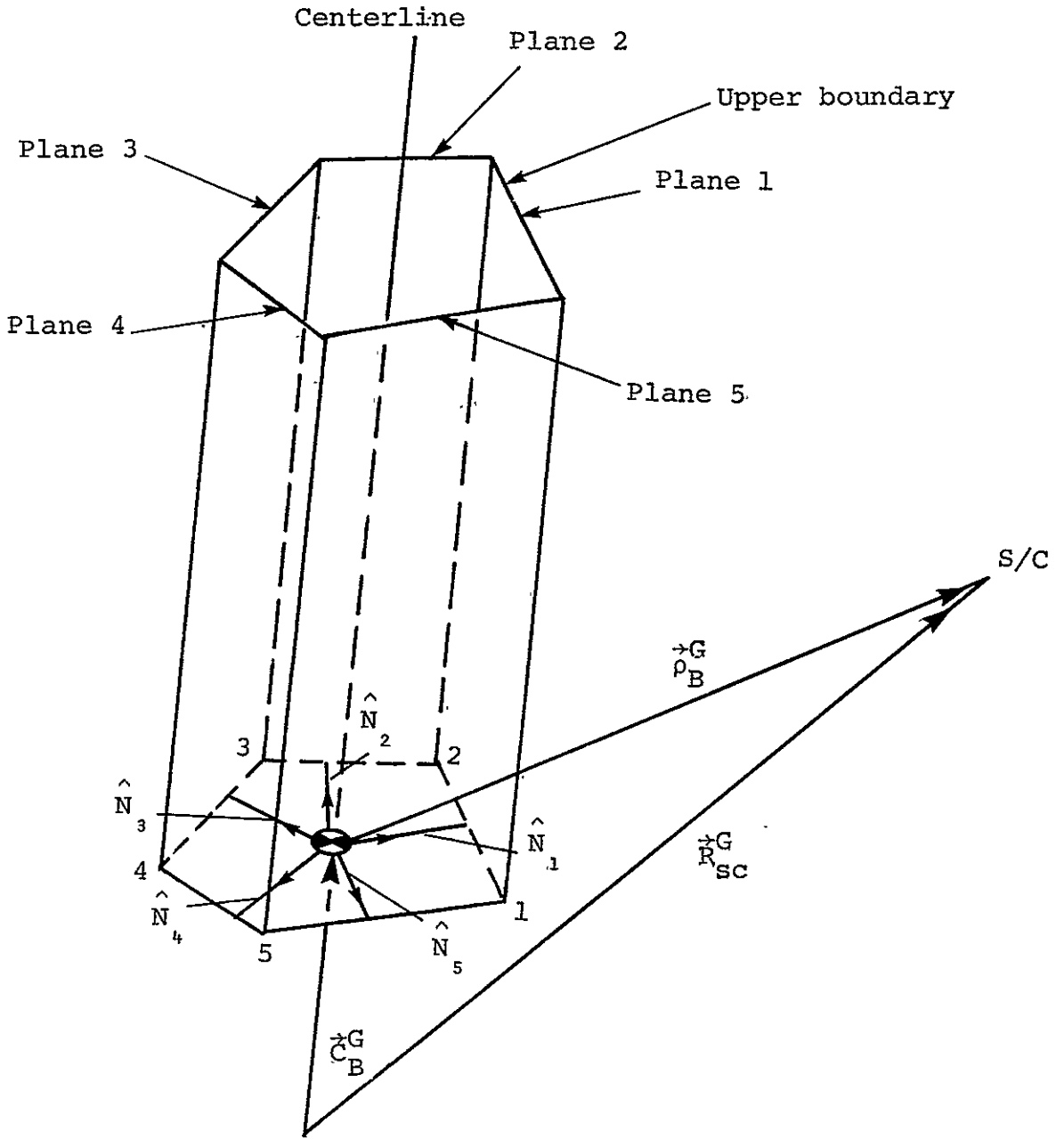

Figure 2-14.- Containment test for constant area polyhedrons.

b. The effects of polar nutation and precession from time t_e to t can be neglected.

c. The vertices are specified in a counterclockwise order as viewed from the top.

d. The planar area of the polyhedron is convex; i.e., the interior angles between the sides defining the vertices are less than 180 degrees.[1]

e. The local horizon for determining whether the S/C is between the upper and lower boundaries is perpendicular to the centroid vector.

f. The distance between two consecutive vertices is sufficient to permit a nonzero cross product (eq. 2-26).

[1]Concave polyhedrons can be accommodated by subdividing them into two or more convex portions as discussed in appendix A.

2.6 CELESTIAL-FIXED SPACE VOLUMES

The celestial-fixed space volumes are arbitrary five-sided polyhedrons which are defined by a lower-limit polygon at an altitude, h_1, and a projection of this polygon to an altitude, h_2. The vertices of the polygon are defined by right ascension and declination and are inertially fixed. Figure 2-12 can also be used to illustrate this type of space volume. As mentioned previously, the planar cross sectional area of this polyhedron remains constant with respect to altitude

2.6.1 Procedure

The basic procedure for this space volume is very similar to the procedure presented in section 2.5.1. It consists of:

a. Computing the centroid vector to the lower boundary in the M50 system.
b. Testing to ensure that the S/C lies above the lower boundary and below the upper boundary. If either of these tests fails, then no further computations are required.
c. Assuming the previous step is passed, further tests will be performed to determine whether the S/C is interior to all planes defined by the sides of the polyhedron.

2.6.2 Equations

The following parameters are required:

α_i and δ_i - right ascension and declination, respectively, of each vertex of the lower boundary in the M50 system ($i = 1,2,3,4,5$)

h_1 - altitude of the lower boundary

h_2 - altitude of the upper boundary

R_{em} - mean equatorial radius

The unit vector to the centroid of the polyhedron, $\hat{C}$, is computed via equations 2-18 through 2-20. The vector to the centroid of the lower boundary is given by

$$\vec{C}_B = \left(R_{em} + h_1\right) \hat{C} \qquad (2\text{-}27)$$

Equations 2-24 and 2-25 (with variables $\vec{R}^G_{sc}$ and $\vec{C}^G_B$ replaced by $\vec{R}_{sc}$ and $\vec{C}_B$, respectively) are then used to ensure that the S/C lies between the upper and lower boundaries.

Assuming equation 2-25 is satisfied, equation 2-26 (with $\vec{C}^G_B$ and $\vec{R}^G_i$ replaced by $\vec{C}_B$ and $\hat{R}_i$, respectively) is used to define the unit normal vectors to each side of the polyhedron. Finally, equations 2-15 and 2-16 are used to determine whether the S/C lies within the space volume.

2.6.3 Assumptions and Limitations

The following assumptions and limitations are implicit in the equations presented in section 2.6.2:

a. The altitudes of the lower and upper boundaries are measured with respect to the mean equatorial radius.
b. The vertices are specified in a counterclockwise order as viewed from the top.
c. The planar area of the polyhedron is convex; i.e., the interior angles between the sides defining the vertices are less than 180 degrees.[1]
d. The distance between two consecutive vertices is sufficient to permit a nonzero cross product (eq. 2-26).

[1] Concave polyhedrons can be accommodated by subdividing them into two or more convex portions as discussed in appendix A.

2.7 SUMMARY OF EQUATIONS

This section summarizes all of the equations presented in the previous sections for the various area targets and space volumes. The order of presentation and equation numbers correspond to the computation sequence discussed in the text.

2.7.1 Earth-Referenced Circles

$$\vec{C}_B^G = \begin{Bmatrix} \left(h + a_F\right) \cos\lambda \cos\phi \\ \left(h + a_F\right) \sin\lambda \cos\phi \\ \left[h + (1 - F)^2 a_F\right] \sin\phi \end{Bmatrix} \tag{2-1}$$

where

$$a_F \doteq \frac{R_{em}}{\sqrt{\cos^2\phi + (1 - F)^2 \sin^2\phi}} \tag{2-2}$$

$$\vec{R}_{sc}^{TEI} = [RNP]_{M50}^{TEI} \vec{R}_{sc} \tag{2-3}$$

$$\vec{R}_{sc}^G = \begin{bmatrix} \cos\Delta\lambda & \sin\Delta\lambda & 0 \\ -\sin\Delta\lambda & \cos\Delta\lambda & 0 \\ 0 & 0 & 1 \end{bmatrix}_{TEI}^{G} \vec{R}_{sc}^{TEI} \tag{2-4}$$

where

$$\Delta\lambda = \omega_e \left(t - t_e\right) \tag{2-5}$$

$$\gamma_A = \left\{ \frac{r_c}{|\vec{C}_B^G|} \right\} \frac{180}{\pi} \tag{2-6}$$

$$\gamma_S = \cos^{-1} \left\{ \frac{\vec{R}_{sc}^G \cdot \vec{C}_B^G}{|\vec{R}_{sc}^G| \; |\vec{C}_B^G|} \right\} \tag{2-7}$$

$$\gamma_S \leq \gamma_A \tag{2-8}$$

2.7.2 Celestial Circles

$$\hat{C}_B = \begin{Bmatrix} \cos \alpha_A \cos \delta_A \\ \sin \alpha_A \cos \delta_A \\ \sin \delta_A \end{Bmatrix} \tag{2-9}$$

$$\gamma_S = \cos^{-1} \left\{ \hat{C}_B \cdot \frac{\vec{R}_{sc}}{|\vec{R}_{sc}|} \right\} \tag{2-10}$$

$$\gamma_S \leq \gamma_A \tag{2-11}$$

2.7.3 Earth-Referenced Polygons

$$\vec{R}_i^G = \begin{Bmatrix} (h_i + a_F) \cos \lambda_i \cos \phi_i \\ (h_i + a_F) \sin \lambda_i \cos \phi_i \\ \left[h_i + (1 - F)^2 a_F\right] \sin \phi_i \end{Bmatrix} \quad i = 1,2,3,\ldots n \tag{2-12}$$

where

$$a_F = \frac{R_{em}}{\sqrt{\cos^2\phi_i + (1 - F)^2 \sin^2\phi_i}} \tag{2-2}$$

$$\vec{R}_{sc}^{TEI} = [RNP]_{M50}^{TEI}\, \vec{R}_{sc} \tag{2-3}$$

$$\vec{R}_{sc}^{G} = \begin{bmatrix} \cos\Delta\lambda & \sin\Delta\lambda & 0 \\ -\sin\Delta\lambda & \cos\Delta\lambda & 0 \\ 0 & 0 & 1 \end{bmatrix}_{TEI}^{G} \vec{R}_{sc}^{TEI} \tag{2-4}$$

where

$$\Delta\lambda = \omega_e \left(t - t_e\right) \tag{2-5}$$

$$\vec{C}_B^G = \frac{\sum_{i=1}^{n} \vec{R}_i^G}{n} \tag{2-13}$$

$$\hat{N}_i^G = \frac{\vec{R}_{i+1}^G \times \vec{R}_i^G}{|\vec{R}_{i+1}^G \times \vec{R}_i^G|} \quad i = 1,2,3,\ldots n-1 \tag{2-14a}$$

$$\hat{N}_n^G = \frac{\vec{R}_1^G \times \vec{R}_n^G}{|\vec{R}_1^G \times \vec{R}_n^G|} \tag{2-14b}$$

$$d_i = \hat{N}_i^G \cdot \left(\vec{R}_i^G - \vec{C}_B^G\right) \quad i = 1,2,3,\ldots n \tag{2-15}$$

$$\hat{N}_i^G \cdot \vec{\rho}_B^G \leq d_i \qquad i = 1,2,3,\ldots n \tag{2-16}$$

where

$$\vec{\rho}_B^G = \vec{R}_{sc}^G - \vec{C}_B^G \tag{2-17}$$

2.7.4 Celestial Polygons

$$\hat{R}_i = \begin{Bmatrix} \cos \alpha_i & \cos \delta_i \\ \sin \alpha_i & \cos \delta_i \\ & \sin \delta_i \end{Bmatrix} \quad i = 1,2,3,...n \tag{2-18}$$

$$\hat{C} = \frac{\vec{C}}{|\vec{C}|} \tag{2-19}$$

where

$$\vec{C} = \frac{\sum_{i=1}^{n} \hat{R}_i}{n} \tag{2-20}$$

$$\vec{\rho}_B = \vec{R}_{sc} - \hat{C} \tag{2-21}$$

$$\hat{N}_i = \frac{\hat{R}_{i+1} \times \hat{R}_i}{|\hat{R}_{i+1} \times \hat{R}_i|} \quad i = 1,2,3,...n-1 \tag{2-14a}$$

$$\hat{N}_n = \frac{\hat{R}_1 \times \hat{R}_n}{|\hat{R}_1 \times \hat{R}_n|} \tag{2-14b}$$

$$d_i = \hat{N}_i \cdot \left(\hat{R}_i - \hat{C}\right) \quad i = 1,2,3,...n \tag{2-15}$$

$$\hat{N}_i \cdot \vec{\rho}_B \leq d_i \qquad i = 1,2,3,...n \tag{2-16}$$

2.7.5 Earth-Referenced Space Volumes

$$\vec{R}_i^G = \begin{Bmatrix} a_F \cos \lambda_i \cos \phi_i \\ a_F \sin \lambda_i \cos \phi_i \\ (1 - F)^2 a_F \sin \phi_i \end{Bmatrix} \quad i = 1,2,3,4,5 \quad (2\text{-}12)$$

where

$$a_F = \frac{R_{em}}{\sqrt{\cos^2 \phi_i + (1 - F)^2 \sin^2 \phi_i}} \quad (2\text{-}2)$$

$$\vec{C}^G = \frac{\sum_{i=1}^{5} \vec{R}_i^G}{5} \quad (2\text{-}22)$$

$$\vec{C}_B^G = \vec{C}^G + h_1 \frac{\vec{C}^G}{|\vec{C}^G|} \quad (2\text{-}23)$$

$$\vec{R}_{sc}^{TEI} = [RNP]_{M50}^{TEI} \vec{R}_{sc} \quad (2\text{-}3)$$

$$\vec{R}_{sc}^G = \begin{bmatrix} \cos \Delta\lambda & \sin \Delta\lambda & 0 \\ -\sin \Delta\lambda & \cos \Delta\lambda & 0 \\ 0 & 0 & 1 \end{bmatrix}_{TEI}^{G} \vec{R}_{sc}^{TEI} \quad (2\text{-}4)$$

where

$$\Delta\lambda = \omega_e \left(t - t_e\right) \quad (2\text{-}5)$$

$$\vec{\rho}_B^G = \vec{R}_{sc}^G - \vec{C}_B^G \quad (2\text{-}24)$$

$$h_2 - h_1 \geq \vec{\rho}_B^G \cdot \frac{\vec{C}_B^G}{|\vec{C}_B^G|} \geq 0 \qquad (2\text{-}25)$$

$$\hat{N}_i^G = \frac{\vec{C}_B^G \times \left(\vec{R}_i^G - \vec{R}_{i+1}^G\right)}{\left|\vec{C}_B^G \times \left(\vec{R}_i^G - \vec{R}_{i+1}^G\right)\right|} \qquad i = 1,2,3,4 \qquad (2\text{-}26a)$$

$$\hat{N}_5^G = \frac{\vec{C}_B^G \times \left(\vec{R}_5^G - \vec{R}_1^G\right)}{\left|\vec{C}_B^G \times \left(\vec{R}_5^G - \vec{R}_1^G\right)\right|} \qquad (2\text{-}26b)$$

$$d_i = \hat{N}_i^G \cdot \left(\vec{R}_i^G - \vec{C}_B^G\right) \qquad i = 1,2,3,4,5 \qquad (2\text{-}15)$$

$$\hat{N}_i^G \cdot \vec{\rho}_B^G \leq d_i \qquad i = 1,2,3,4,5 \qquad (2\text{-}16)$$

2.7.6 Celestial-Fixed Space Volumes

$$\hat{R}_i = \begin{Bmatrix} \cos\alpha_i & \cos\delta_i \\ \sin\alpha_i & \cos\delta_i \\ & \sin\delta_i \end{Bmatrix} \qquad i = 1,2,3,4,5 \qquad (2\text{-}18)$$

$$\hat{C} = \frac{\vec{C}}{|\vec{C}|} \qquad (2\text{-}19)$$

where

$$\vec{C} = \frac{\sum_{i=1}^{5} \hat{R}_i}{5} \qquad (2\text{-}20)$$

$$\vec{C}_B = \left(R_{em} + h_1\right) \hat{C} \qquad (2\text{-}27)$$

$$\vec{\rho}_B = \vec{R}_{sc} - \vec{C}_B \tag{2-24}$$

$$h_2 - h_1 \geq \vec{\rho}_B \cdot \frac{\vec{C}_B}{|\vec{C}_B|} \geq 0 \tag{2-25}$$

$$\hat{N}_i = \frac{\vec{C}_B \times \left(\hat{R}_i - \hat{R}_{i+1}\right)}{\left|\vec{C}_B \times \left(\hat{R}_i - \hat{R}_{i+1}\right)\right|} \quad i = 1,2,3,4 \tag{2-26a}$$

$$\hat{N}_5 = \frac{\vec{C}_B \times \left(\hat{R}_5 - \hat{R}_1\right)}{\left|\vec{C}_B \times \left(\hat{R}_5 - \hat{R}_1\right)\right|} \tag{2-26b}$$

$$d_i = \hat{N}_i \cdot \left(\hat{R}_i - \vec{C}_B\right) \qquad i = 1,2,3,4,5 \tag{2-15}$$

$$\hat{N}_i \cdot \vec{\rho}_B \leq d_i \qquad i = 1,2,3,4,5 \tag{2-16}$$

3.0 SEMIANALYTICAL ALGORITHM TO PREDICT AOS AND LOS TIMES

This section presents a semianalytic technique for predicting AOS and LOS times. This technique is designed to bound the actual visibility periods and uses a simplified geometry model in conjunction with unperturbed orbital motion. Its principal purpose is to reduce the burden on the precise numerical search by eliminating regions of the S/C orbit where AOS and LOS times are physically impossible.

The basic procedure consists of the following:

a. Determining the parameters of an outer boundary cone which circumscribes the entire area target or space volume.
b. Determining whether the orientation of the S/C orbit plane will permit any intersections of the outer boundary cone with the S/C orbit plane.
c. Assuming intersections are possible for the following:
    (1) Celestial-fixed targets
        (a) Compute the conic intersection points of the outer boundary cone with the S/C orbit plane.
        (b) Compute predictions of AOS and LOS times (t_{AOS_K} and t_{LOS_K}, respectively) for each revolution based upon these intersection points.
    (2) Earth-fixed targets
        (a) Compute the time of closest approach (TCA) of the S/C position vector with the centerline of the outer boundary cone and the corresponding closest approach angle (γ_{CA}). These computations are performed on a revolution-by-revolution basis.
        (b) If γ_{CA} is less than or equal to the half-cone angle of the outer boundary cone, then compute predictions of AOS and LOS times based upon the times when the S/C lies on the perimeter of the

outer boundary cone. These times are denoted by t_{AOS_K} and t_{LOS_K}.

After the AOS and LOS time predictions are determined, the precise numerical search (using the detailed area target and space volume geometry model discussed in sec. 2) can then be performed over the reduced time regions from t_{AOS_K} to t_{LOS_K}.

The following parameters are required to predict the AOS and LOS times:

t_{start} - start time for the search

t_{end} - end time for the search

Δt - time increment for the search. For the purposes of this algorithm, Δt will be used as a tolerance for converging upon the AOS and LOS times for Earth-referenced targets.

$\vec{R}_{sc_o}$ - S/C position vector in the M50 system at t_{start}.

$\vec{V}_{sc_o}$ - S/C velocity vector in the M50 system at t_{start}.

$[RNP]^{TEI}_{M50}$ - RNP matrix to transform from the M50 to the TEI system.

t_e - epoch time corresponding to the RNP matrix.

The following subsections provide the necessary equations. Section 3.1 discusses the computation of the outer boundary cone parameters. Section 3.2 discusses the technique to determine whether any AOS or LOS times are possible. Section 3.3 presents the equations to predict AOS and LOS times. Section 3.4 discusses the assumptions and limitations implicit in these equations.

Two reference coordinate systems are used in these computations. The M50 coordinate system is used when dealing with celestial-fixed targets and the TEI system is used for Earth-referenced

targets. The TEI system was selected for Earth-referenced targets in order to model the effects of polar nutation and precession on the Earth's spin axis.

For celestial-fixed targets, the M50 Keplerian elements (a, e, i, Ω, ω and M_o) at the start time will be computed from $\vec{R}_{sc_o}$ and $\vec{V}_{sc_o}$.

For Earth-referenced targets, the TEI Keplerian elements at the start time will be computed from $\vec{R}^{TEI}_{sc_o}$ and $\vec{V}^{TEI}_{sc_o}$. Where

$$\vec{R}^{TEI}_{sc_o} = [RNP]^{TEI}_{M50} \vec{R}_{sc_o} \tag{3-1}$$

$$\vec{V}^{TEI}_{sc_o} = [RNP]^{TEI}_{M50} \vec{V}_{sc_o} \tag{3-2}$$

3.1 COMPUTING OUTER BOUNDARY CONE PARAMETERS

The outer boundary cone is defined by

α_o - right ascension of the centerline

ϕ_o - latitude of the centerline

γ_A - half-cone angle

For Earth-referenced targets these parameters will be defined in the TEI system at t_{start}.[1] For celestial-fixed targets, these parameters will be defined in the M50 system and remain invariant with respect to time.

3.1.1 Earth-Referenced Circles

The unit vector along the centerline of the cone is given in the TEI system by

$$\hat{C}^{TEI} = \begin{bmatrix} \cos\Delta\lambda & -\sin\Delta\lambda & 0 \\ \sin\Delta\lambda & \cos\Delta\lambda & 0 \\ 0 & 0 & 1 \end{bmatrix}_G^{TEI} \frac{\vec{C}_B^G}{|\vec{C}_B^G|} \qquad (3\text{-}3)$$

where

$\vec{C}_B^G$ is given by equation 2-1

$\Delta\lambda$ is given by equation 2-5 with t equal to t_{start}

Thus, the right ascension and latitude of the centerline is given in the TEI system (at the start of the search) by

$$\alpha_o = \tan^{-1}\left\{\frac{C_y^{TEI}}{C_x^{TEI}}\right\} \qquad (3\text{-}4)$$

[1] The TEI system is selected for Earth-referenced targets in order to model the polar nutation and precession from M50 reference to the epoch time of the RNP matrix.

$$\phi_o = \sin^{-1} \left\{ C_z^{TEI} \right\} \tag{3-5}$$

where

$$\hat{C}^{TEI} \Rightarrow \left(C_x^{TEI}, C_y^{TEI}, C_z^{TEI} \right)$$

The half-cone angle, γ_A, is given by equation 2-6.

3.1.2 Celestial Circles

The right ascension, latitude, and half-cone angle in the M50 system are given via input

$$\alpha_o = \alpha_A \tag{3-6}$$

$$\phi_o = \delta_A \tag{3-7}$$

3.1.3 Earth-Referenced Polygons

The unit vector along the centerline of the outer boundary cone is given in the TEI system by equation 3-3 where equation 2-13 is used to compute $\vec{C}_B^G$. Equations 3-4 and 3-5 are then used to compute α_o and ϕ_o, respectively. The outer boundary cone is centered along the centroid vector and has an angular radius which contains the vertex furthest from the centroid vector (fig. 3-1). Thus, the half-cone angle is given by

$$\gamma_A = \max \left[\cos^{-1} \left\{ \frac{\vec{R}_i^G \cdot \vec{C}_B^G}{|\vec{R}_i^G| \; |\vec{C}_B^G|} \right\} \quad i = 1,2,3,\ldots n \right] \tag{3-8}$$

where

max implies the maximum algebraic value

$\vec{R}_i^G$ is given by equation 2-12.

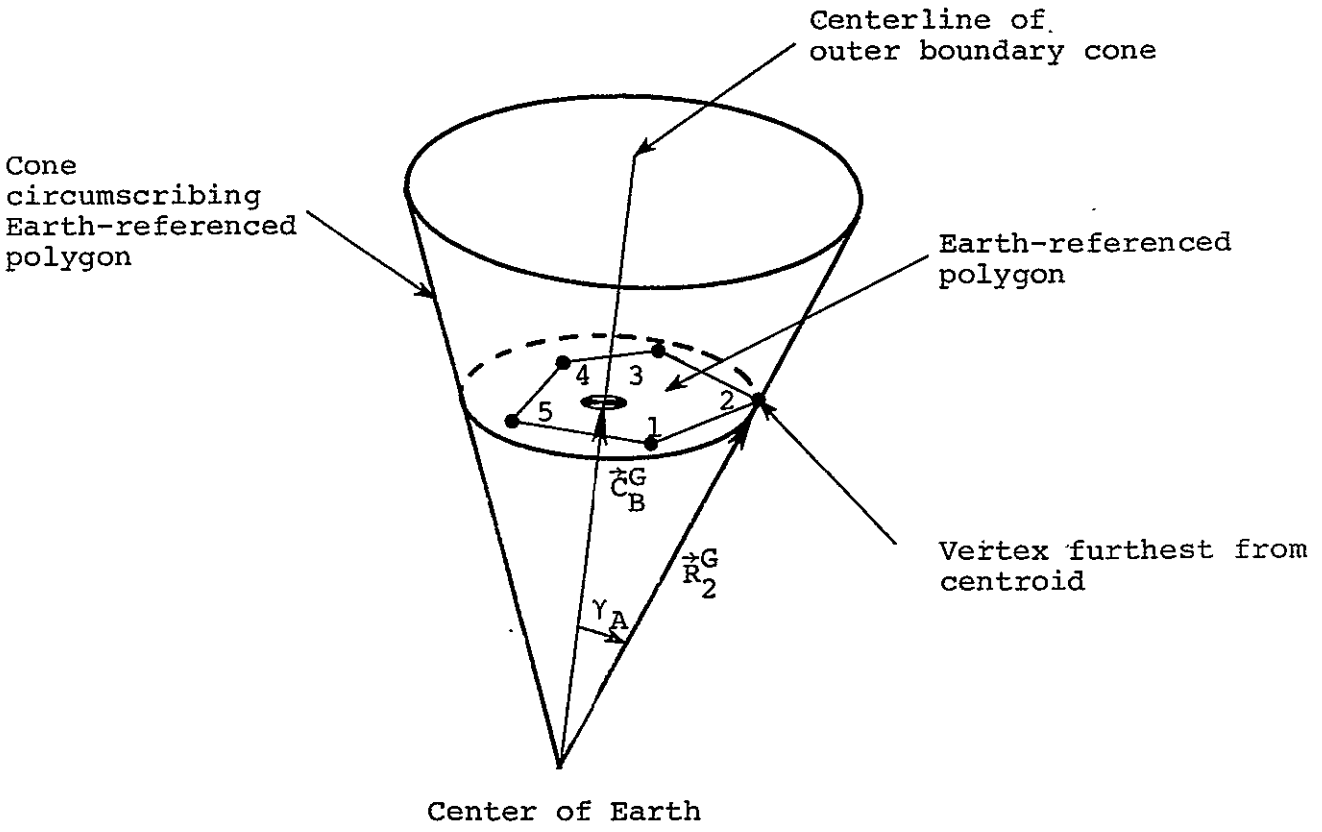

Figure 3-1.- Circumscribing polygons.

3.1.4 Celestial Polygons

The unit vector along the centerline of the celestial polygon is given by equation 2-19. Equations 3-4 and 3-5 (with $\hat{C}^{TEI}$ replaced by $\hat{C}$) are then used to compute α_o and ϕ_o, respectively. The half-cone angle which contains the vertex furthest from the centroid is given by

$$\gamma_A = \max \left[\cos^{-1} \left\{ \hat{R}_i \cdot \hat{C} \right\} \quad i = 1,2,3,\ldots n \right] \qquad (3\text{-}9)$$

where

$\hat{R}_i$ is given by equation 2-18.

3.1.5 Earth-Referenced Space Volumes

The unit vector along the centerline of the outer boundary cone for Earth-referenced space volumes is given by equation 3-3 with $\vec{C}_B^G$ replaced by $\vec{C}^G$ (eq. 2-22). Equations 3-4 and 3-5 are then used to compute α_o and ϕ_o, respectively. Since the Earth-referenced space volume represents a constant area polyhedron (sec. 2.5), the outer boundary cone to be used for predicting AOS and LOS times circumscribes the space volume planar area at the S/C altitude. However, for noncircular orbits, the S/C altitude varies as a function of time and thus the size of the outer boundary cone would also vary as a function of time. The size of the cone is largest at perigee and smallest at apogee. Since the purpose of the outer boundary cone is to bound the actual visibility region, the half-cone angle at the S/C perigee altitude will be computed and held constant with respect to time. The vector from the center of the Earth to each vertex of the space volume projected to the S/C perigee altitude, $\vec{R}_i^{G'}$, (fig. 3-2) is given by

$$\vec{R}_i^{G'} = \vec{R}_i^G + \left[R_p - |\vec{C}_B^G| \right] \frac{\vec{C}_B^G}{|\vec{C}_B^G|} \qquad i = 1,2,3,\ldots n \quad (3\text{-}10)$$

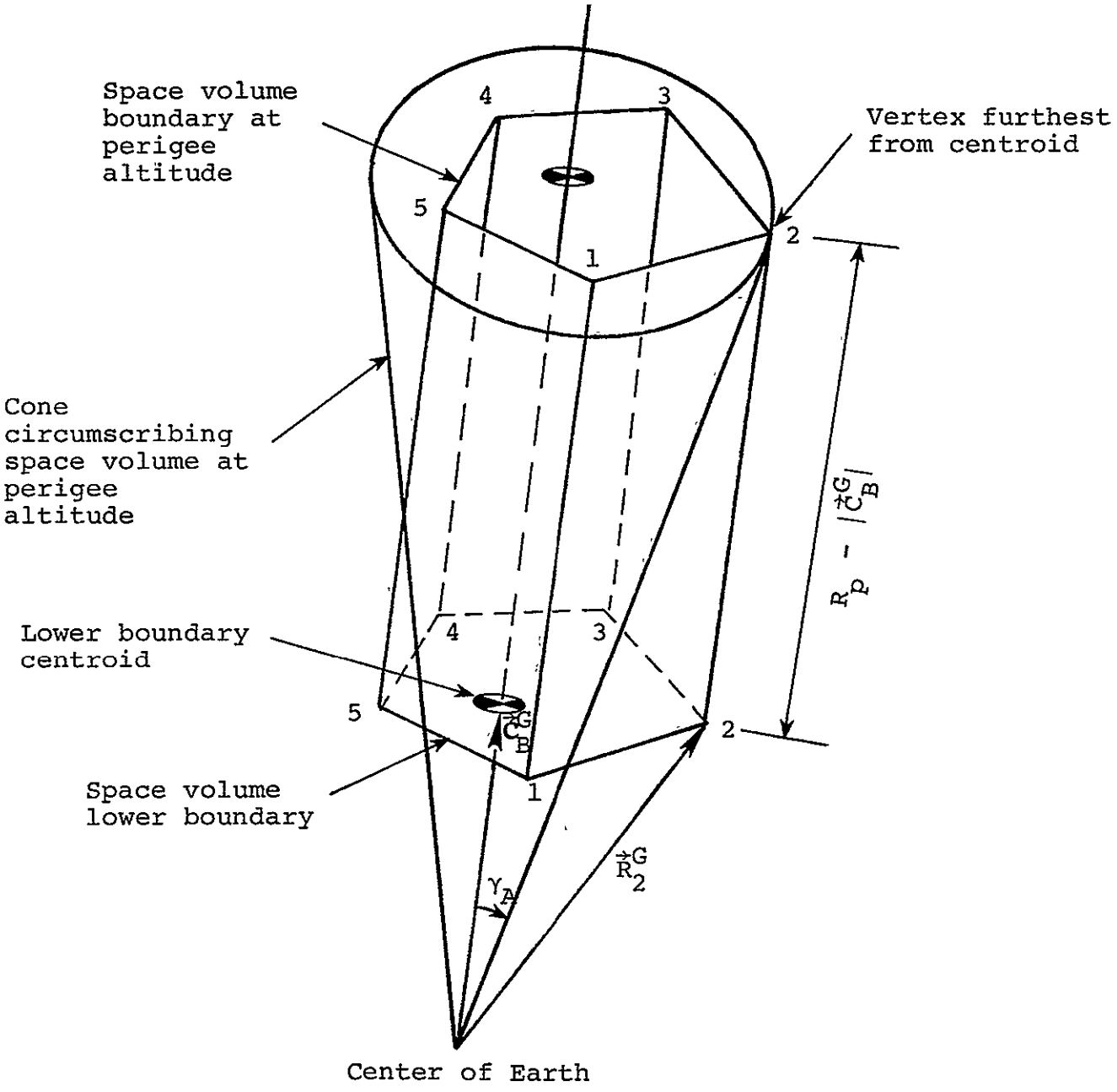

Figure 3-2.- Circumscribing space volumes.

where

$\vec{R}_i^G$ is given by equation 2-12

$\vec{C}_B^G$ is given by equation 2-23

R_p is the S/C perigee radius

$= a(1 - e)$ (3-11)

Thus the half-cone angle which contains the vertex furthest from the centerline of the cone is given by

$$\gamma_A = \max \left[\cos^{-1} \left\{ \frac{\vec{R}_i^{G'} \cdot \vec{C}_B^G}{|\vec{R}_i^{G'}| \; |\vec{C}_B^G|} \right\} \quad i = 1,2,3,\ldots n \right] \qquad (3\text{-}12)$$

3.1.6 Celestial-Fixed Space Volumes

The unit vector along the centerline of the outer boundary cone for celestial-fixed space volumes is given by equation 2-19. Equations 3-4 and 3-5 (with $\hat{C}^{TEI}$ replaced by $\hat{C}$) are then used to compute α_o and ϕ_o, respectively. Since the celestial-fixed space volume also represents a constant area polyhedron (sec. 2.6), the outer boundary cone to be used for predicting AOS and LOS times circumscribes the space volume planar area at the S/C perigee altitude (sec. 3.1.5). The vector from the center of the Earth to each vertex of the space volume at the S/C perigee altitude, $\vec{R}_i'$, is given by

$$\vec{R}_i' = \hat{R}_i + \left[R_p - |\vec{C}_B| \right] \hat{C} \qquad (3\text{-}13)$$

where

$\hat{R}_i$ is given by equation 2-18

$\vec{C}_B$ is given by equation 2-27

R_p is the S/C perigee radius (equation 3-11)

Thus

$$\gamma_A = \max \left[\cos^{-1} \left\{ \frac{\vec{R}_i'}{|\vec{R}_i'|} \cdot \hat{C} \right\} \quad i = 1,2,3,\ldots n \right] \qquad (3\text{-}14)$$

3.2 DETERMINING WHETHER AOS AND LOS TIMES ARE POSSIBLE

The following computations will determine whether the relative orientation of the S/C orbit plane and the outer boundary cone will permit any intersections between these two figures. If no intersections are possible, then no AOS or LOS times are possible. Since the Earth-referenced targets rotate with the Earth and the celestial-fixed targets remain inertially fixed, two different types of tests are required. The celestial-fixed situation is the simplest and is discussed first.

3.2.1 Celestial-Fixed Targets

Figure 3-3 illustrates a celestial-fixed outer boundary cone and a S/C orbit plane. The S/C orbit plane is perpendicular to the unit angular momentum vector which is given by

$$\hat{h} = \frac{\vec{R}_{sc_o} \times \vec{V}_{sc_o}}{|\vec{R}_{sc_o} \times \vec{V}_{sc_o}|} \tag{3-15}$$

where

$\vec{R}_{sc_o}$ and $\vec{V}_{sc_o}$ are the S/C position and velocity vectors, respectively, in the M50 system at the beginning of the search.

The centerline of the outer boundary cone, $\hat{C}$, is given in the M50 system by

$$\hat{C} = \begin{Bmatrix} \cos \alpha_o \cos \phi_o \\ \sin \alpha_o \cos \phi_o \\ \sin \phi_o \end{Bmatrix} \tag{3-16}$$

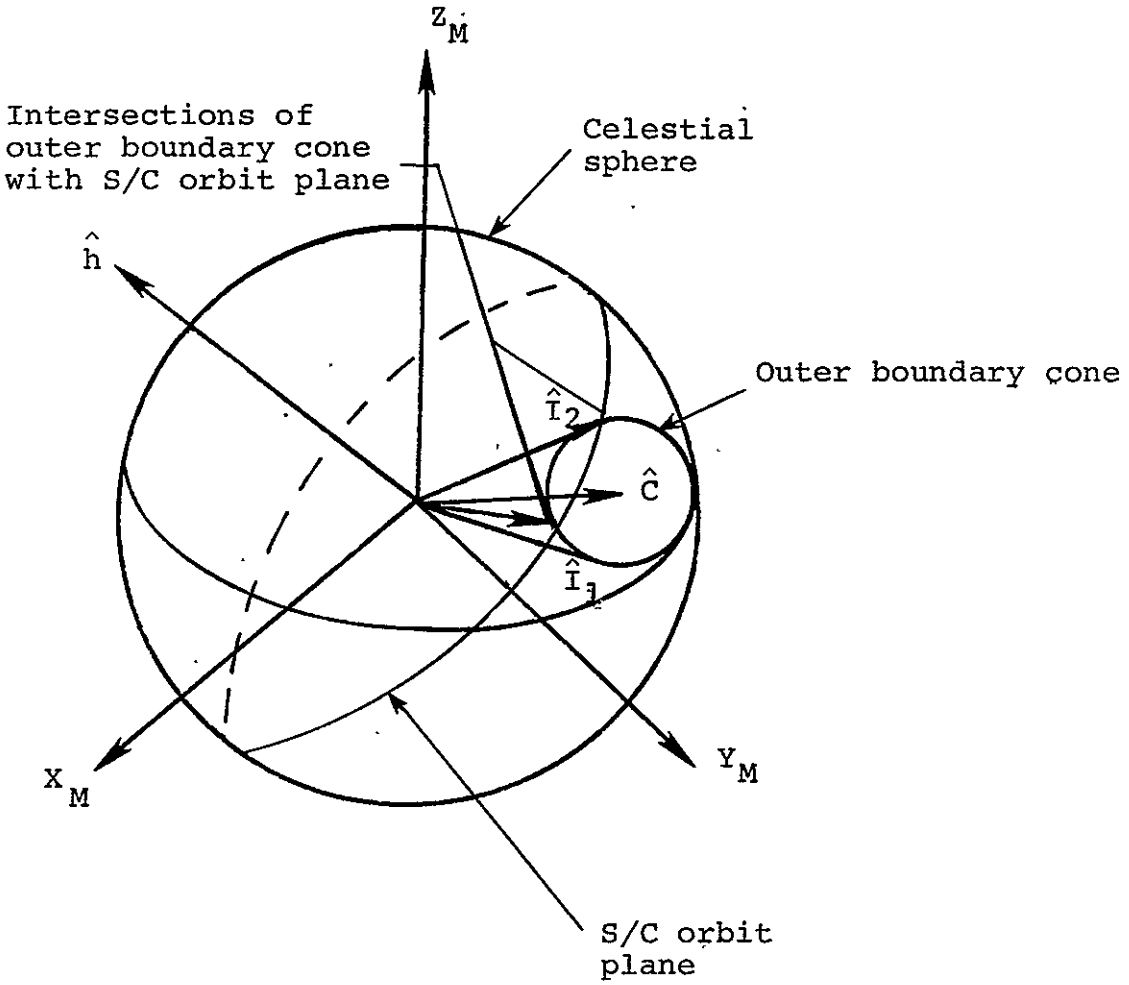

Figure 3-3.- Intersection of celestial-fixed outer boundary cone with S/C orbit plane.

where

α_o and ϕ_o were computed using the procedure discussed in section 3.1.

The intersection points of the outer boundary cone with the S/C orbit plane are denoted by $\hat{I}_1$ and $\hat{I}_2$ on figure 3-3. These vectors can be found by solving the following conic intersection equations[1]

$$\hat{h} \cdot \hat{I} = 0 \qquad (3\text{-}17a)$$

$$\hat{C} \cdot \hat{I} = \cos \gamma_A \qquad (3\text{-}17b)$$

$$\hat{I} \cdot \hat{I} = 1 \qquad (3\text{-}17c)$$

These equations provide 0, 1, or 2 solutions for $\hat{I}$. If no solutions are produced, then the relative orientation of the outer boundary cone and the S/C orbit plane does not permit intersections, and no AOS or LOS times are possible. If only one solution is produced, the AOS and LOS times are the same. If two solutions are produced, the AOS and LOS times predictions are made using the method outlined in section 3.3.

[1]The method for solving these equations is presented in appendix B.

3.2.2 Earth-Referenced Targets

Figure 3-4 illustrates an Earth-referenced outer boundary cone at a particular instant of time. This cone rotates about the Earth's polar axis. Hence, over one sidereal day, the volume of space swept out by the outer boundary cone describes a spherical sector whose upper and lower limits are determined by γ_A and ϕ_o (fig. 3-5). Intersections of the S/C orbit plane with this volume of space are possible only if the S/C orbit inclination exceeds the lower limit of the spherical sector.

For posigrade and polar orbits, the S/C orbit plane will intersect the spherical sector only if[1]

$$i \geq |\phi_o| - \gamma_A \qquad (3\text{-}18a)$$

For retrograde orbits, intersections are possible only if[1]

$$180 - i \geq |\phi_o| - \gamma_A \qquad (3\text{-}18b)$$

where

i is the S/C orbit inclination in the TEI system

If equation 3-18 is not satisfied, then no intersections are possible and thus no AOS or LOS times are possible. If equation 3-18 is satisfied, then the approach presented in section 3.3 is used to predict AOS and LOS times.

[1]The absolute value sign is used in these equations to accommodate targets in both the northern and southern hemispheres.

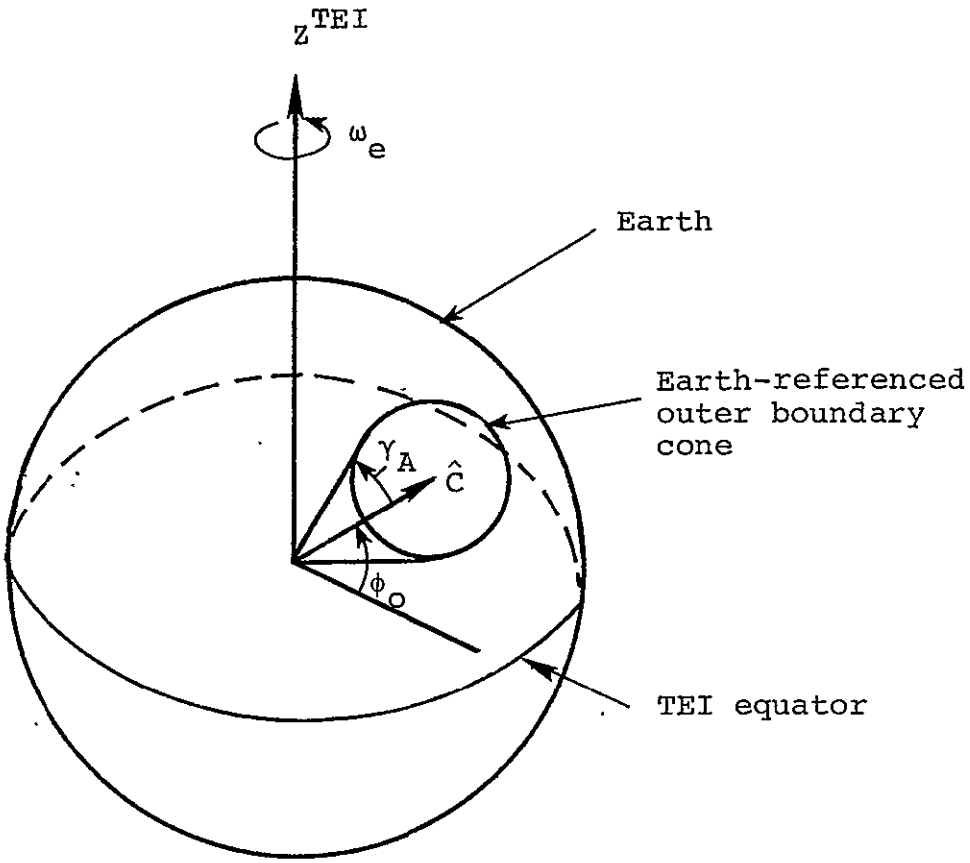

Figure 3-4.- Earth-referenced outer boundary cone.

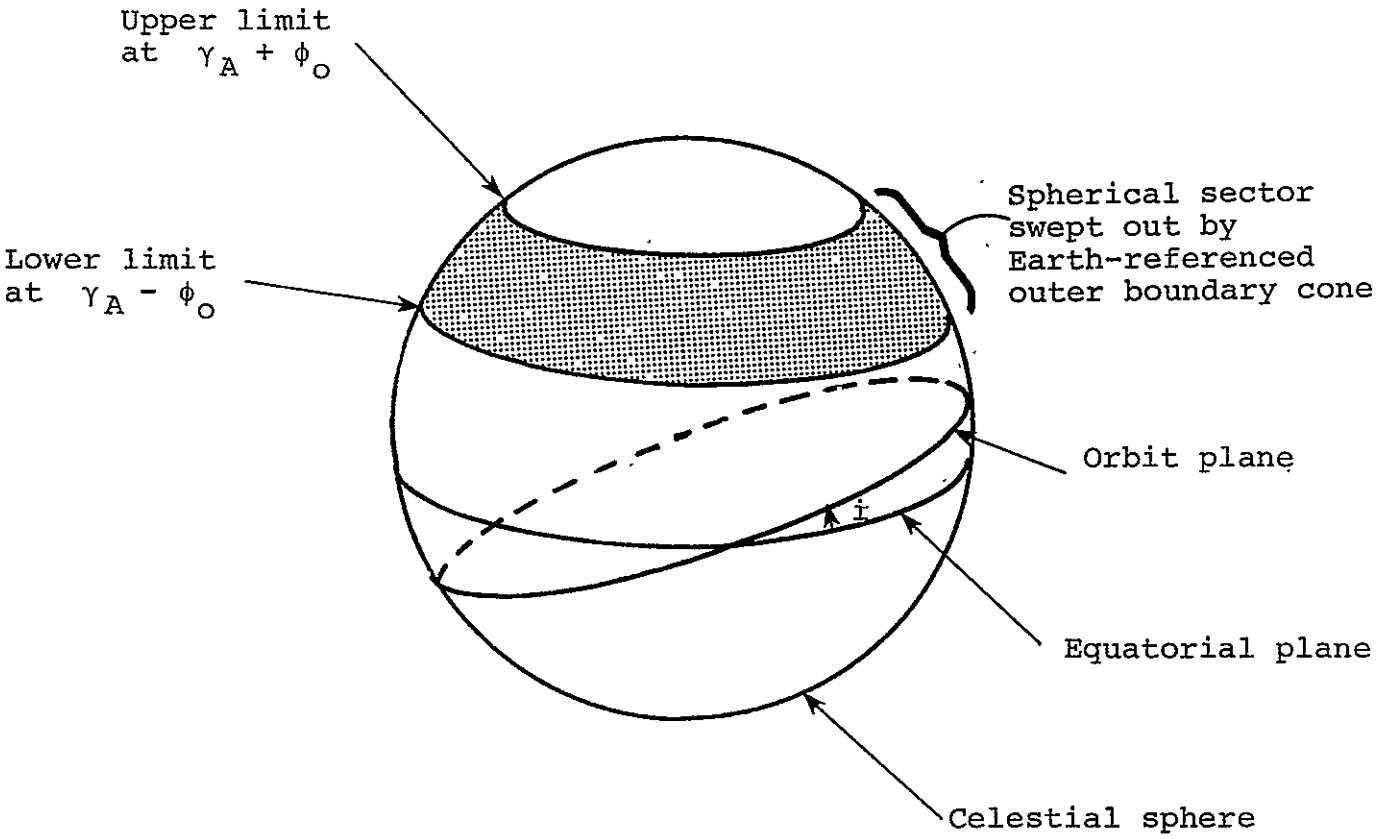

Figure 3-5.- Spherical sector swept out by Earth-referenced outer boundary cone.

3.3 PREDICTING AOS AND LOS TIMES

The following subsections present the equations necessary to predict AOS and LOS times for celestial-fixed and Earth-referenced targets. These equations assume that the tests performed in section 3.2 have indicated that intersections of the outer boundary cone with the S/C orbit plane are possible.

3.3.1 Celestial-Fixed Targets

The intersection vectors, $\hat{I}_1$ and $\hat{I}_2$ (sec. 3.2.1), can be used directly to predict the AOS and LOS times. Figure 3-6 illustrates the geometry. The unit vector in the direction of the ascending node, $\hat{\Omega}$, is given by

$$\hat{\Omega} = \begin{Bmatrix} \cos \Omega \\ \sin \Omega \\ 0 \end{Bmatrix} \qquad (3\text{-}19)$$

where

Ω = right ascension of the ascending node in the M50 system

The angles between $\hat{\Omega}$ and the two intersection vectors are given by

$$u_1 = \tan^{-1}\left\{\frac{\hat{h} \cdot (\hat{\Omega} \times \hat{I}_1)}{\hat{\Omega} \cdot \hat{I}_1}\right\} \qquad (3\text{-}20a)$$

$$u_2 = \tan^{-1}\left\{\frac{\hat{h} \cdot (\hat{\Omega} \times \hat{I}_2)}{\hat{\Omega} \cdot \hat{I}_2}\right\} \qquad (3\text{-}20b)$$

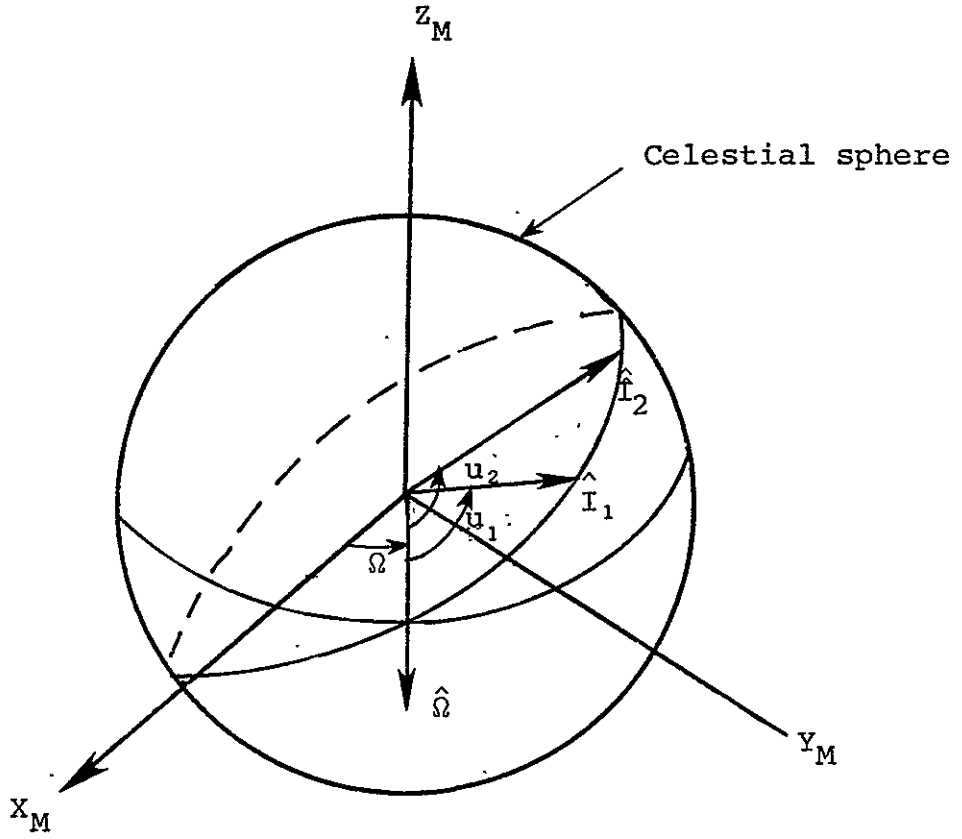

Figure 3-6.- Definition of intersection points.

One of these angles corresponds to the AOS point and the other to the LOS point. The appropriate angle can be determined by noting that the visibility period must be less than or equal to one half of the orbit.

Thus let

$$K = \tan^{-1}\left\{\frac{\hat{h} \cdot (\hat{I}_1 \times \hat{I}_2)}{\hat{I}_1 \cdot \hat{I}_2}\right\} \tag{3-21}$$

If $K \geq 0$

$$u_{AOS} = u_1 \tag{3-22a}$$

$$u_{LOS} = u_2 \tag{3-23a}$$

If $K < 0$

$$u_{AOS} = u_2 \tag{3-22b}$$

$$u_{LOS} = u_1 \tag{3-23b}$$

The true anomalies of the AOS and LOS points are given by

$$f_{AOS/LOS} = u_{AOS/LOS} - \omega \tag{3-24}$$

where

ω is the argument of perigee of the S/C orbit.

These can be converted to AOS and LOS times by

$$t_{AOS/LOS} = \frac{M_{AOS/LOS}}{\dot{M}} + \tau \tag{3-25}$$

where

$$M_{AOS/LOS} = E_{AOS/LOS} - e \sin E_{AOS/LOS} \tag{3-26}$$

$$E_{AOS/LOS} = 2 \tan^{-1} \left\{ \sqrt{\frac{1 - e}{1 + e}} \tan \left(\frac{f_{AOS/LOS}}{2} \right) \right\} \qquad (3\text{-}27)$$

$$\dot{M} = \frac{360}{T} \quad \text{(in degrees per unit of time)} \qquad (3\text{-}28)$$

$$T = 2 \pi \sqrt{\frac{a^3}{\mu}} \qquad (3\text{-}29)$$

$$\tau = t_{start} - \frac{M_o}{\dot{M}} + (R - 1) T \qquad (3\text{-}30)$$

R is the revolution number measured with respect to t_{start}

a is the semimajor axis of the S/C orbit

e is the eccentricity of the S/C orbit

M_o is the S/C mean anomaly at t_{start}

μ is the gravitational constant

Since both the orbit plane and the celestial-fixed target remain inertially fixed, u_{AOS} and u_{LOS} remain constant. Thus, the AOS and LOS times for future revolutions differ by only the orbital period. The AOS and LOS times for the subsequent N revolutions are given by

$$t_{AOS/LOS_{K+1}} = t_{AOS/LOS_K} + T \qquad K = 1,2,3...N \qquad (3\text{-}31)$$

3.3.2 Earth-Referenced Targets

Computation of AOS and LOS times for Earth-referenced targets is somewhat more complicated than for celestial-fixed targets since the orientation of the Earth-referenced target varies as a function of time. The following procedure will be used to estimate the AOS and LOS times:

a. The TCA of the center of the Earth-referenced outer boundary cone with the S/C position vector will be determined along with the corresponding closest approach angle, γ_{CA}. These computations will be performed on a revolution-by-revolution basis.

b. The closest approach angle from the previous step will be compared with γ_A. If $\gamma_{CA} > \gamma_A$, then no AOS or LOS times are possible for that revolution, and the previous step will be repeated for the next revolution. If $\gamma_{CA} \leq \gamma_A$, then AOS and LOS times will be computed by solving for the times when the angle between the center of the outer boundary cone and the S/C position vector is equal to γ_A.

3.3.2.1 Determining TCA

The closest approach point occurs when the S/C position vector and the center of the outer boundary cone lie in the same hemisphere and are coplanar (fig. 3-7). Both the S/C and the center of the outer boundary cone are moving with time. The center of the cone is rotating about the Earth's Z axis at the Earth's rotation rate. The S/C is moving about the orbit angular momentum vector at a rate which is dependent upon both the orbit period and eccentricity. As a result, the TCA cannot be analytically determined for noncircular/nonequatorial orbits. The TCA can, however, be determined iteratively by the following:

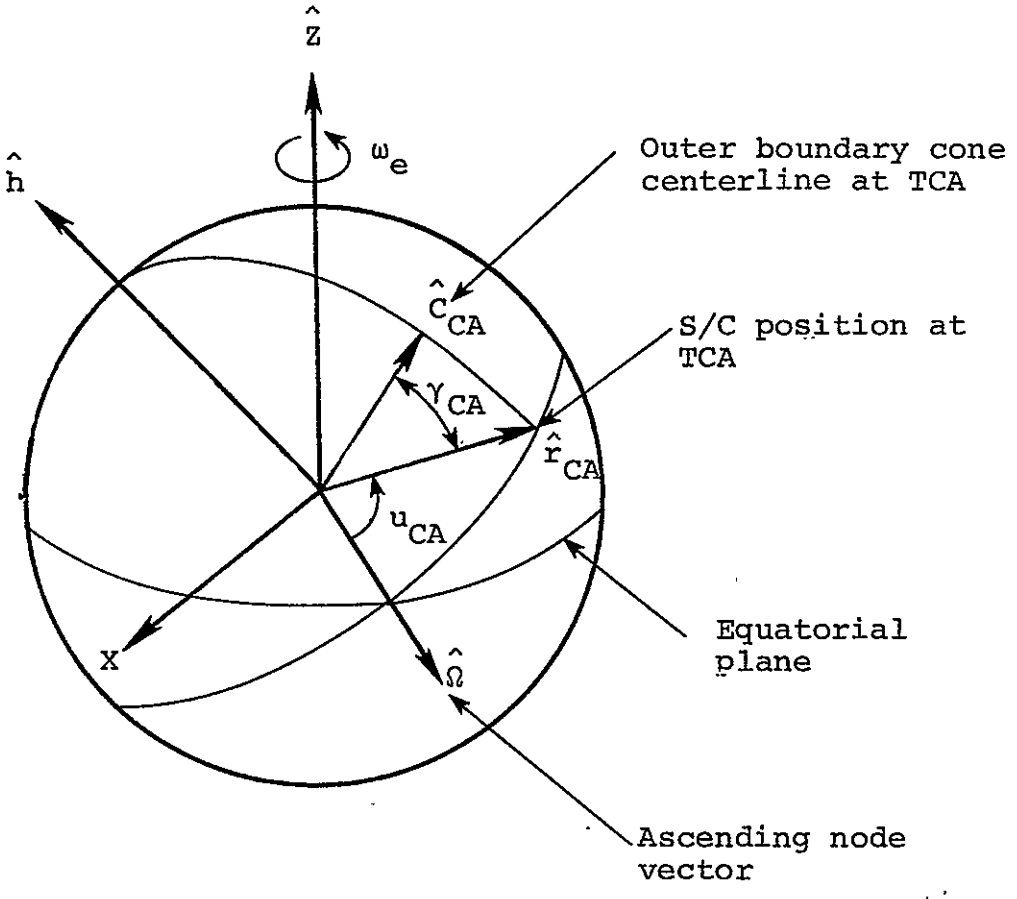

Figure 3-7.- Closest approach point.

a. Estimating the closest approach point (for the first revolution, this estimate would be based upon t_{start}; for subsequent revolutions, this estimate would be based upon the TCA of the previous revolution plus one orbital period).

b. Determining the time at which the S/C will reach this point.

c. Updating the closest approach point based upon the time estimate from the previous step.

d. Repeating the two previous steps until the difference in time between two successive iterations is less than or equal to the time step, Δt.

The following discussion develops the equations necessary to compute the TCA.

The unit vector from the center of the Earth to the center of the outer boundary cone is given by

$$\hat{C} = \begin{Bmatrix} \cos \alpha \cos \phi_o \\ \sin \alpha \cos \phi_o \\ \sin \phi_o \end{Bmatrix} \tag{3-32}$$

where

$$\alpha = \alpha_o + \omega_e (t - t_{start}) \tag{3-33}$$

α_o is the initial right ascension of the centerline (sec. 3.1)

ω_e is the Earth rotation rate

ϕ_o is the latitude of the centerline (sec. 3.1)

The closest approach point, $\hat{r}_{CA}$, occurs when

$$\hat{r}_{CA} = \frac{\hat{h} \times \hat{C}}{|\hat{h} \times \hat{C}|} \times \hat{h} \qquad (3\text{-}34)$$

where $\hat{h}$ is the angular momentum vector in the TEI system (computed via eq. 3-15 using $R_{sc_o}^{TEI}$ and $V_{sc_o}^{TEI}$ from eqs. 3-1 and 3-2).

The angle from the ascending node to this point, u_{CA}, is given by

$$u_{CA} = \tan^{-1} \left\{ \frac{\hat{h} \cdot (\hat{\Omega} \times \hat{r}_{CA})}{\hat{\Omega} \cdot \hat{r}_{CA}} \right\}$$

which can be simplified to

$$u_{CA} = \tan^{-1} \left\{ \frac{\hat{h} \cdot (\hat{\Omega} \times \hat{C})}{\hat{\Omega} \cdot \hat{C}} \right\} \qquad (3\text{-}35)$$

where $\hat{\Omega}$ is computed by equation 3-19 using the right ascension of the ascending node in the TEI system.

The TCA, t_{CA}, is then given by

$$f_{CA} = u_{CA} - \omega \qquad (3\text{-}36)$$

$$E_{CA} = 2 \tan^{-1} \left\{ \sqrt{\frac{1-e}{1+e}} \tan \left(\frac{f_{CA}}{2} \right) \right\} \qquad (3\text{-}37)$$

$$M_{CA} = E_{CA} - e \sin E_{CA} \qquad (3\text{-}38)$$

$$t_{CA} = \frac{M_{CA}}{\dot{M}} + \tau \qquad (3\text{-}39)$$

where

τ is given by equation 3-30

$\dot{M}$ is given by equation 3-28

e is the orbit eccentricity

ω is the argument of perigee

This time would then be used in equations 3-32 and 3-33 to update the value of $\hat{C}$. Equations 3-35 through 3-39 would be repeated until the value of t_{CA} between two successive iterations is less than or equal to the time step, Δt. After the TCA has been found, the corresponding closest approach angle, γ_{CA}, would be computed.

The unit vector from the center of the Earth to the S/C is given by

$$\hat{r} = \begin{Bmatrix} \cos \Omega \cos u - \sin \Omega \sin u \cos i \\ \sin \Omega \cos u + \cos \Omega \sin u \cos i \\ \sin u \sin i \end{Bmatrix} \qquad (3\text{-}40)$$

The closest approach angle is given by

$$\gamma_{CA} = \cos^{-1} \left\{ \hat{r}_{CA} \cdot \hat{C}_{CA} \right\} \qquad (3\text{-}41)$$

where

$\hat{r}_{CA}$ is given by equation 3-40 evaluated at u_{CA}

$\hat{C}_{CA}$ is given by equations 3-32 and 3-33 evaluated at t_{CA}.

If γ_{CA} is greater than the outer boundary cone angle, γ_A (sec. 3.1), then no AOS or LOS times are possible for this revolution. In this event, the procedure outlined is repeated for the next revolution. The initial estimate of TCA for the next revolution would be equal to the TCA for the current revolution plus one orbital period. The process continues until either $\gamma_{CA} \leq \gamma_A$ or the TCA exceeds the end time of the search, t_{end}. If $\gamma_{CA} \leq \gamma_A$, estimates of AOS and LOS times are made using the method outlined in section 3.3.2.2.

3.3.2.2 Determining AOS and LOS Times

After a feasible TCA has been found, the AOS and LOS times can be computed by solving the following equations.

$$\hat{r} \cdot \hat{C} = \cos \gamma_A \tag{3-42}$$

Substituting equations 3-40 and 3-32 into this expression and simplifying yields

$$\cos (\Omega - \alpha) \cos \phi_o \cos u - \sin (\Omega - \alpha) \cos \phi_o \cos i \sin u + \sin \phi_o \sin i \sin u = \cos \gamma_A \tag{3-43}$$

Equation 3-43 cannot be explicitly solved for time for noncircular/nonequatorial orbits. However, this equation can be solved numerically using the method of successive substitution. For convenience, equation 3-43 can be rewritten as

$$A_1 \cos u + B_1 \sin u = C_1 \tag{3-44}$$

where

$$A_1 = \cos \phi_o \cos (\Omega - \alpha) \tag{3-45}$$

$$B_1 = \sin \phi_o \sin i - \cos \phi_o \cos i \sin (\Omega - \alpha) \tag{3-46}$$

$$C_1 = \cos \gamma_A \tag{3-47}$$

Assuming α is constant between iterations, equation 3-44 has the following solution

$$u_{AOS/LOS} = \tan^{-1}\left\{\frac{B_1}{A_1}\right\} \pm \cos^{-1}\left\{\frac{C_1}{\sqrt{A_1^2 + B_1^2}}\right\} \qquad (3\text{-}48)$$

The minus sign will produce AOS solutions and the plus sign will produce LOS solutions. The procedure is as follows:

a. Solving for AOS times, t_{AOS}

(1) Use initial estimate of $t_{AOS} = t_{CA}$.

(2) Compute A_1, B_1, and C_1 using equations 3-33, 3-45, 3-46, and 3-47.

(3) Compute u_{AOS} using equation 3-48 with the minus sign.

(4) Compute revised estimate of AOS time using equations 3-24 through 3-30.

(5) If the change in time from the previous iteration is less than Δt, then a solution has been found. Otherwise, repeat steps (2) through (5) with the revised time estimate.

b. Solving for LOS time, t_{LOS}

The solution for LOS time is similar to the procedure for AOS time except that

(1) The initial estimate of LOS time in step a(1) is given by

$$t_{LOS} = t_{CA} + (t_{CA} - t_{AOS}) \qquad (3\text{-}49)$$

(2) u_{LOS} is computed in step a(3) by using equation 3-48 with the plus sign.

(3) The revised estimate of LOS time is produced in step a(4).

The computations discussed in this section are performed for each revolution in which γ_{CA} was found to be less than or equal to γ_A. In the special case where γ_{CA} is exactly equal to γ_A, the AOS and LOS times are identical and equal to the TCA. Hence computation of AOS and LOS times can be bypassed.

3.4 ASSUMPTIONS AND LIMITATIONS

The following assumptions are implicit in the equations presented in sections 3.1 through 3.3.

a. Unperturbed orbital motion over the time period $t_{end} \geq t \geq t_{start}$.

b. The effects of polar nutation and precession from t_e to t_{end} can be neglected.

4.0 FUNCTIONAL OVERVIEW OF AOS AND LOS TIME COMPUTATIONS

This section provides a functional overview of the ATSVP. The overall procedure for determining precise AOS and LOS times is presented and discussed. The basic procedure consists of predicting the AOS and LOS times using the algorithm presented in section 3 and then refining these predictions by performing a sequential time search using the equations presented in section 2.

The AOS times are defined to be the time point at which the S/C first enters the area target or space volume. If the S/C lies within the area target or space volume at the beginning of the user-specified search period (t_{start}), the first AOS time will be set equal to the start time. LOS times are defined to be the last time point prior to the S/C exiting the area target or space volume. If the S/C lies within the area target or space volume at the end of the user-specified search period (t_{end}), then the last LOS time will be set equal to the end time. It should be noted that the time increment used to perform the sequential time search will limit the accuracy and resolution of the AOS and LOS times (e.g., if the time increment is 1 minute, this implies that the AOS and LOS times will be determined to the nearest minute and that visibility periods of less than 1 minute may be skipped).

The area targets and space volumes defined in section 1 fall into two general categories:

a. Earth-referenced which include
   (1) Earth-referenced circles.
   (2) Earth-referenced polygons.
   (3) Earth-referenced space volumes.
b. Celestial-fixed which include
   (1) celestial-fixed circles.
   (2) celestial-fixed polygons.
   (3) celestial-fixed space volumes.

The logic for computing the AOS and LOS times for each of these categories is presented in the following subsections.

4.1 EARTH-REFERENCED AREA TARGETS AND SPACE VOLUMES

Figure 4-1 provides a functional flowchart for the Earth-referenced area targets and space volumes. The required inputs are

a. Target table (either the ground target, ground polygon, or ground-fixed space volume table).
b. Target ID.
c. Start and end times and time increment (t_{start}, t_{end}, and Δt, respectively).
d. S/C ephemeris and ephemeris ID.
e. RNP matrix and associated epoch time.

A brief description of the process is provided herein. The heading numbers correspond to the numbered blocks on figure 4-1.

1. The geodetic parameters defining the area target or space volume are obtained from the appropriate target table based upon the input target ID. Sections 2.1.2, 2.3.2, and 2.5.2 describe the specific parameters which are required.
2. The RNP matrix and its associated epoch time are obtained.
3. The geodetic coordinates of the area target or space volume are transformed to the rotating geocentric coordinate system (secs. 2.1.2, 2.3.2, and 2.5.2).
4. The number of visibility periods between t_{start} and t_{end} are determined along with predictions of AOS and LOS times. Section 3 describes this process.
5. A test is performed to determine whether any visibility periods were found. If this test is failed, then no AOS/LOS times are possible and processing is terminated.
6. A loop is established which will process each visibility period found in step 4.

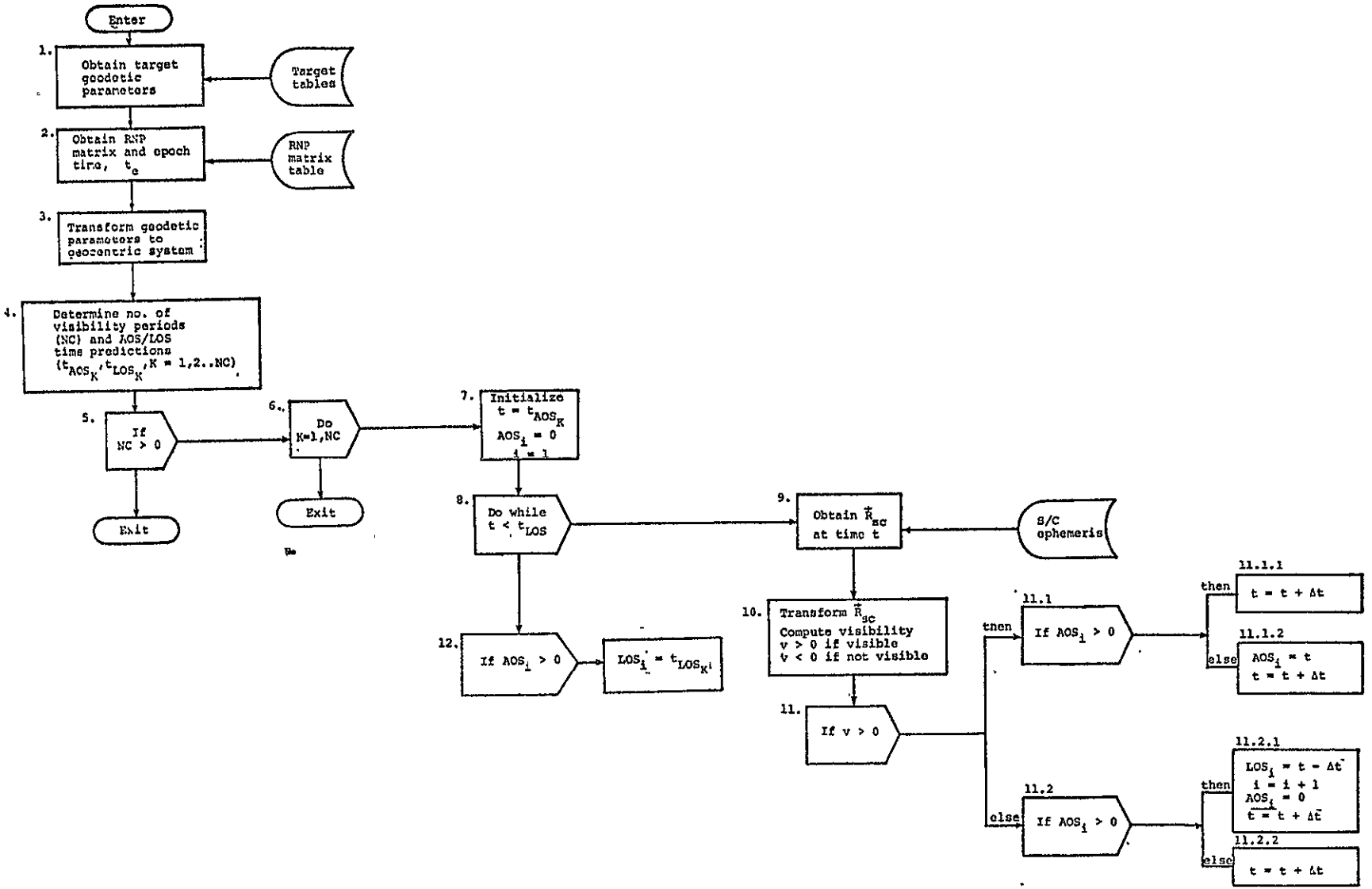

Figure 4-1.- Functional flow for Earth-referenced area targets and space volumes.

7. The current time, t, is initialized to the AOS time prediction, t_{AOS_K}. The initial value of the precise AOS time, AOS_1, is set to zero. The AOS/LOS counter, i, is initialized to one.[1]
8. A loop is established which will terminate when t exceeds the LOS time prediction, t_{LOS_K}.
9. The S/C position vector (at time t in the M50 system) is obtained from the ephemeris file based upon the ephemeris ID.
10. The S/C position vector is transformed to the rotating geocentric system and computations are performed to determine whether the S/C lies within the area target or space volume (secs. 2.1.2, 2.3.2, 2.5.2, and app. A).

    Based upon the results of these tests, the S/C visibility parameter, V, is set

    $V > 0$ if the S/C lies within the area target or space volume

    $V < 0$ if the S/C lies exterior to the area target or space volume
11. A test is performed on V.

    If $V > 0$

    11.1 a further test is performed on AOS_i to determine whether the S/C was also visible during one or more of the previous time steps.

    If $AOS_i > 0$

    11.1.1 then the S/C was visible during one or more of the previous time steps. Hence, no transi-

[1] Depending upon the target geometry and the S/C groundtrack, multiple AOS/LOS times could occur during a single visibility period.

tion has occurred. The current time is incremented by Δt and the search continues.

If $AOS_i \leq 0$

11.1.2 then a transition into the area target or space volume has occurred. The current AOS time, AOS_i, is set equal to the current time. The current time is incremented by Δt and the search continues.

If $V < 0$

11.2 a further test is performed on AOS_i to determine whether the S/C was visible during the previous time step.

If $AOS_i > 0$

11.2.1 then the S/C was visible during the previous time step and a transition out of the area target or space volume has occurred. The current LOS time, LOS_i, is set equal to the time of the previous time step ($t - \Delta t$). The AOS/LOS counter, i, is incremented by one. The next AOS time is initialized to zero. The current time is incremented by Δt and the search continues.

11.2.2 the S/C was not visible during the preceding time step. Thus no transition has occurred. The current time is incremented by Δt and the search continues.

12. At the completion of the sequential time search, a test is made to determine whether the S/C was visible at the end time. If the test is true, the last LOS time is set equal to t_{LOS_K}.

4.2 CELESTIAL-FIXED AREA TARGETS AND SPACE VOLUMES

Figure 4-2 illustrates the logic flow for the celestial-fixed area targets and space volumes. This logic is similar to the approach presented in section 4.1. The required inputs are

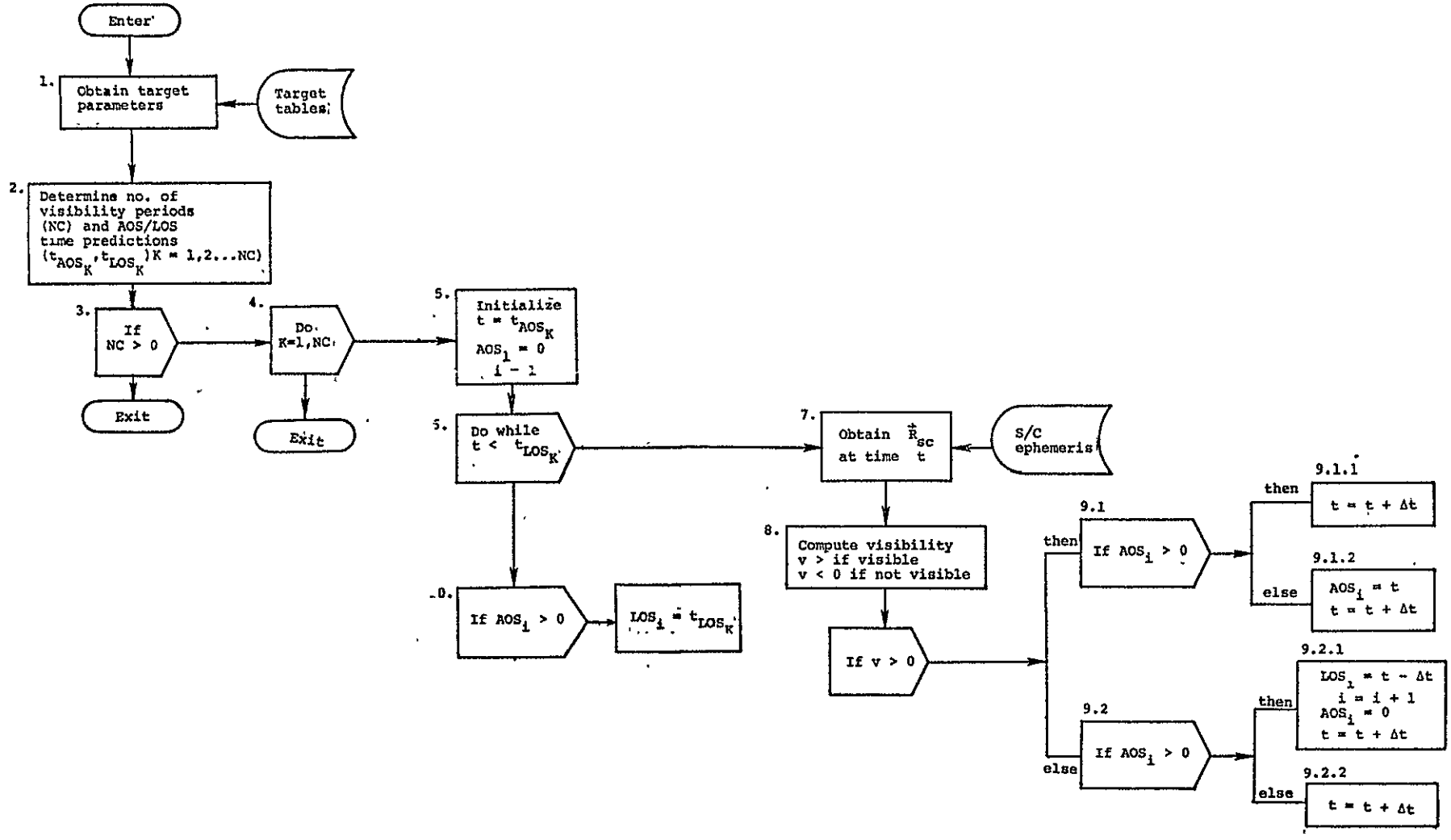

Figure 4-2.- Functional flow for celestial-fixed area targets and space volumes.

a. Target table (either celestial circles, celestial polygons, or celestial-fixed space volumes table).
b. Target ID.
c. Start and end times and time increment (t_{start}, t_{end}, and Δt, respectively).
d. S/C ephemeris and ephemeris ID.

A brief description of the process is provided herein. The heading numbers correspond to the numbered blocks on figure 4-2.

1. The parameters defining the celestial-fixed area target or space volume are obtained from the appropriate target table based upon the input target ID. Sections 2.2.2, 2.4.2, and 2.6.2 describe the specific parameters which are required.

2. The number of visibility periods between t_{start} and t_{end} are determined along with predictions of AOS and LOS times. Section 3 describes this process.

3. A test is performed to determine whether any visibility periods were found. If this test is failed, then no AOS/LOS times are possible and processing is terminated.

4. A loop is established which will process each visibility period found in step 2.

5. The current time, t, is initialized to the AOS time prediction, t_{AOS_K}. The initial value of the precise AOS time, AOS_1, is set to zero. The AOS/LOS counter, i, is initialized to one.[1]

6. A loop is established which will terminate when t exceeds the LOS time prediction, t_{LOS_K}.

7. The S/C position vector (at time t in the M50 system) is obtained from the ephemeris file based upon ephemeris ID.

8. Computations are performed to determine whether the S/C lies within the area target or space volume (secs. 2.2.2, 2.4.2,

[1] Depending upon the target geometry and the S/C groundtrack, multiple AOS/LOS times could occur during a single visibility period.

2.6.2, and app. A). Based upon the results of these tests, the S/C visibility parameter, V, is set

V > 0 if the S/C lies within the area target or space volume

V < 0 if the S/C lies exterior to the area target or space volume

9. A test is performed on V.

If V > 0

9.1 a further test is performed on AOS_i to determine whether the S/C was also visible during one or more of the previous time steps.

If $AOS_i > 0$

9.1.1 then the S/C was visible during one or more of the previous time steps. Hence, no transition has occurred. The current time is incremented by Δt and the search continues.

If $AOS_i \leq 0$

9.1.2 then a transition into the area target or space volume has occurred. The current AOS time, AOS_i, is set equal to the current time. The current time is incremented by Δt and the search continues.

If V < 0

9.2 a further test is performed on AOS_i to determine whether the S/C was visible during the previous step.

If $AOS_i > 0$

9.2.1 then the S/C was visible during the previous time step and a transition out of the area target or space volume has occurred. The current LOS time, LOS_i, is set equal to the time of the previous time step $(t - \Delta t)$. The AOS/LOS counter, i, is

incremented by one. The next AOS time is initialized to zero. The current time is incremented by Δt and the search continues.

9.2.2 the S/C was not visible during the preceding time step. Thus, no transition has occurred. The current time is incremented by Δt and the search continues.

10. At the completion of the sequential time search, a test is made to determine whether the S/C was visible at the end time. If the test is true, the last LOS time is set equal to t_{LOS_K}.

5.0 DETAILED LOGIC FLOW

Figure 5-1 presents the detailed logic flow for the area targets and space volumes processor. This flowchart integrates the functional overview presented in section 4 with the equations and approach presented in sections 2 and 3 and the appendixes.

Annotations are provided on the flowchart to describe the computations and tests that are performed. In order to simplify figure 5-1, several notations have been used to represent corresponding FORTRAN functions, e.g.,

$\phi(I)$	represents an array of longitudes indexed by the variable I.
$\vec{R}(I)$	represents a two-dimensional array [i.e., R(3,5)] in which the first dimension represents the Cartesian components of the vector and the second dimension is indexed by the variable I. Hence, operations involving vector quantities imply a "DO loop" on the innermost dimension.
$\hat{N}(J,I)$	represents a three-dimensional array [i.e., N(3,5,3)] in which the first dimension represents the Cartesian components of the vector and the second and third dimensions are indexed by variables J and I, respectively. Operations involving these vector quantities also imply a DO loop on the innermost dimension.
$\sum_{L=1}^{K-1}$	implies summation over the indicated range using the variable specified by the lower bound (e.g., the variable L will be used to perform the summation over the range L = 1 to L = K - 1).

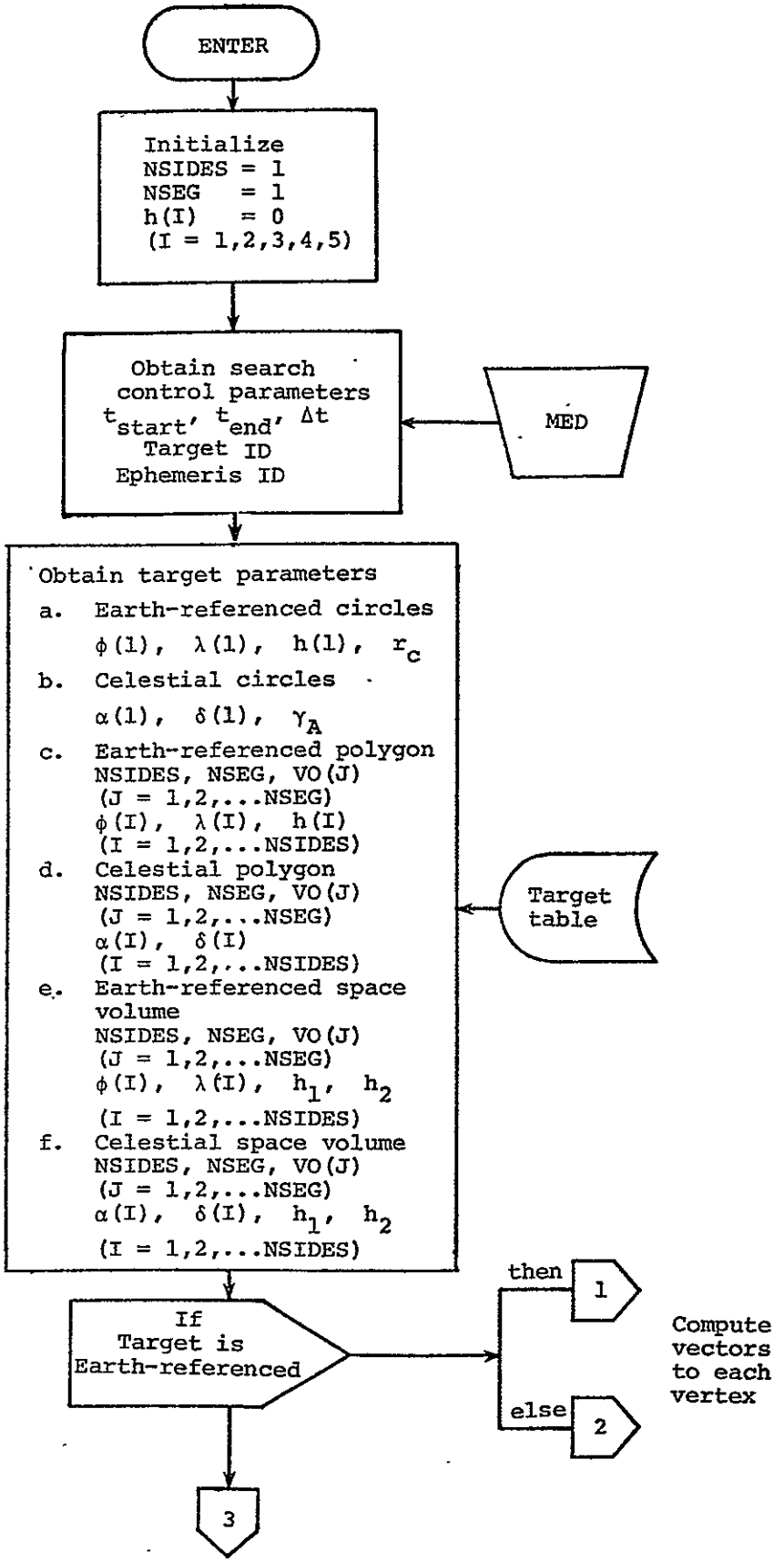

Figure 5-1.- Detailed flowchart.

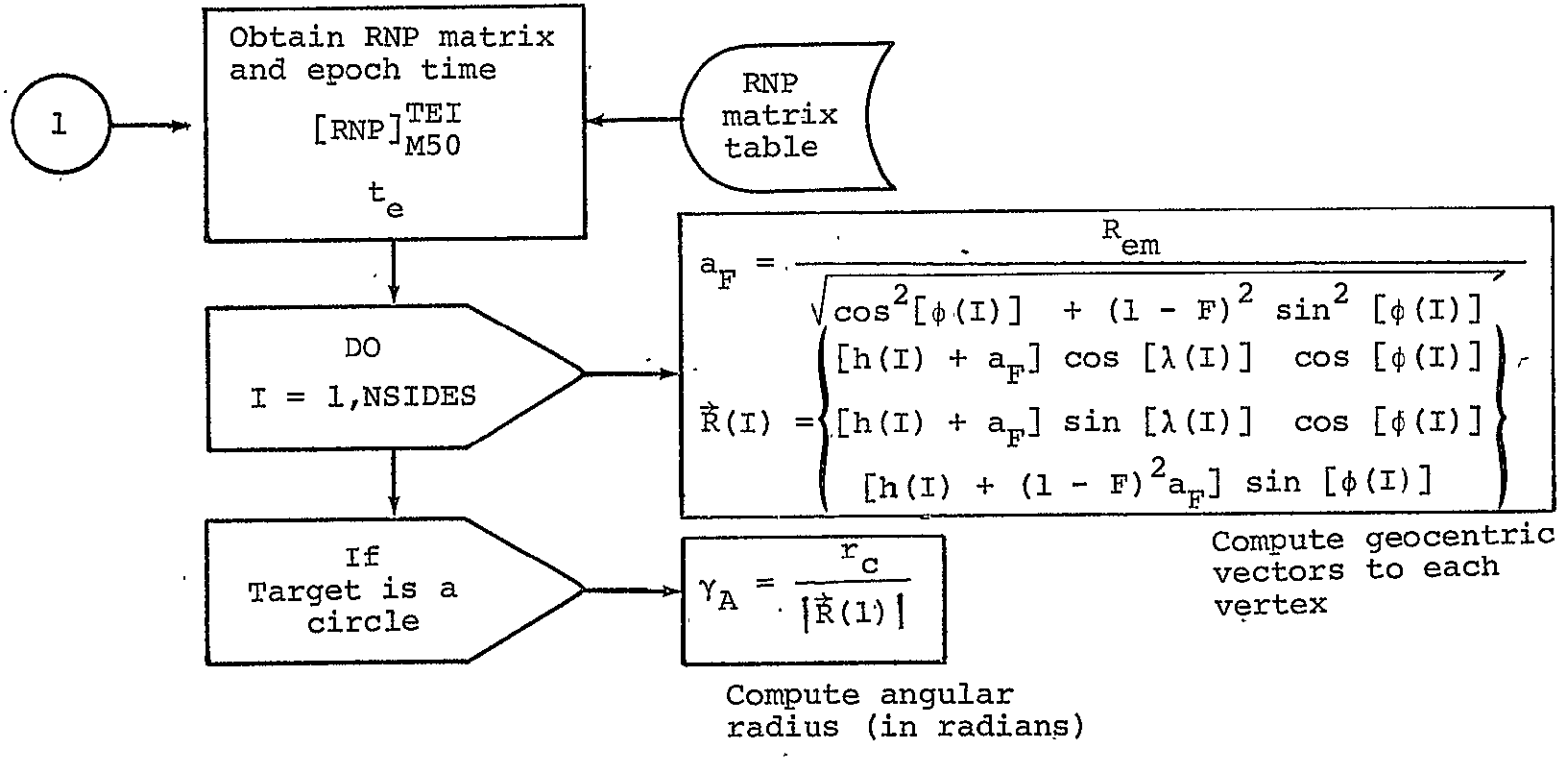

Figure 5-1.- Continued.

Celestial-fixed targets

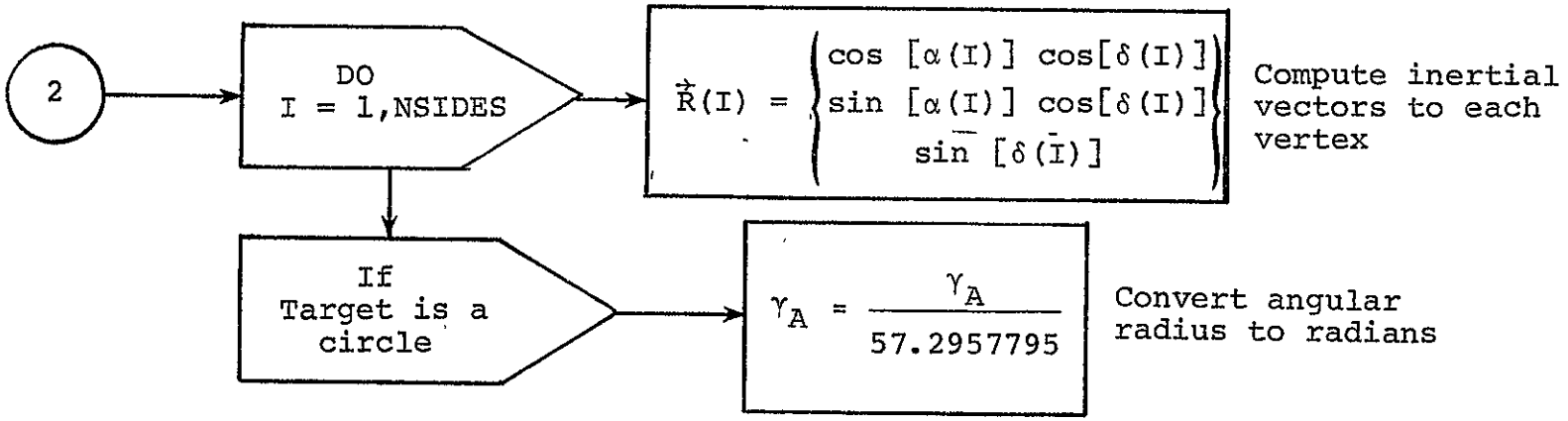

Figure 5-1.- Continued.

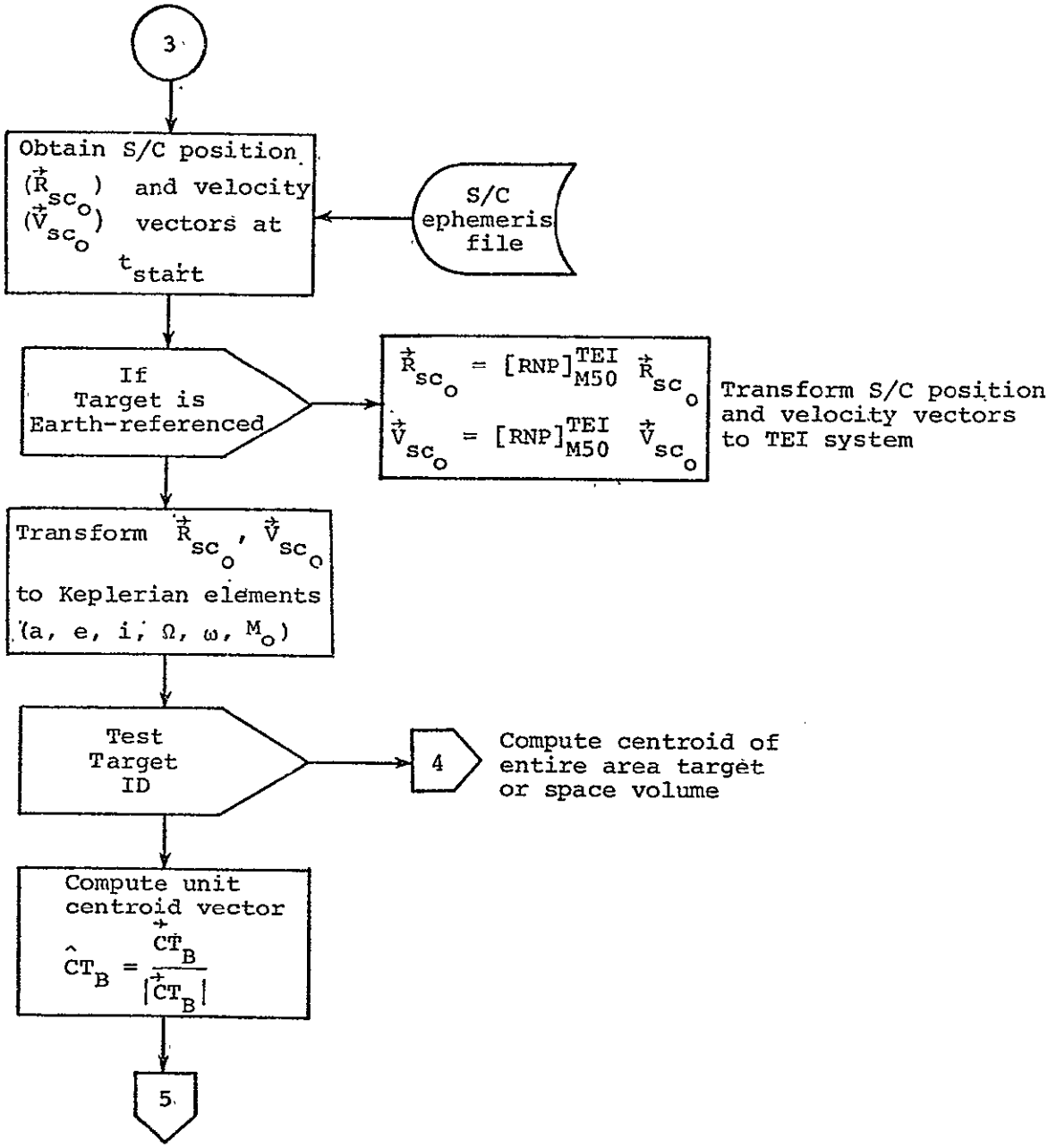

Figure 5-1.- Continued.

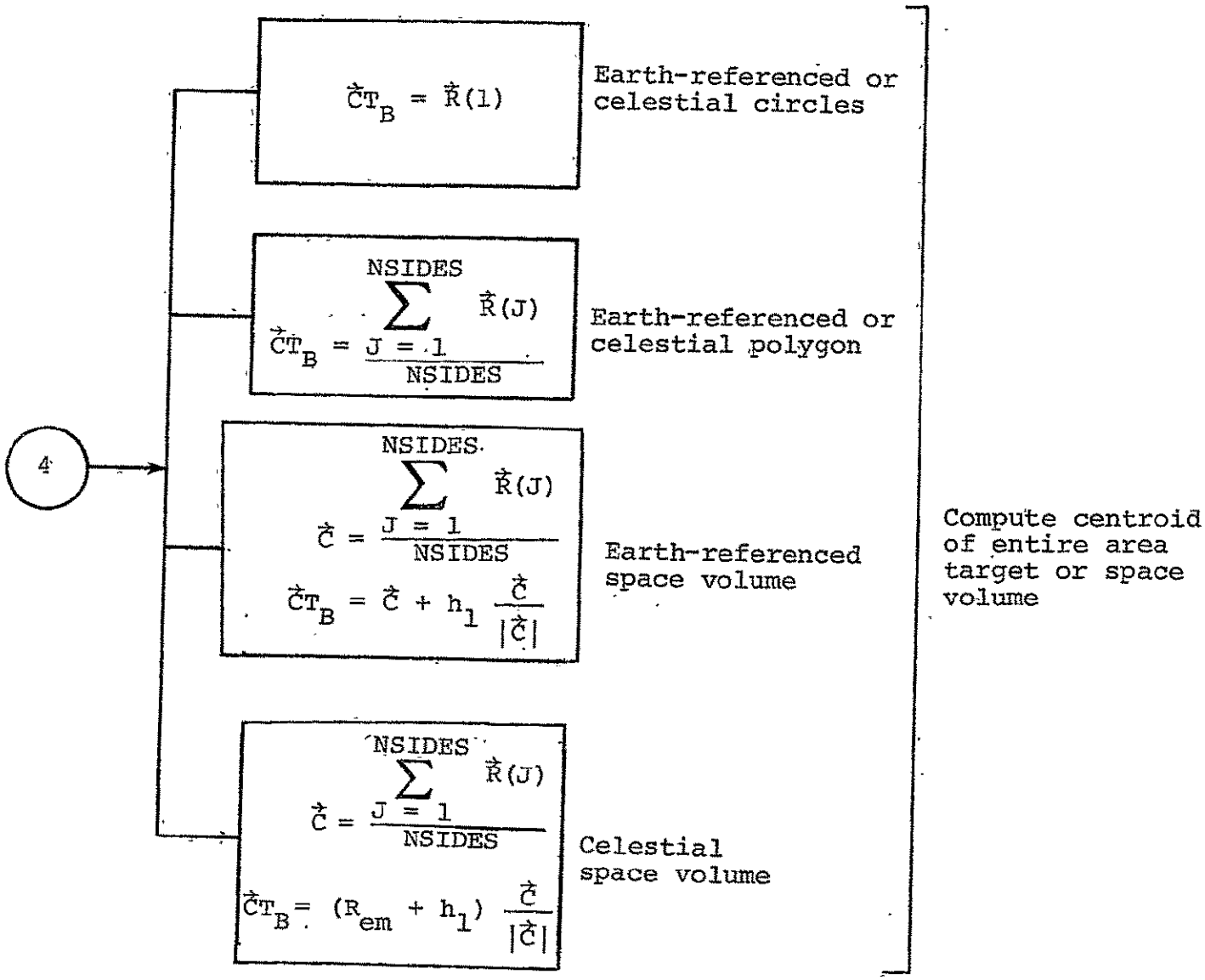

Figure 5-1.- Continued.

C-2

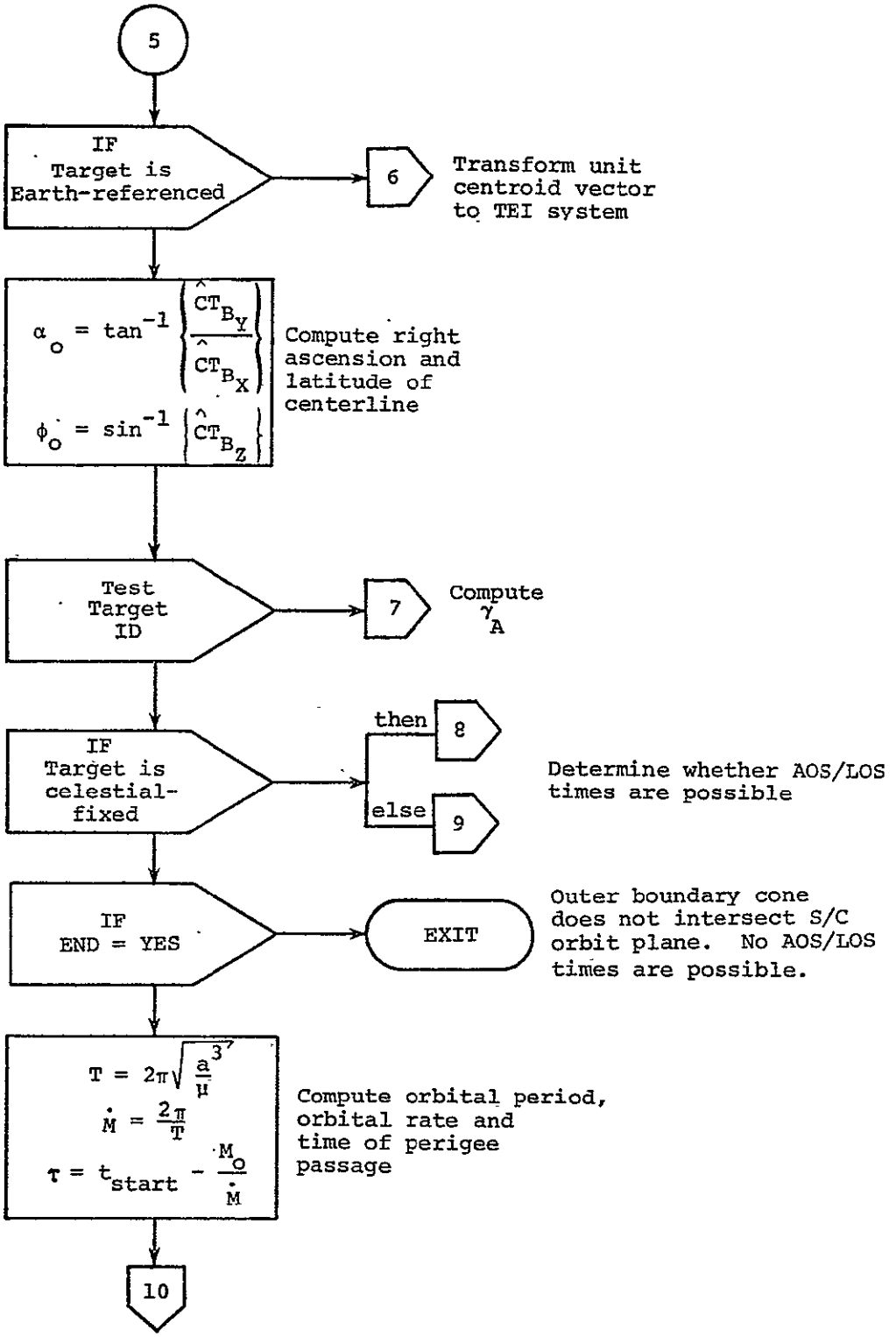

Figure 5-1.- Continued.

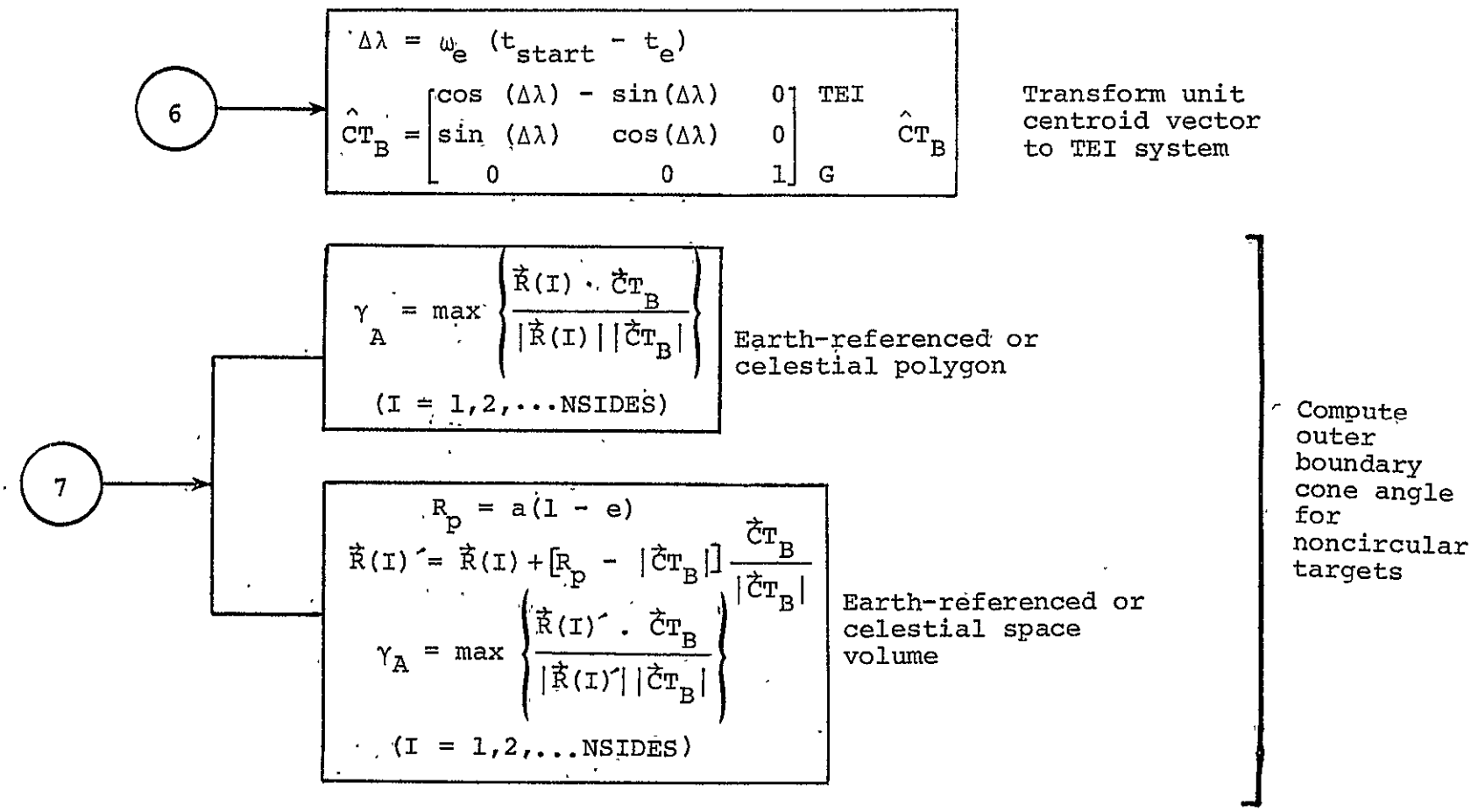

Figure 5-1.- Continued.

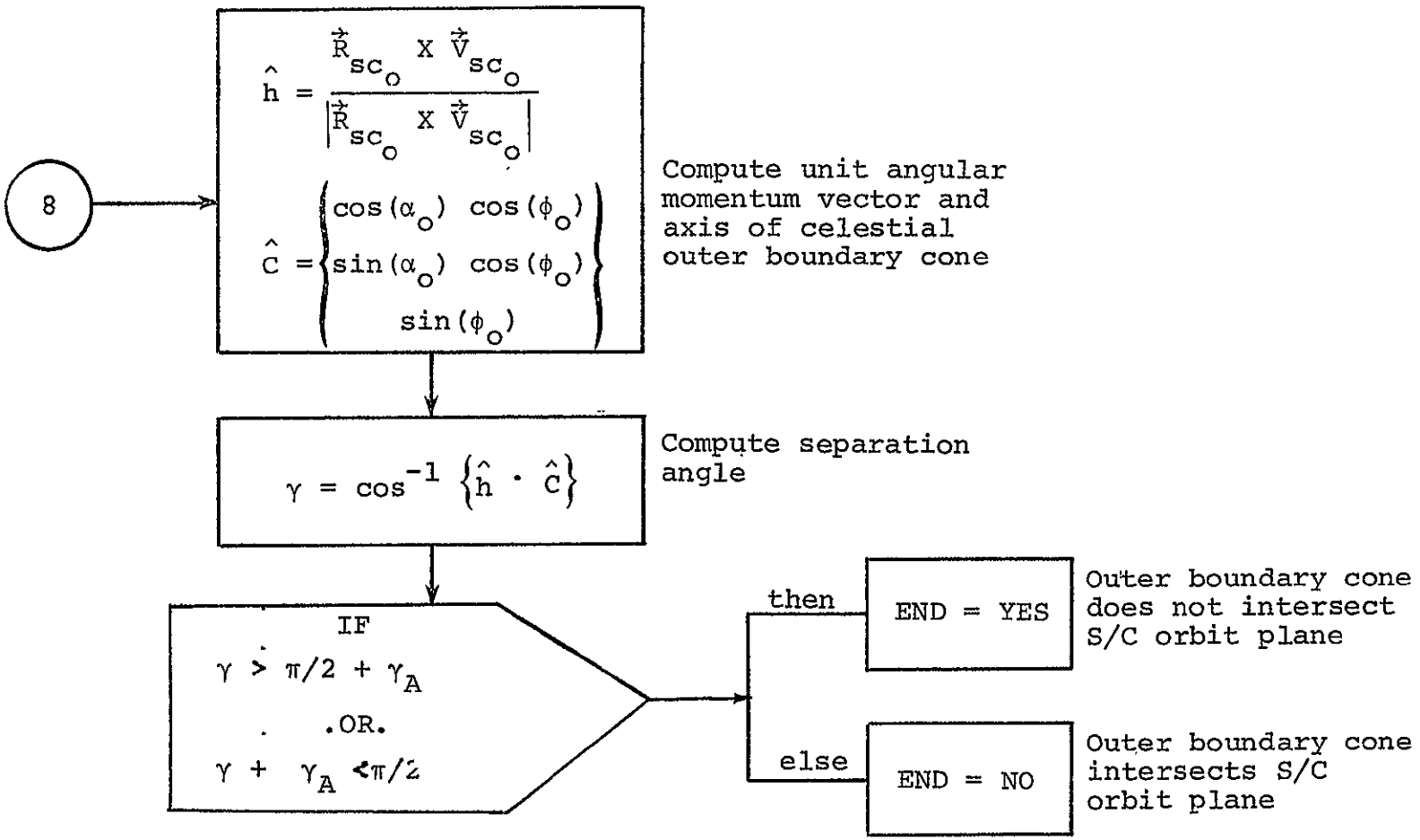

Figure 5-1.- Continued.

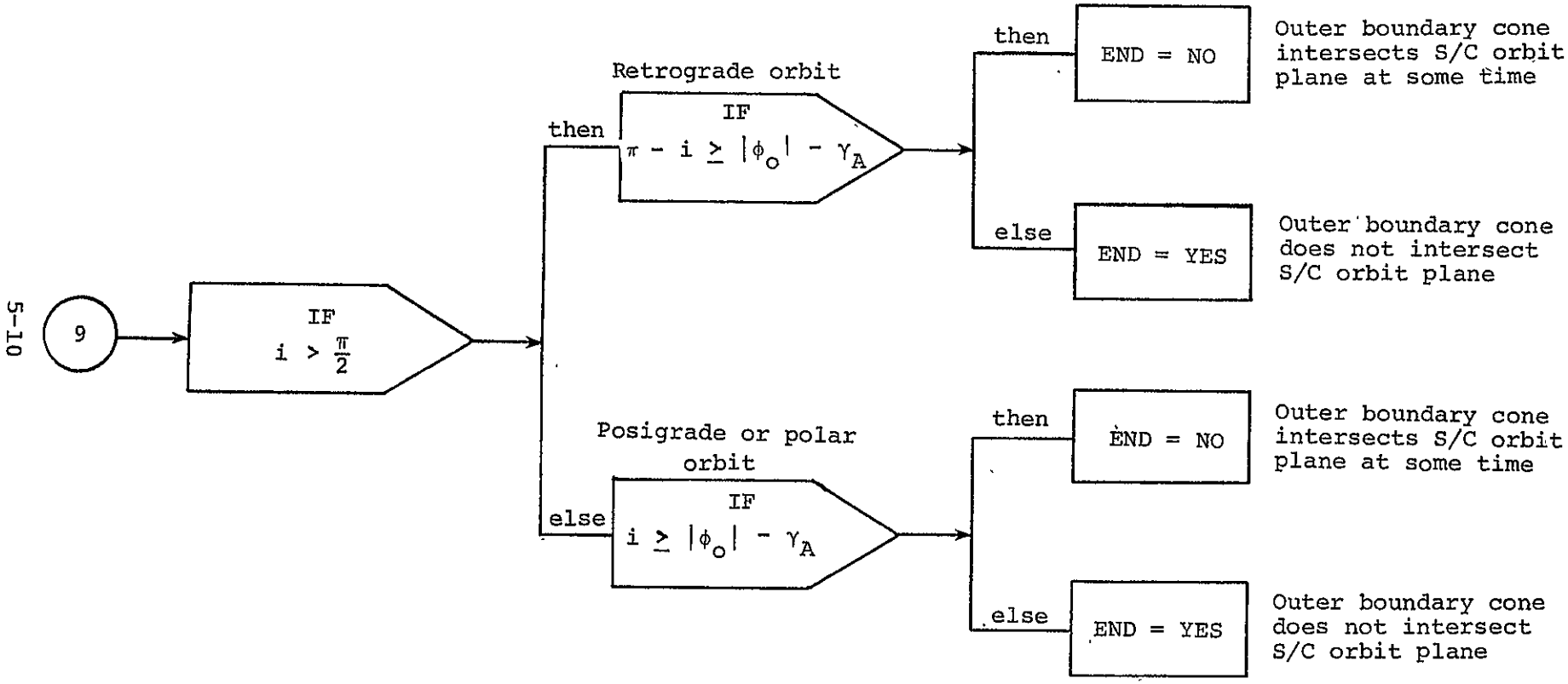

Figure 5-1.- Continued.

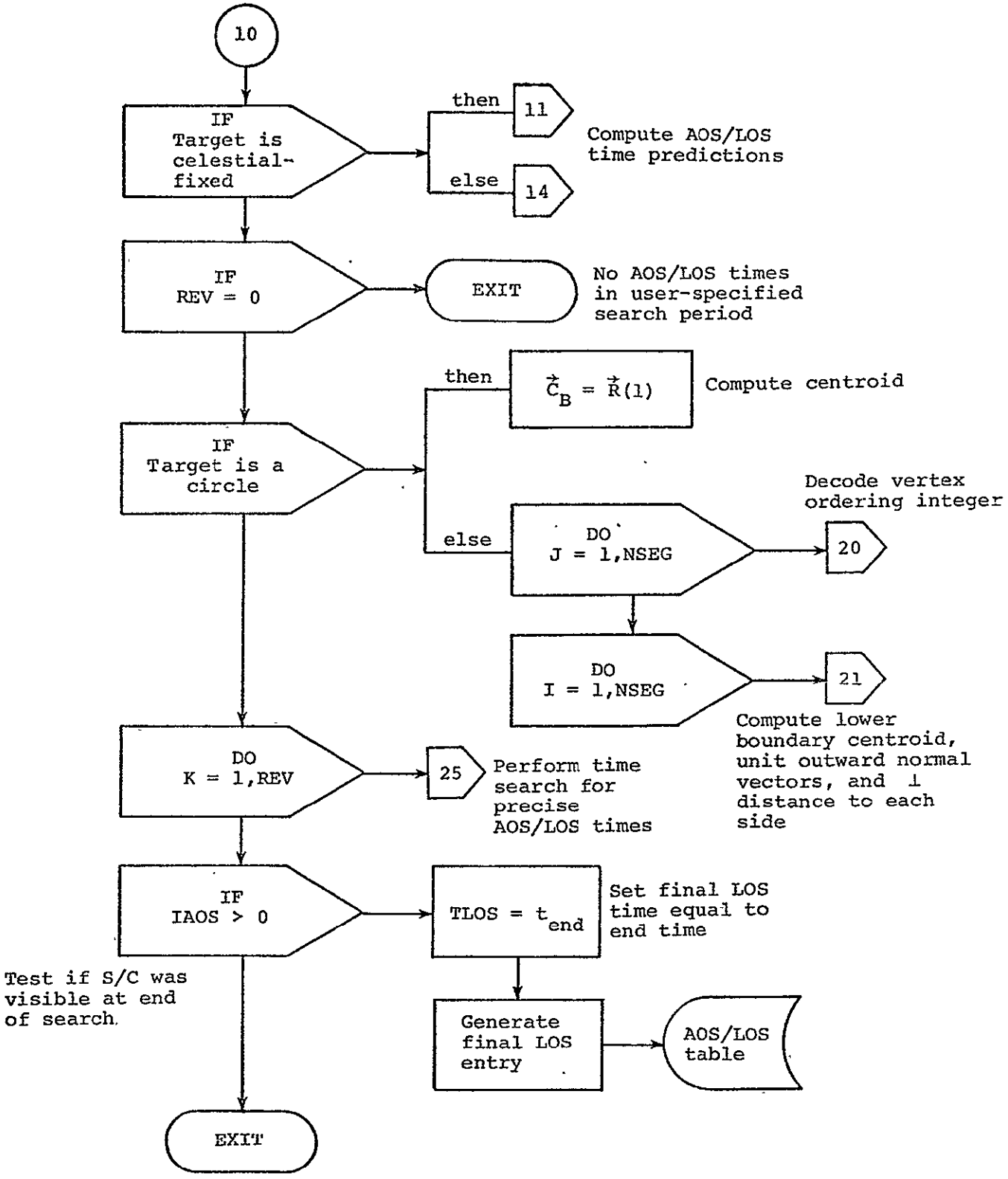

Figure 5-1.- Continued.

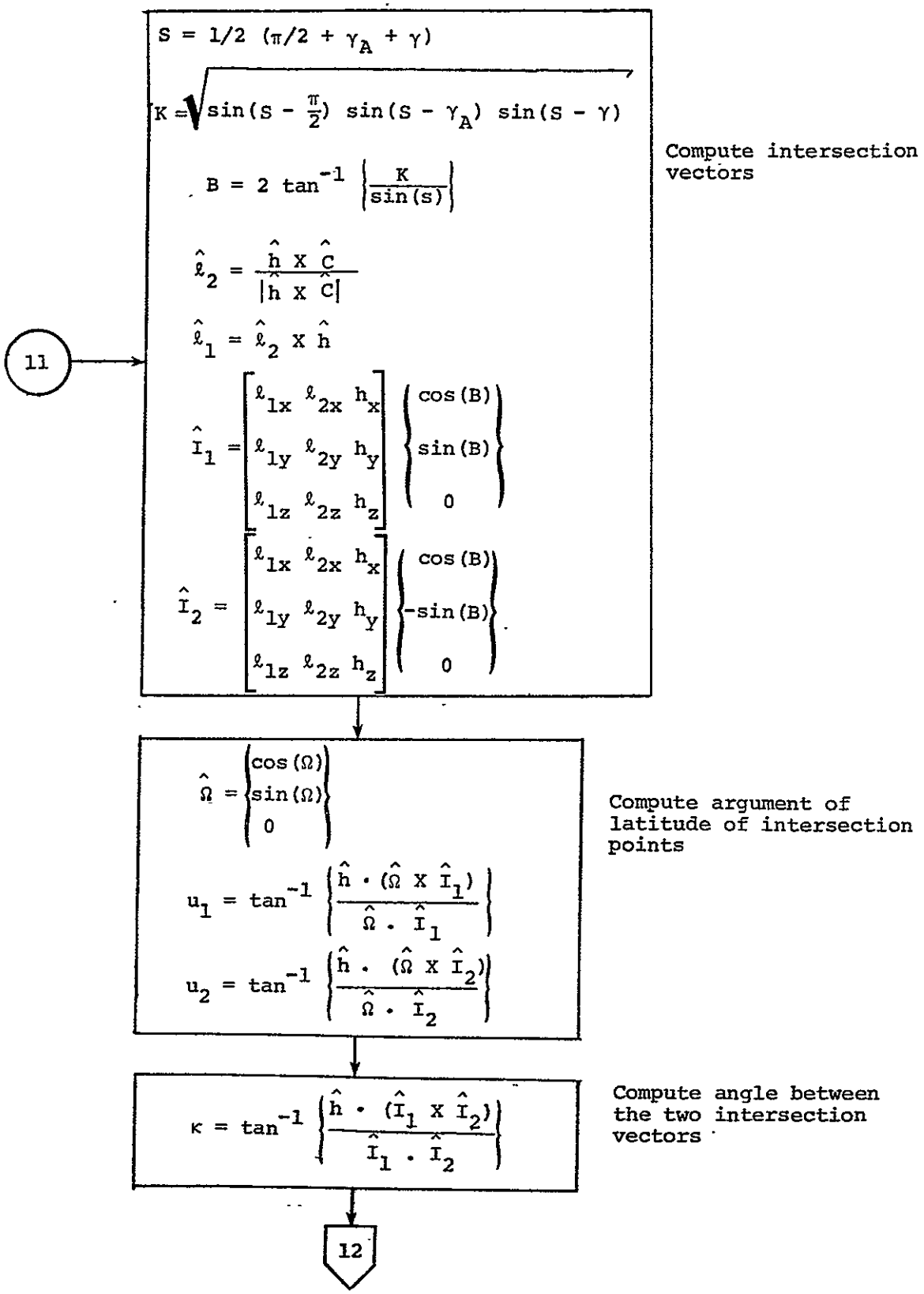

Figure 5-1.- Continued.

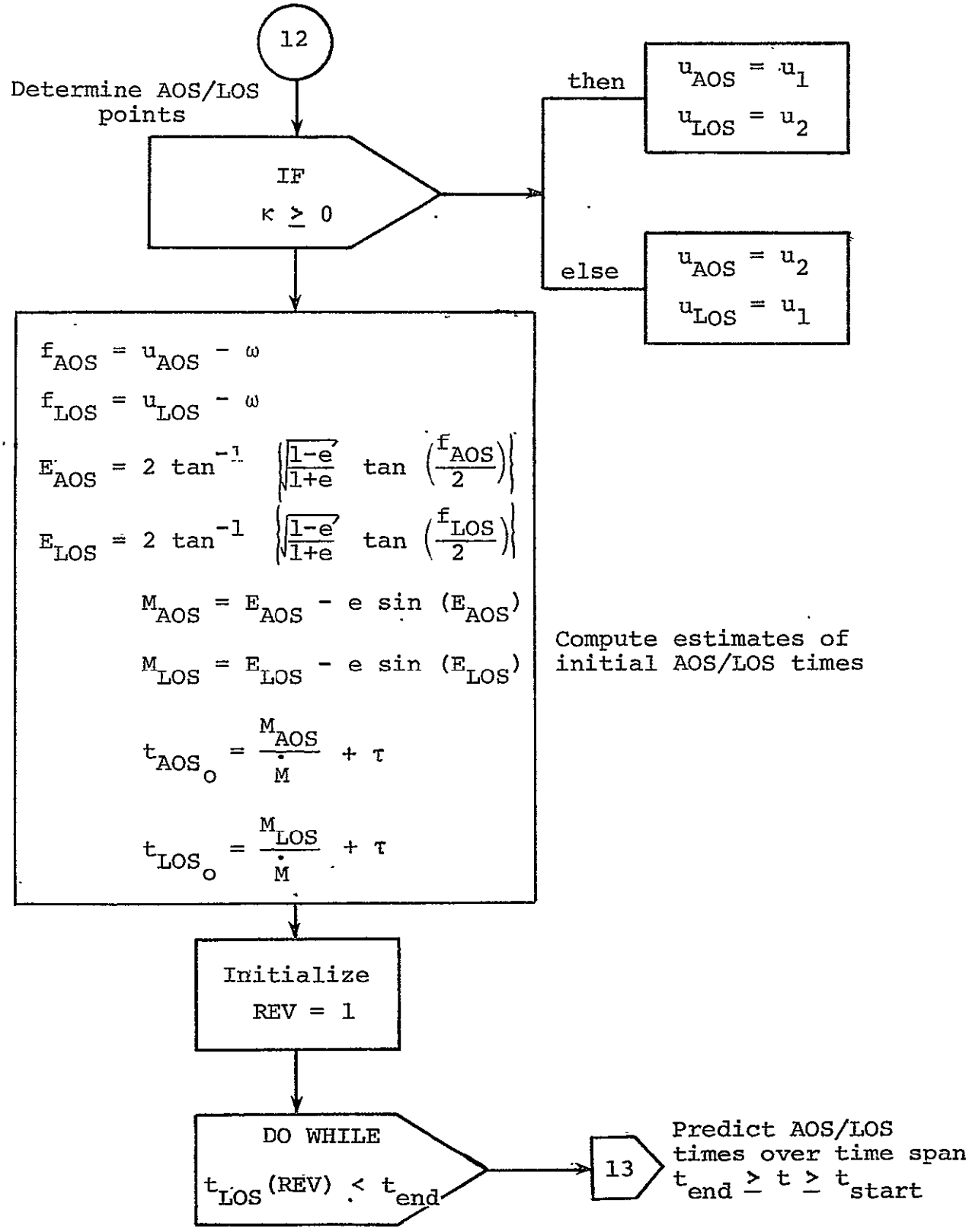

Figure 5-1.- Continued.

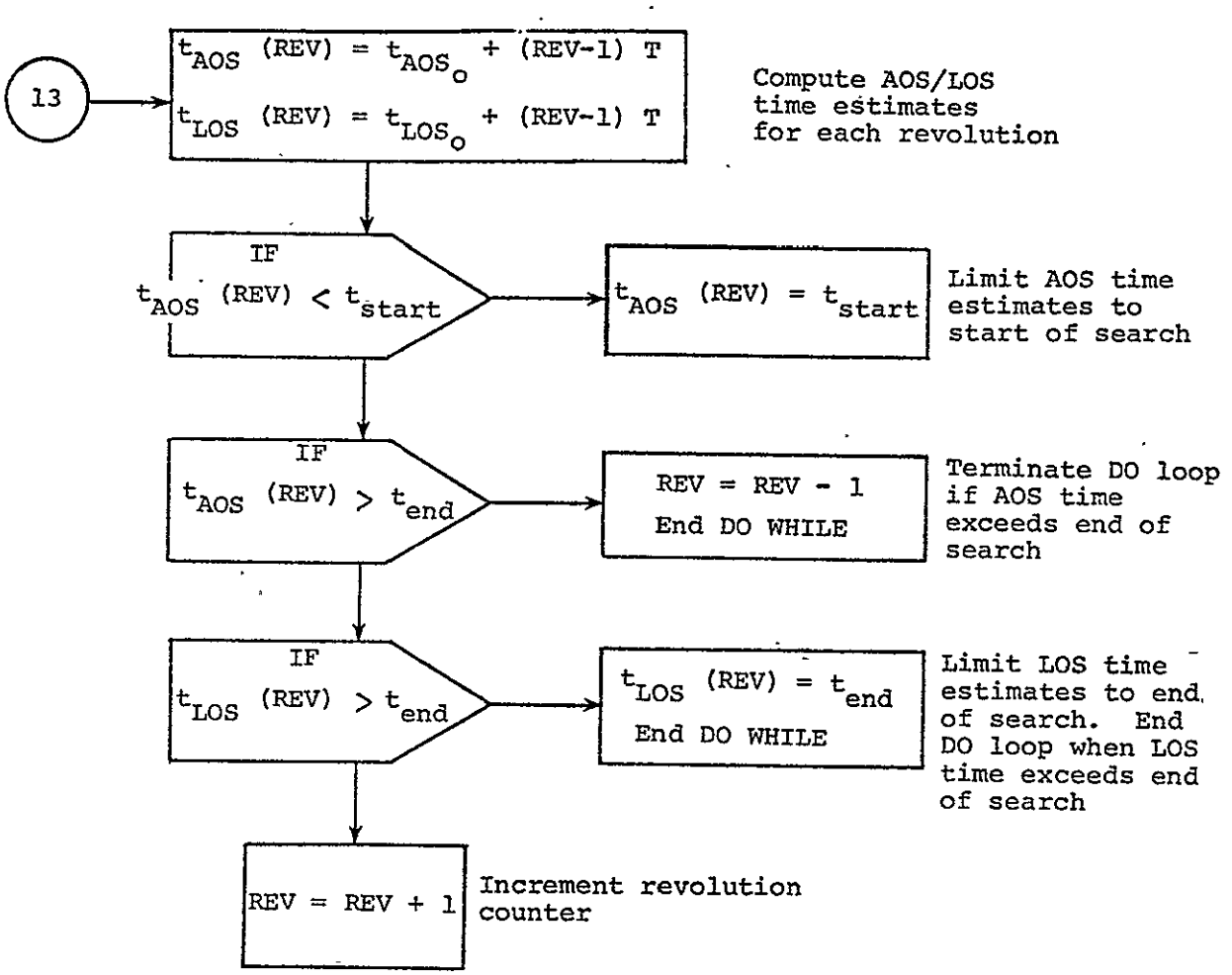

Figure 5-1.- Continued.

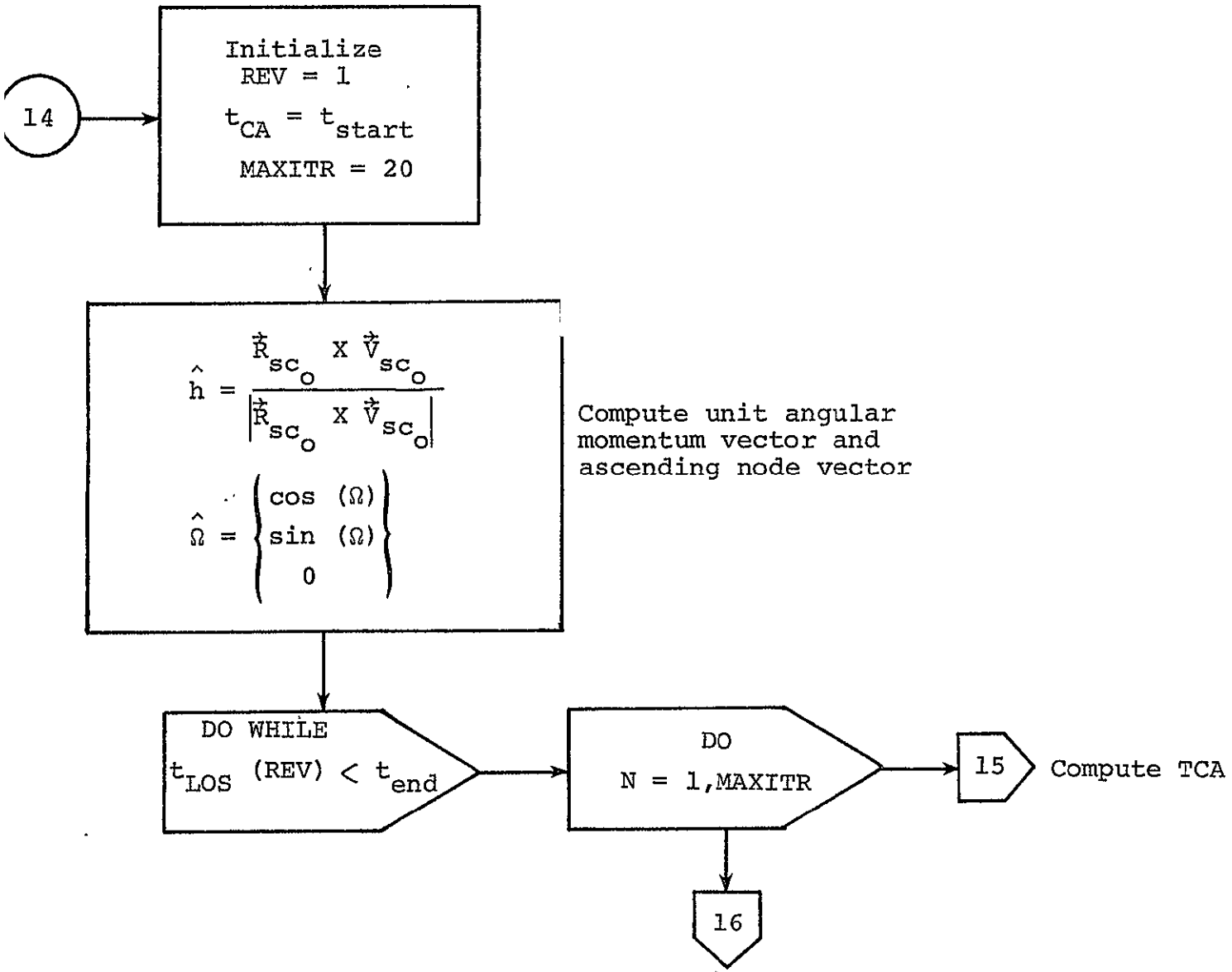

Figure 5-1.- Continued.

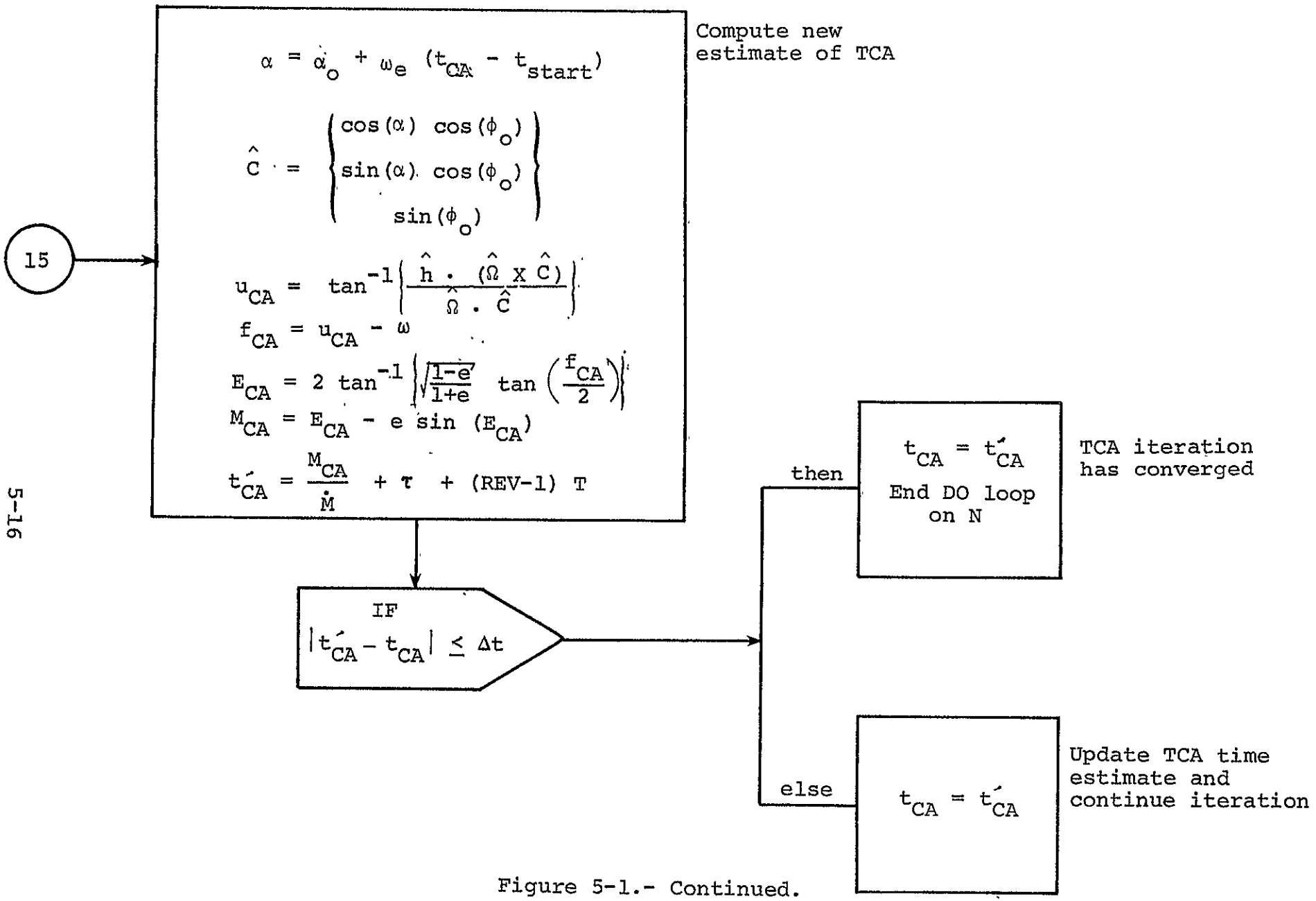

Figure 5-1.- Continued.

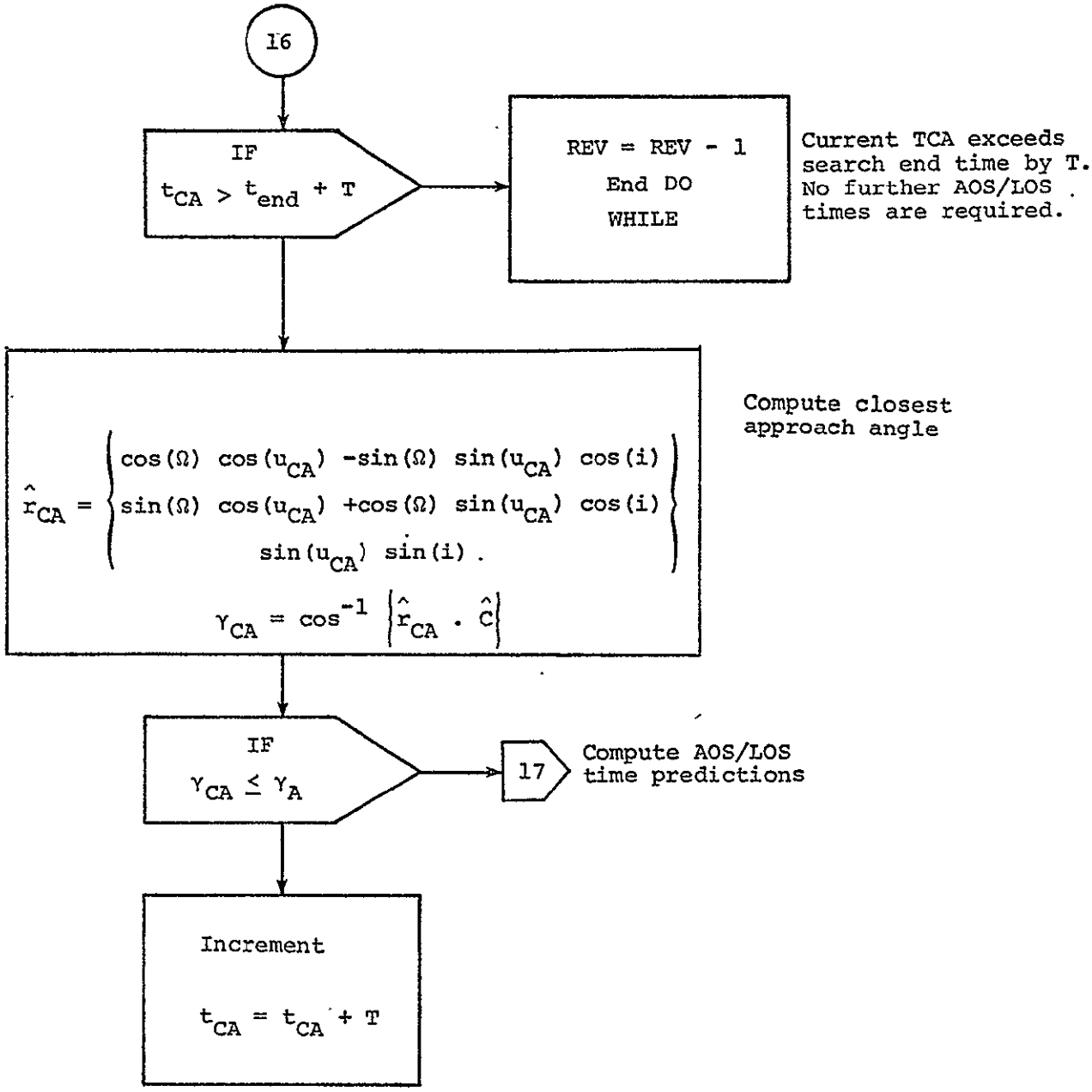

Figure 5-1.- Continued.

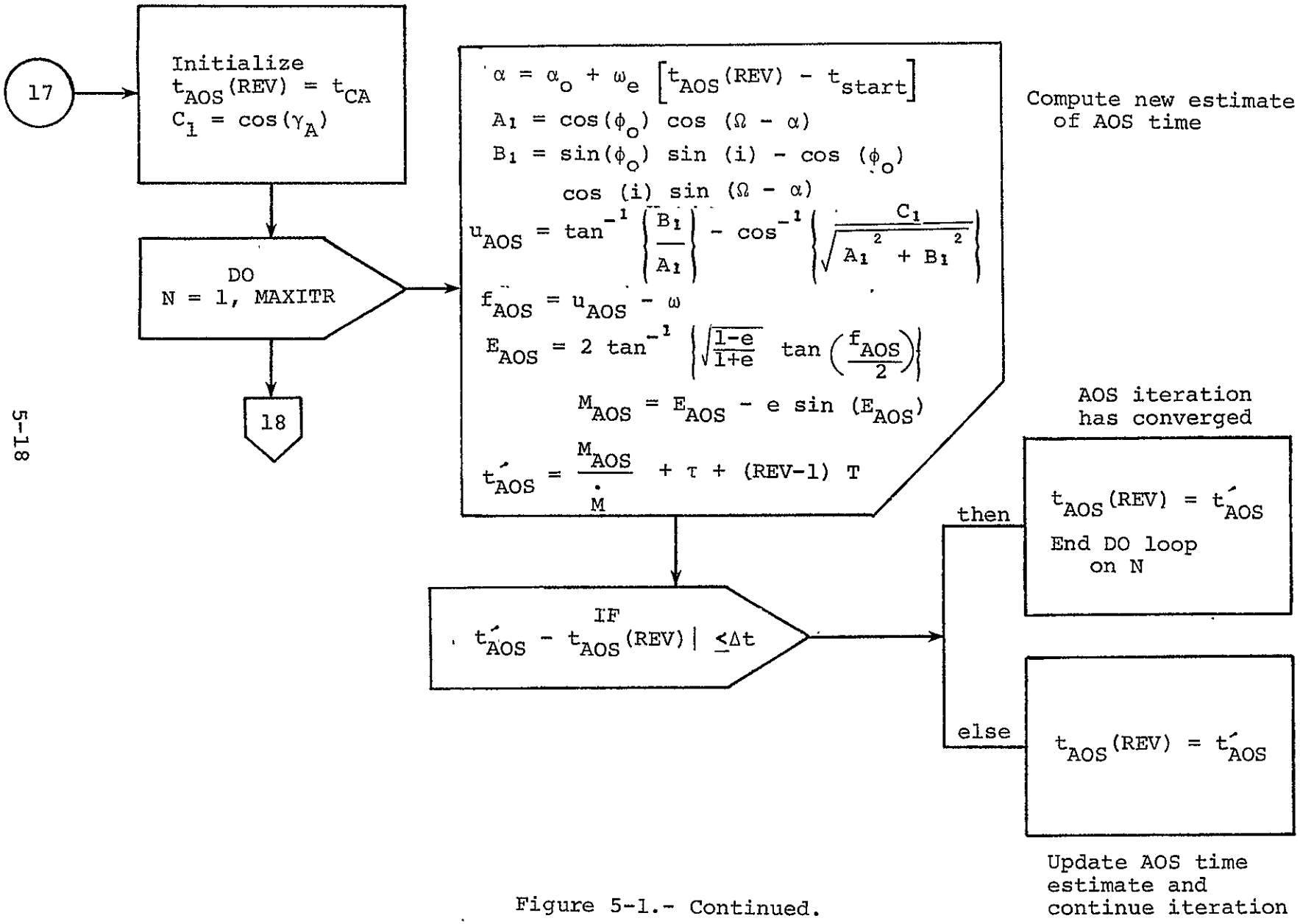

Figure 5-1.- Continued.

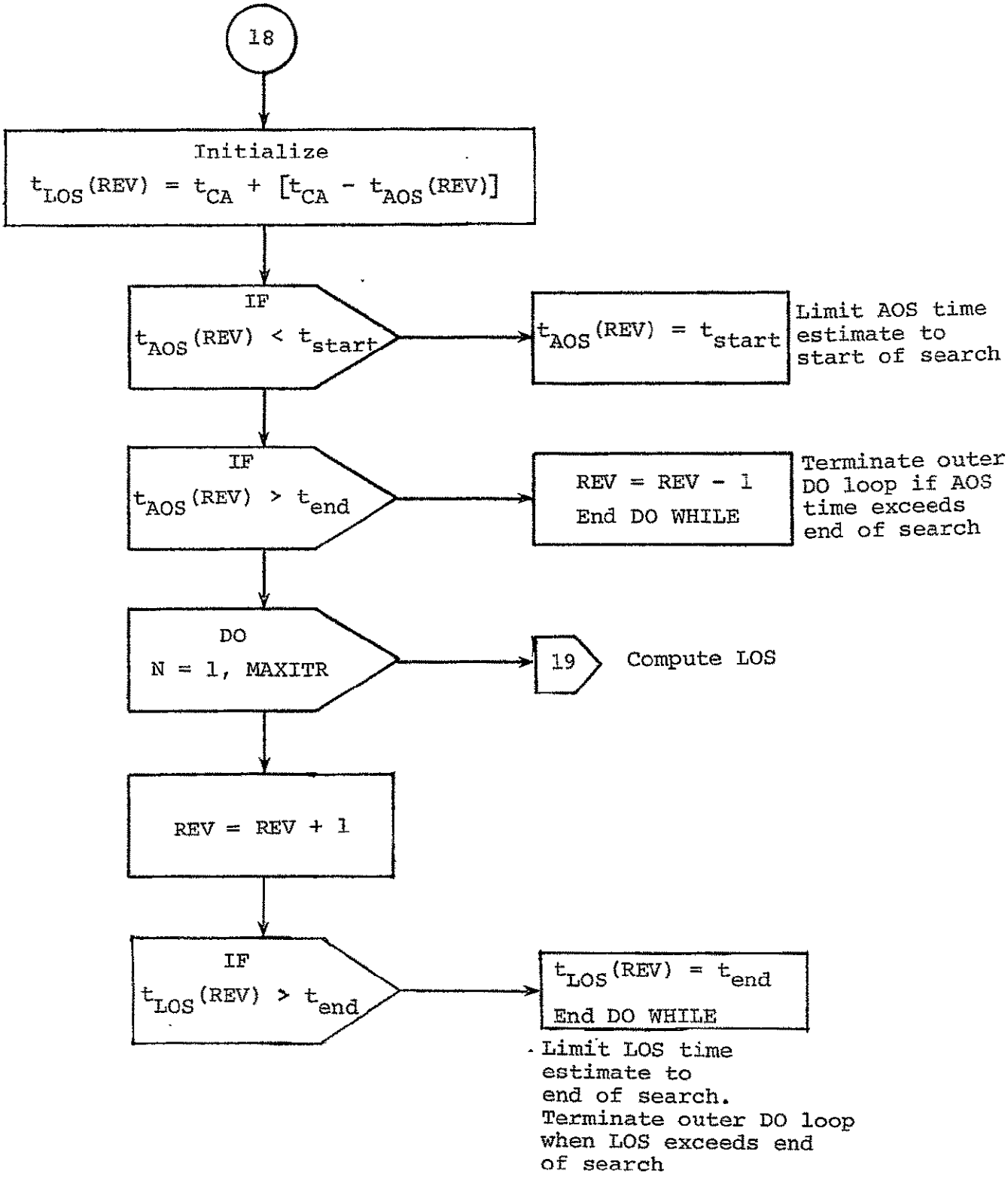

Figure 5-1.- Continued.

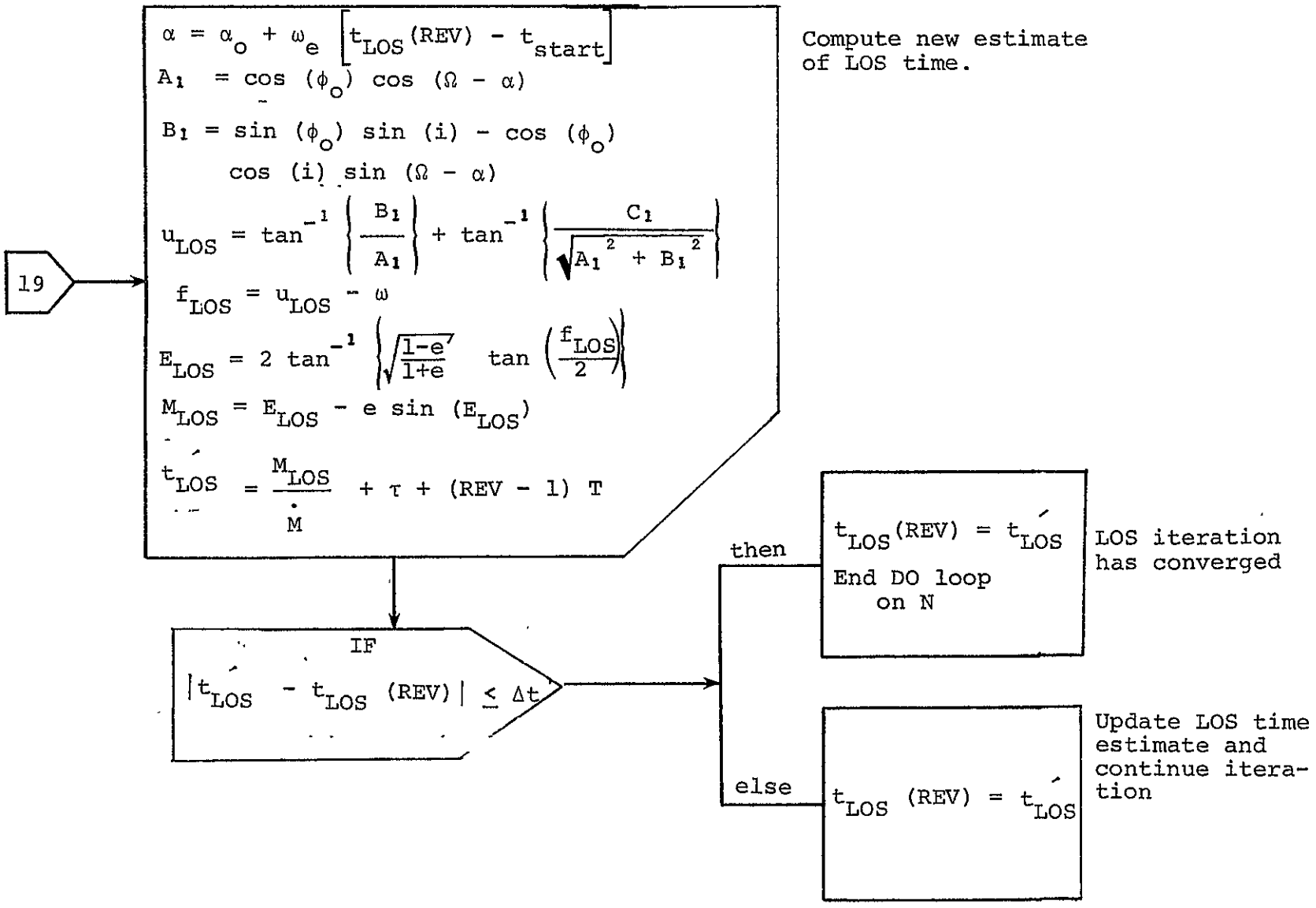

Figure 5-1.- Continued.

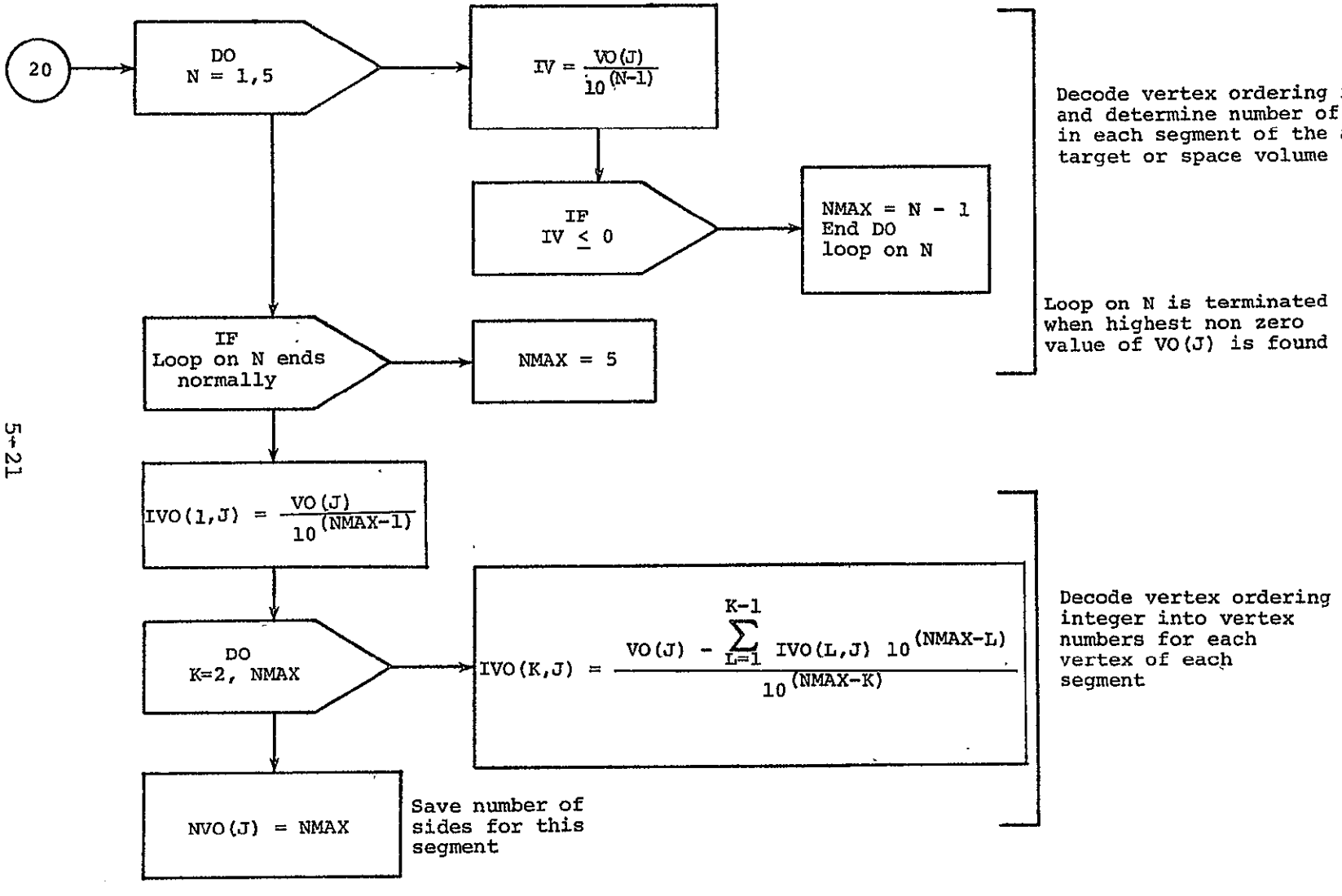

Figure 5-1.- Continued.

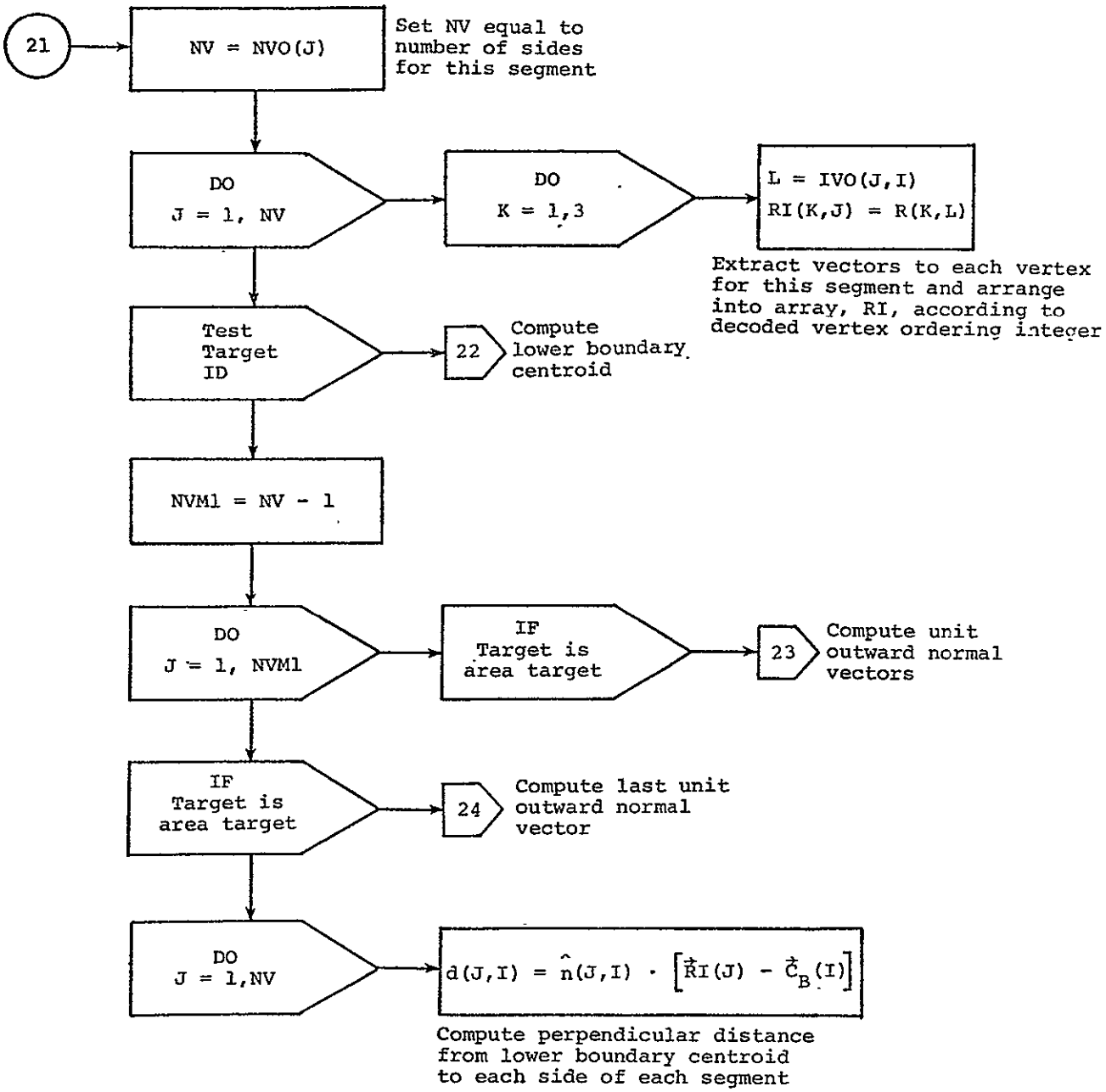

Figure 5-1.- Continued.

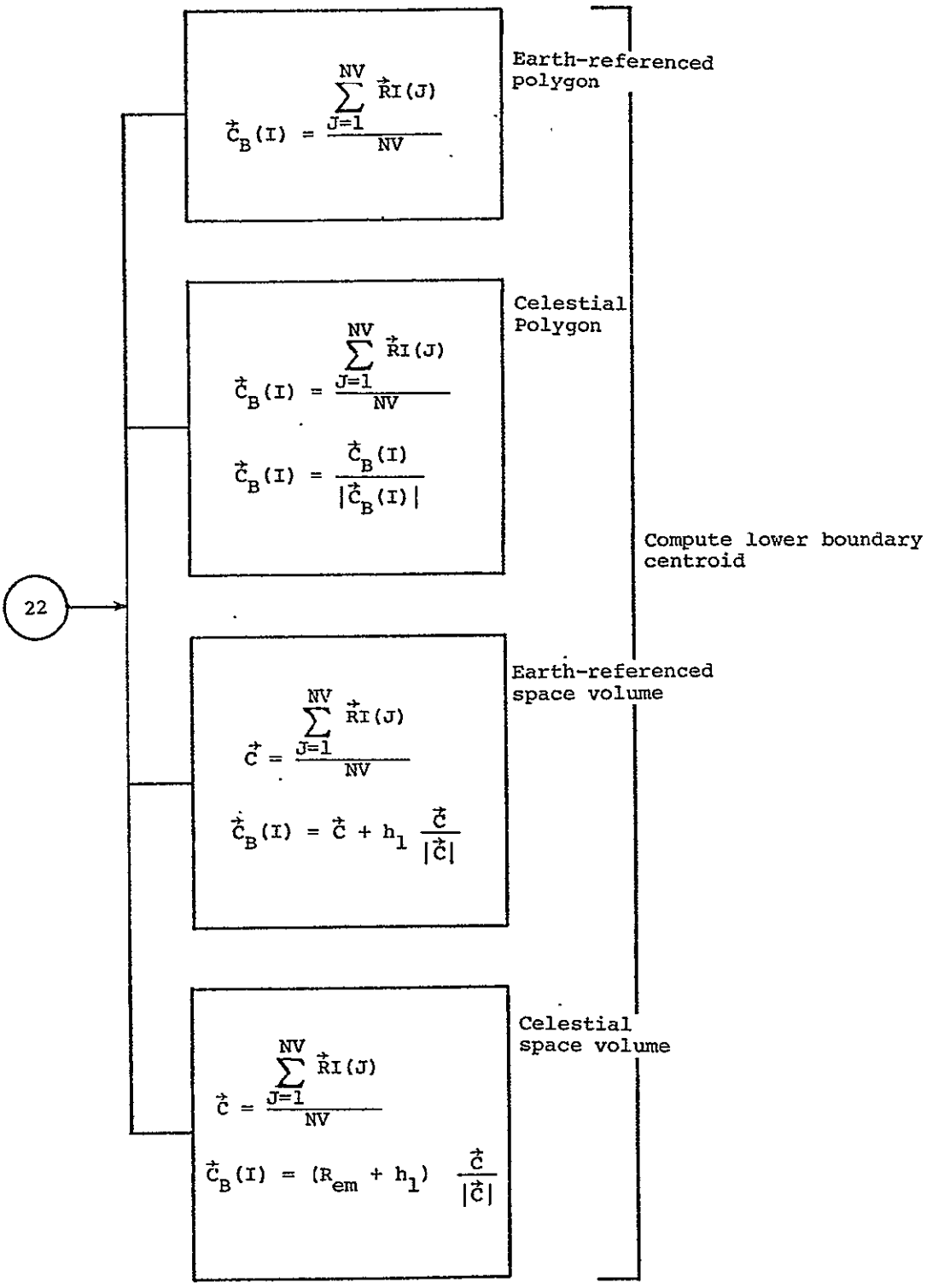

Figure 5-1.- Continued.

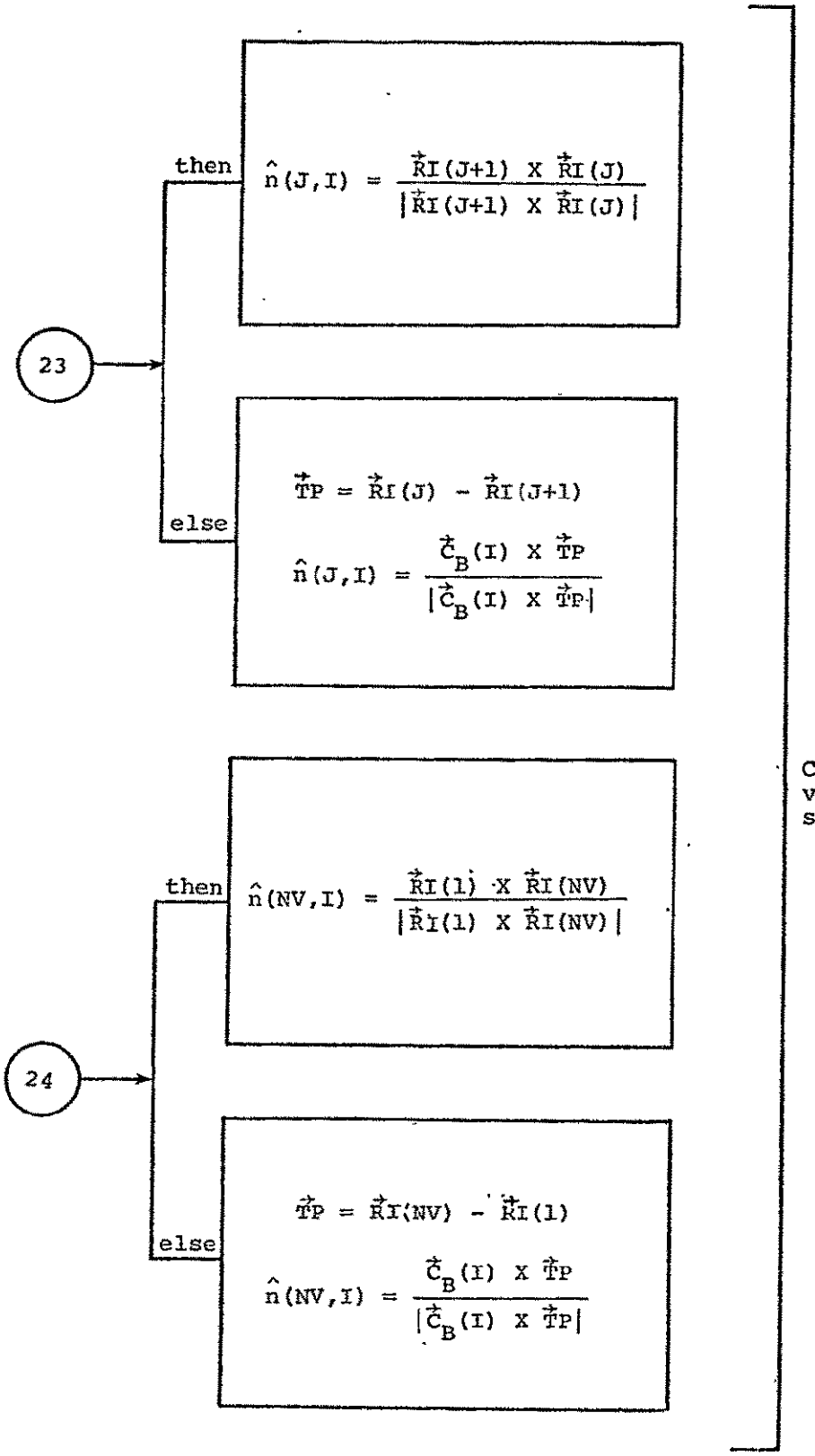

Figure 5-1.- Continued.

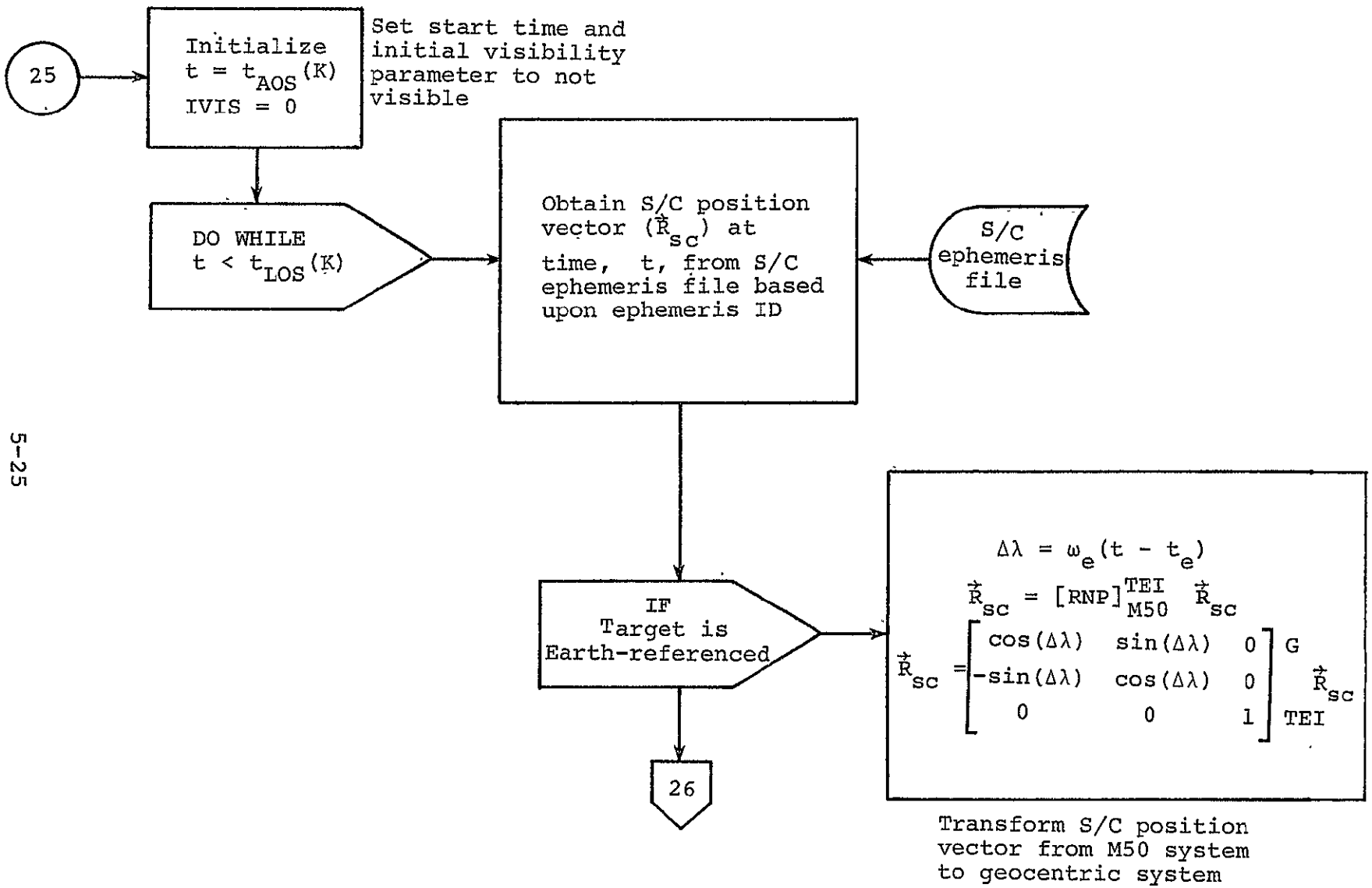

Figure 5-1.- Continued.

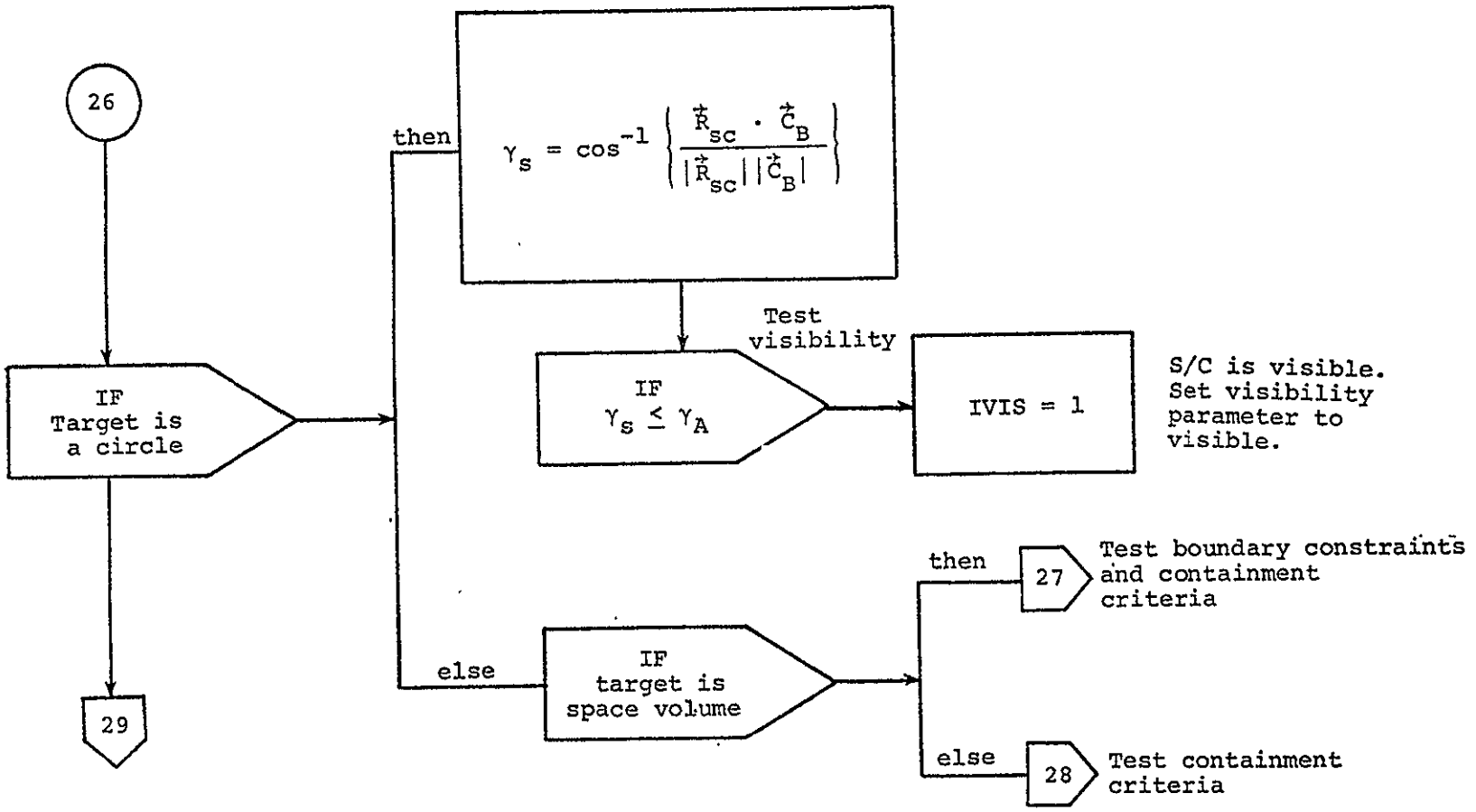

Figure 5-1.- Continued.

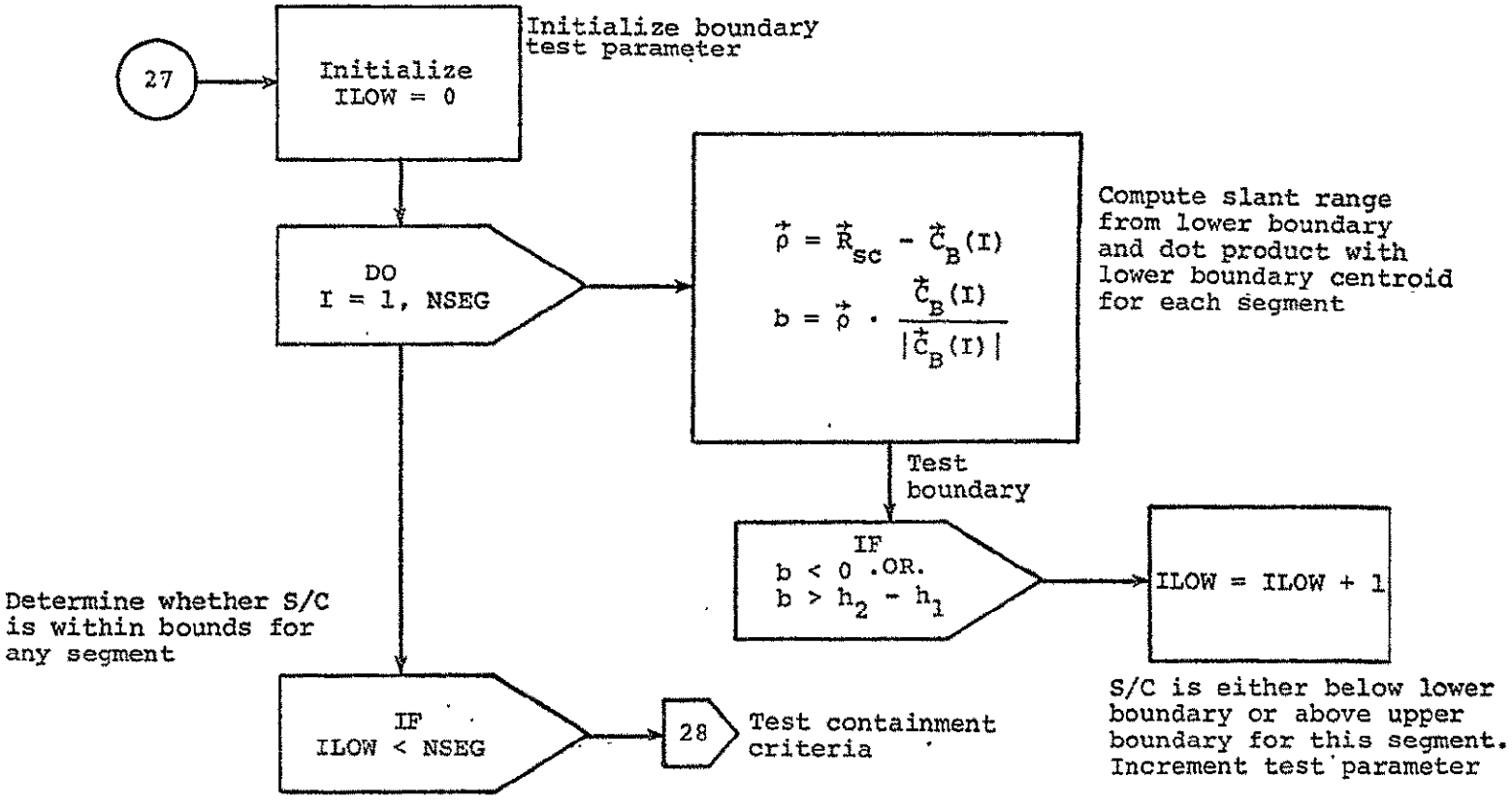

Figure 5-1.- Continued.

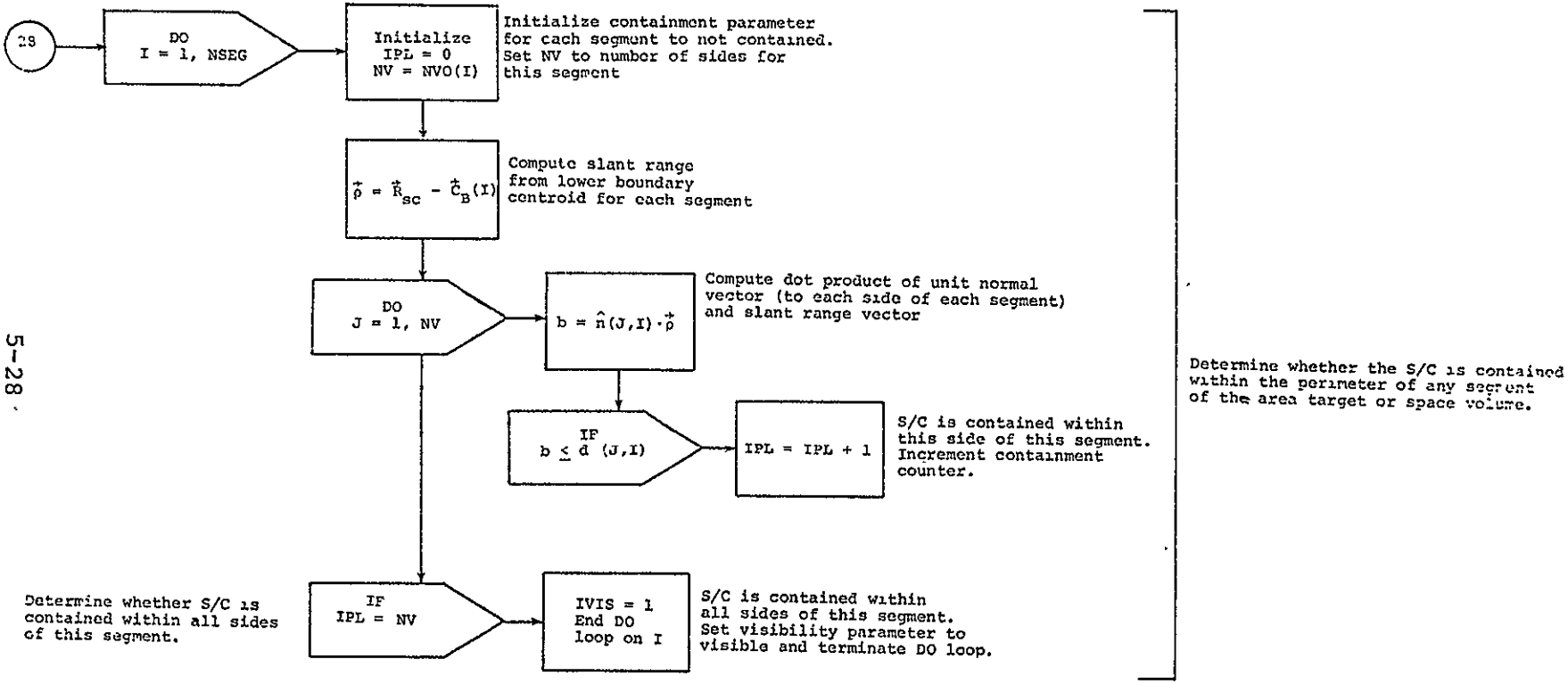

Figure 5-1.- Continued.

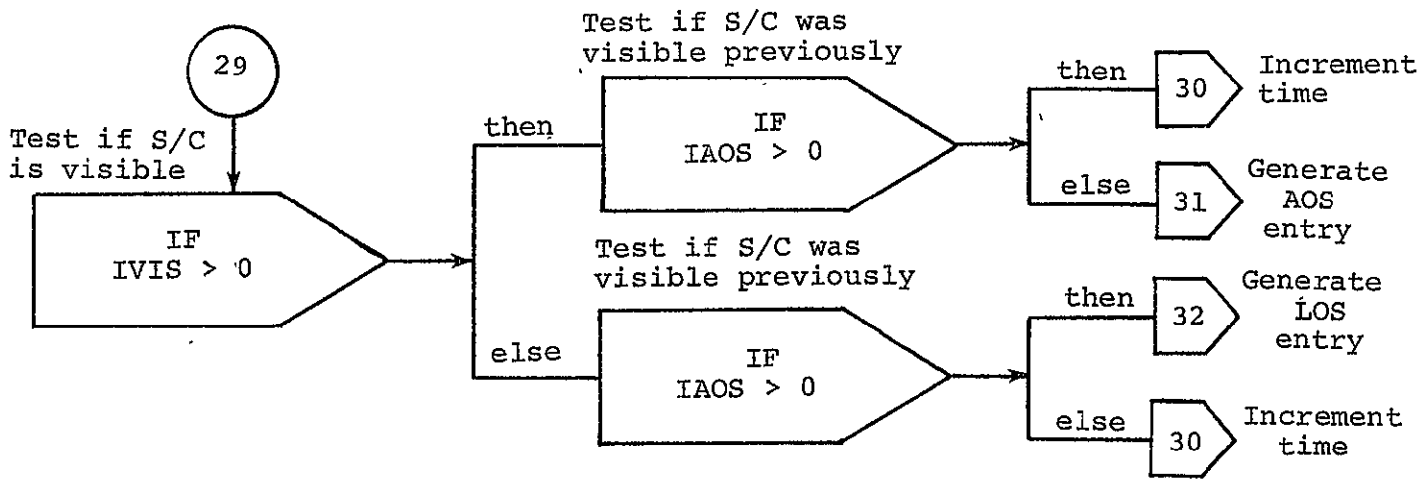

Figure 5-1.- Continued.

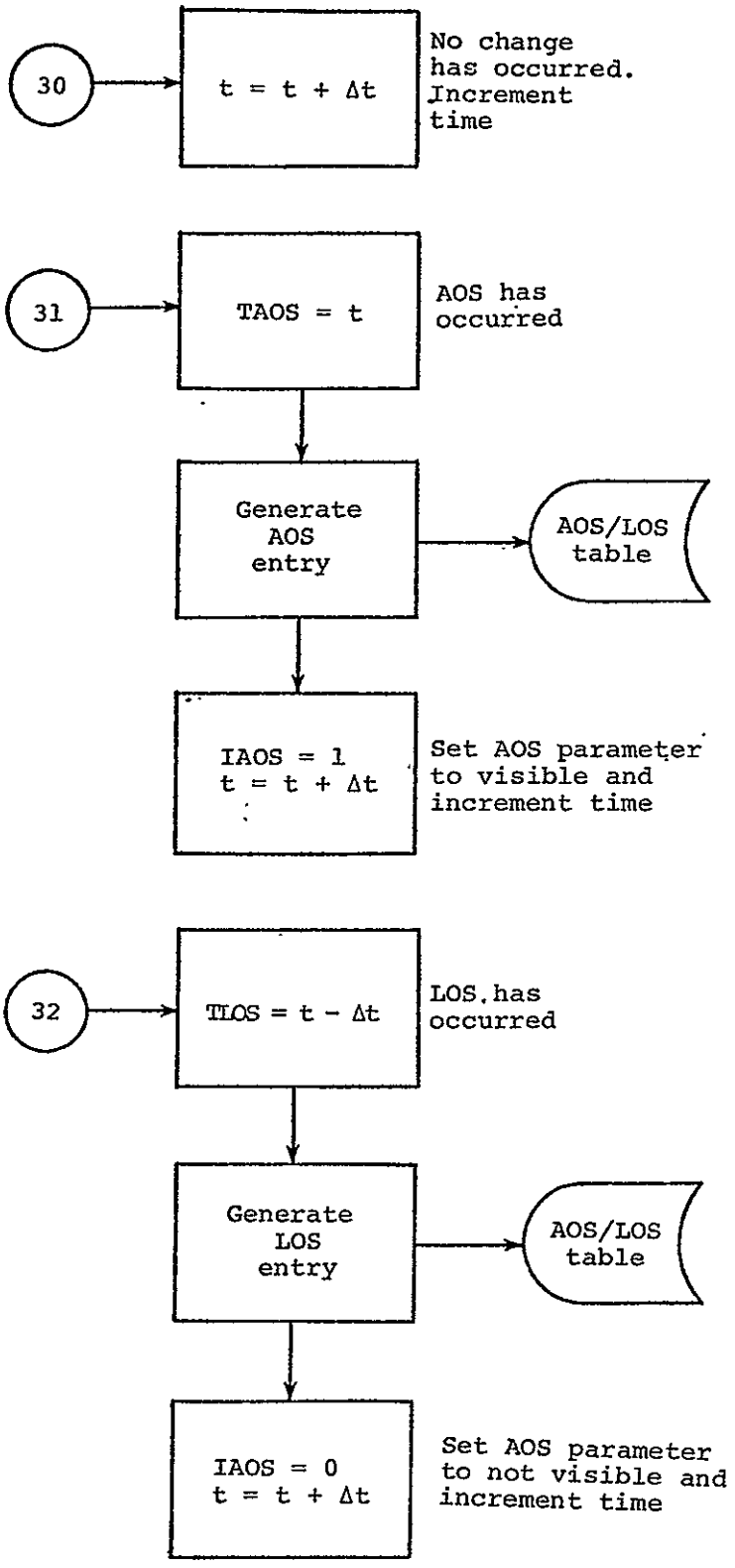

Figure 5-1.- Concluded.

APPENDIX A

SUBDIVIDING CONCAVE POLYGONS

SUBDIVIDING CONCAVE POLYGONS

This appendix discusses the procedure for subdividing complex concave polygons into two or more simpler convex segments.[1] The purpose of this subdivision process is to permit the equations in section 2 to be used on a segment-by-segment basis to test for containment. The criterion for the S/C (or S/C subsatellite point) to be contained in the concave area target or space volume is that it must be contained in any one of its segments. For convenience, the equations and figures presented in this appendix will use a pentagon as an example.[2] However, this approach is easily extended to any n-sided polygon.

Figure A-1 presents three examples of concave pentagons. Figure A-1(a) illustrates a pentagon having one concave vertex. Figures A-1(b) and A-1(c) illustrate pentagons having two concave vertices. These pentagons can always be subdivided into triangles by selecting an "appropriate" vertex and connecting nonadjacent vertices (fig. A-2). The maximum number of triangles necessary to completely subdivide any arbitrarily shaped polygon is

$$N_{seg_{max}} = n - 2 \qquad \text{(A-1)}$$

where

n = number of sides

---

[1] A concave polygon is defined to be a polygon that has one or more interior vertex angles exceeding 180 degrees. A convex polygon is defined to be a polygon that has all of its interior angles less than 180 degrees.

[2] This corresponds to the maximum number of sides specifically addressed in the requirements defined in reference 1.

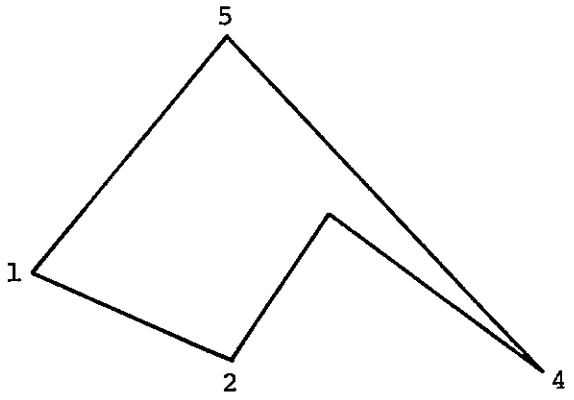

(a) One concave vertex.

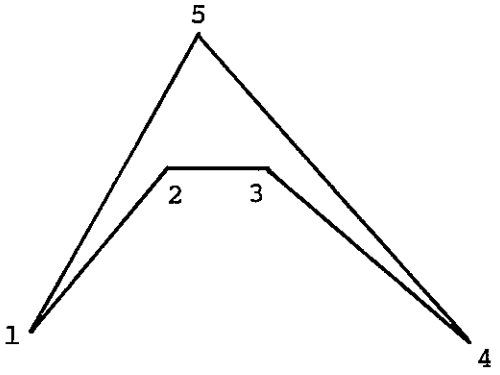

(b) Two adjacent concave vertices.

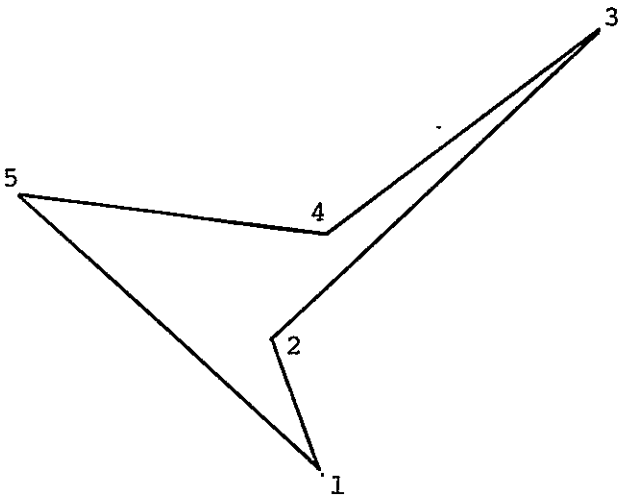

(c) Two nonadjacent concave vertices.

Figure A-1.- Examples of concave pentagons.

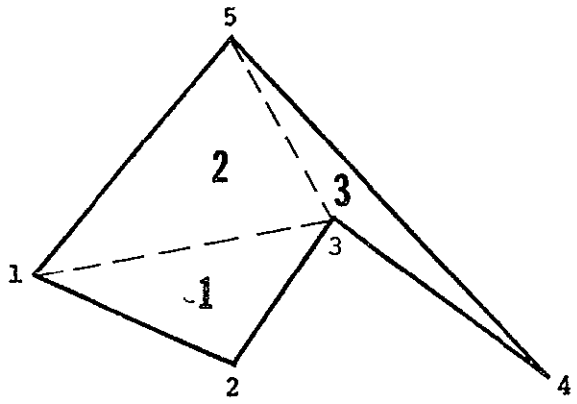

(a) One concave vertex.

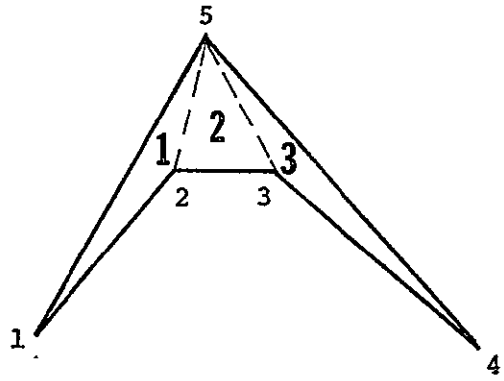

(b) Two adjacent concave vertices.

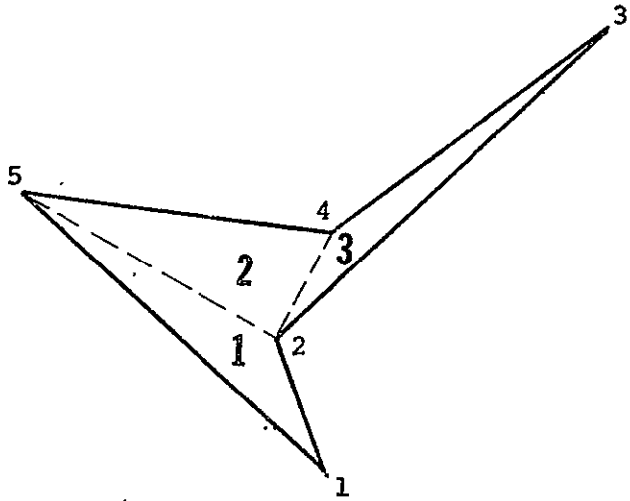

(c) Two nonadjacent concave vertices.

Figure A-2.- Examples of subdividing concave pentagons.

Furthermore, the maximum number of interior angles exceeding 180 degrees can also be determined by noting that the sum of the interior angles of the polygon must be equal to the sum of the interior angles of all triangles into which it can be subdivided. Thus, the sum of the interior vertex angles for any arbitrarily shaped polygon is given by

$$\sum_{i=1}^{n} \gamma_i = (n - 2)\ 180 \qquad \text{(A-2)}$$

where

γ_i = interior vertex angles of the polygon

Thus, the maximum number of interior vertex angles exceeding 180 degrees, γ^*, is given by

$$N(\gamma^*)_{max} = (n - 3) \qquad \text{(A-3)}$$

This equation limits the maximum number of concave vertices for a pentagon to two. Figures A-1(b) and A-1(c) illustrate two examples. In figure A-1(b), the two concave vertices are adjacent to each other. In figure A-1(c), the two concave vertices are non-adjacent.

The selection of the "appropriate" vertex to begin the subdivision process is highly dependent upon the shape of the polygon and the number and relationship of the concave vertices. Also, it is not always necessary to subdivide the polygon into triangles. Figure A-3 illustrates another method for subdividing the pentagon of figure A-1(a). In this case, the concave pentagon is subdivided into a four-sided convex polygon and one triangle. Furthermore, figure A-1 by no means exhausts all of the potential pentagon shapes that could be constructed.

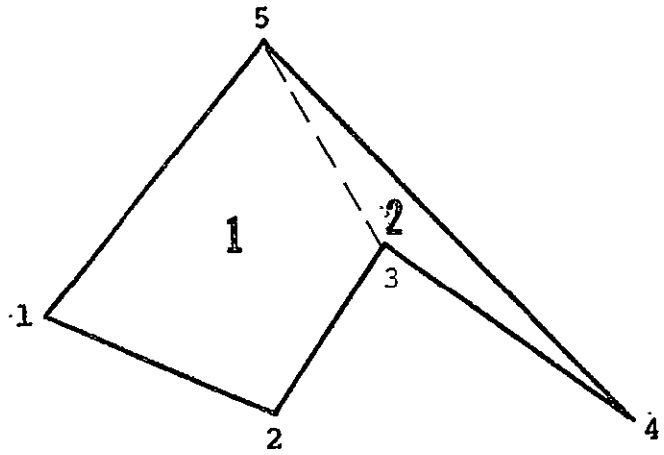

Figure A-3.- Alternate subdivision.

Since the shape of the area targets and space volumes will remain static during a mission, it is recommended that the subdivision process be performed manually.[1] There are two distinct advantages to this approach:

a. It eliminates the coding and execution of complex subdivision logic.
b. It can be performed once for each concave area target and space volume and does not have to be repeated each time AOS and LOS times are desired.

The treatment of concave polygons will place additional requirements on the target tables other than those specifically mentioned in reference 1. In addition to the number of sides and coordinates for each vertex, the target tables must also contain the following for each polygon-shaped target

N_{seg} - number of segments into which the target is subdivided ($3 \geq N_{seg} \geq 1$ for polygons having five or less sides)

VO_i - integers defining the counterclockwise ordering of the vertices for each segment ($i = 1,2,...N_{seg}$)

The use of these additional parameters can best be illustrated by example. For figure A-3, this pentagon is subdivided into two segments. The first segment is a four-sided polygon defined by vertices 1, 2, 3, and 5. The second segment is a triangle defined by vertices 3, 4, and 5. The corresponding parameters for this pentagon would be

$$N_{seg} = 2$$
$$VO_1 = 1235 \text{ (or } 2351 \text{ or } 3512 \text{ or } 5123)$$
$$VO_2 = 345 \text{ (or } 453 \text{ or } 534)$$

[1] This can easily be performed by plotting the vertex points on a Mercator projection.

Similarly, for figures A-2(b) and A-2(c):

a. Figure A-2(b)

$$N_{seg} = 3$$
$$VO_1 = 125 \text{ (or } 251 \text{ or } 512)$$
$$VO_2 = 235 \text{ (or } 352 \text{ or } 523)$$
$$VO_3 = 345 \text{ (or } 453 \text{ or } 534)$$

b. Figure A-2(c)

$$N_{seg} = 3$$
$$VO_1 = 125 \text{ (or } 251 \text{ or } 512)$$
$$VO_2 = 245 \text{ (or } 452 \text{ or } 524)$$
$$VO_3 = 234 \text{ (or } 342 \text{ or } 423)$$

For consistency, this approach can also be used for convex polygons. In this case, N_{seg} would be one and VO_1 would be set to the counterclockwise vertex sequence.

For computational purposes, the number of sides for each segment, n_i, can be extracted from the vertex ordering integer, VO_i, as follows

$$n_i = \text{highest values of } n_i \text{ where TRUNC} \left\{ \frac{VO_i}{10^{n_i - 1}} \right\} > 0 \qquad \text{(A-4)}$$

where

TRUNC implies integer truncation.

The vertex numbers, V_j, corresponding to each vertex of the i^{th} subpolygon can also be extracted from the vertex ordering integer as follows

$$V_1 = \text{TRUNC}\left\{\frac{VO_i}{10^{n_i-1}}\right\} \qquad \text{(A-5a)}$$

$$V_j = \text{TRUNC}\left\{\frac{VO_i - \sum_{\ell=1}^{j-1} V_\ell \, 10^{n_i-\ell}}{10^{n_i-j}}\right\} \quad j = 2,3,\ldots n_i \qquad \text{(A-5b)}$$

APPENDIX B

CONIC INTERSECTIONS

CONIC INTERSECTIONS

This appendix presents the equations to compute the intersection points between two right circular cones.[1] The required input parameters are

$\hat{V}_1$ - unit vector along the axis of the first cone

γ_1 - half-cone angle of the first cone

$\hat{V}_2$ - unit vector along the axis of the second cone

γ_2 - half-cone angle of the second cone

The quantities to be computed are

$\hat{I}_1$ and $\hat{I}_2$ - unit vectors to the intersection points of the two cones

Figure B-1 illustrates the two right circular cones and the intersection points. The coordinate system for the cones is arbitrary and the only restriction is that both $\hat{V}_1$ and $\hat{V}_2$ must have a common origin and must be expressed in the same system. The first step is to determine whether the relative orientation of the two cones permits any intersections. This can be determined by computing the angle between the axes of the two cones.

$$\gamma = \cos^{-1} \{\hat{V}_1 \cdot \hat{V}_2\} \qquad \text{(B-1)}$$

[1] These equations can also be used to compute the intersection points between a right circular cone and a plane or the intersection points between two planes.

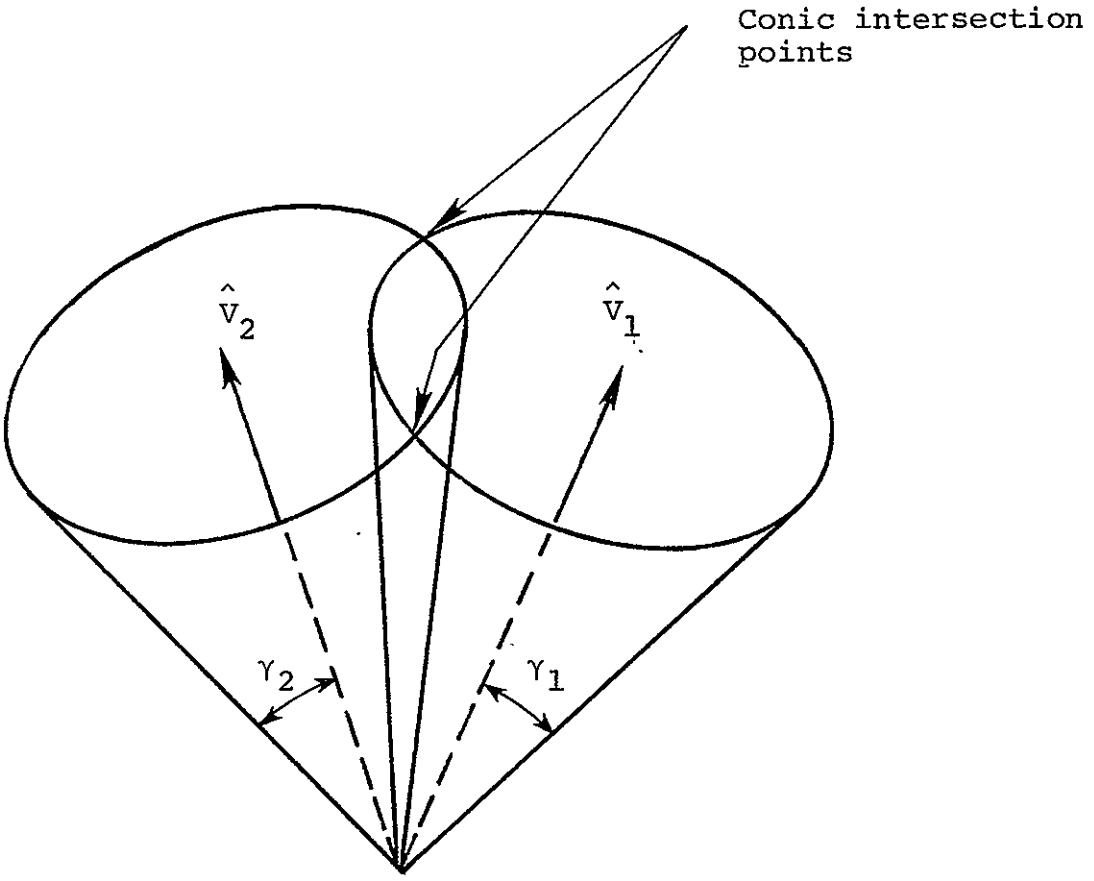

Figure B-1.- Intersection of two cones.

The cones will not intersect if

$$\gamma > \gamma_1 + \gamma_2 \qquad \text{[fig. B-2(a)]} \quad \text{(B-2)}$$

or

$$\gamma + \text{smaller}\{\gamma_1: \gamma_2\} < \text{greater}\{\gamma_1: \gamma_2\} \quad \text{[fig. B-2(b)]} \quad \text{(B-3)}$$

Assuming intersections are possible (i.e., neither equation B-2 nor B-3 is satisfied), the next step is to compute the intersection vectors. Figure B-3 illustrates the geometry. The intersection vectors are symetrically located on either side of the arc connecting vectors $\hat{V}_1$ and $\hat{V}_2$. Furthermore, the intersection vectors lie on the perimeter of both cones. Thus, all of the sides of the spherical triangle connecting vectors $\hat{V}_1$, $\hat{V}_2$, and $\hat{I}_1$ are known

$$\text{side a (connecting } \hat{V}_1 \text{ and } \hat{I}_1\text{)} = \gamma_1$$
$$\text{side b (connecting } \hat{V}_2 \text{ and } \hat{I}_1\text{)} = \gamma_2$$
$$\text{side c (connecting } \hat{V}_1 \text{ and } \hat{V}_2\text{)} = \gamma$$

The angle from side 'c' to side 'a' can be determined using the half-angle formula for spherical triangles. The result is

$$B = 2 \tan^{-1} \left\{ \frac{K}{\sin(S - \gamma_2)} \right\} \qquad \text{(B-4)}$$

where

$$K = \pm \sqrt{\frac{\sin(S - \gamma_1) \sin(S - \gamma_2) \sin(S - \gamma)}{\sin(S)}} \qquad \text{(B-5)}$$

$$S = 1/2 \ (\gamma_1 + \gamma_2 + \gamma) \qquad \text{(B-6)}$$

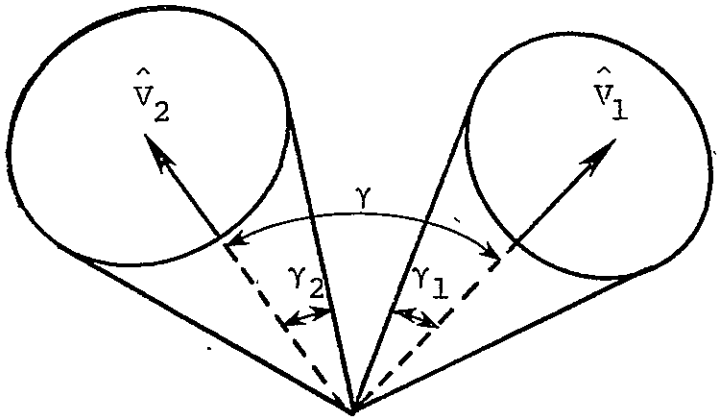

(a) $\gamma > \gamma_1 + \gamma_2$

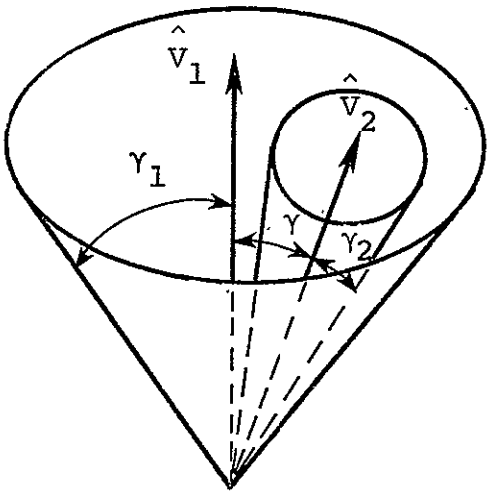

(b) γ + smaller $\{\gamma_1 : \gamma_2\}$ < greater $\{\gamma_1 : \gamma_2\}$

Figure B-2.- Conditions when cones do not intersect.

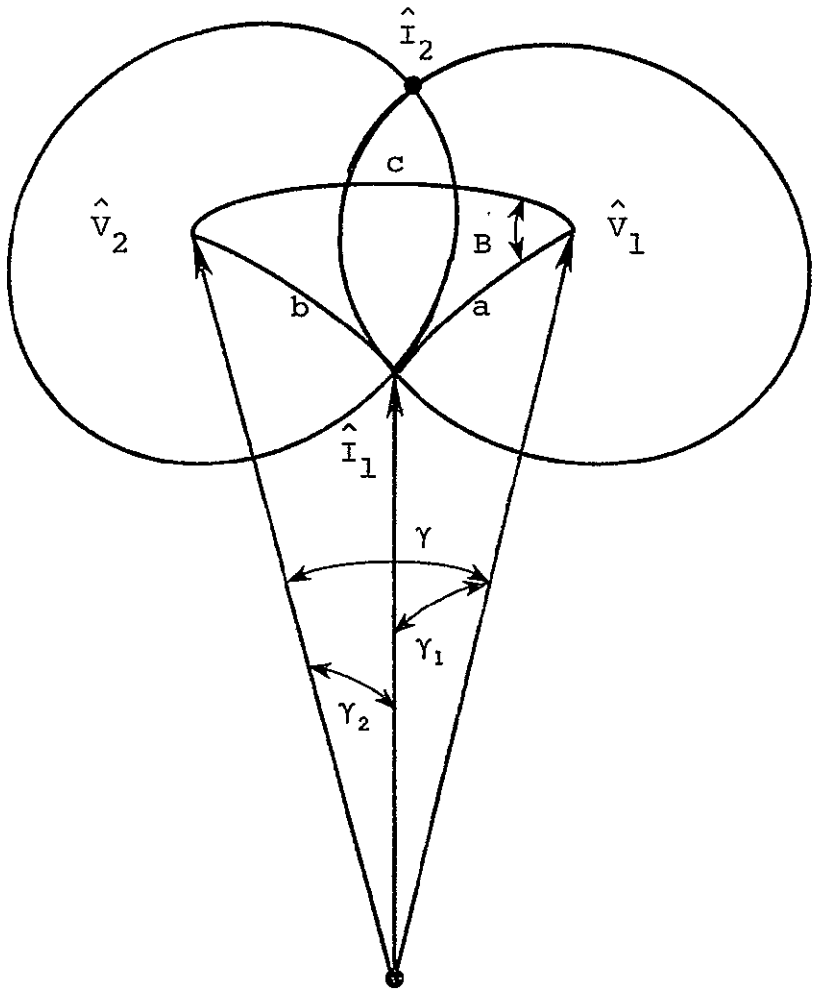

Figure B-3.- Spherical geometry to compute intersection points.

The dual value of K in equation B-5 produces two values of B in equation B-4. These values of B are equal in magnitude but opposite in sign and correspond to the two intersection points.[1] The unit vectors to the two intersection points are given by

$$\hat{I}_{1,2} = \begin{bmatrix} \ell_{1x} & \ell_{2x} & V_{1x} \\ \ell_{1y} & \ell_{2y} & V_{1y} \\ \ell_{1z} & \ell_{2z} & V_{1z} \end{bmatrix} \begin{Bmatrix} \cos B \sin \gamma_1 \\ \pm \sin B \sin \gamma_1 \\ \cos \gamma_1 \end{Bmatrix} \qquad \text{(B-7)}$$

where

$$\hat{V}_1 \Rightarrow (V_{1x}, V_{1y}, V_{1z})$$

$$\hat{\ell}_2 \Rightarrow (\ell_{2x}, \ell_{2y}, \ell_{2z}) = \frac{\hat{V}_1 \times \hat{V}_2}{|\hat{V}_1 \times \hat{V}_2|} \qquad \text{(B-8)}$$

$$\hat{\ell}_1 \Rightarrow (\ell_{1x}, \ell_{1y}, \ell_{1z}) = \hat{\ell}_2 \times \hat{V}_1 \qquad \text{(B-9)}$$

[1] For the special case of $B = 0$, the two intersection vectors are coincident. This physically corresponds to the situation when the two cones are tangent.

REFERENCE

1. Torres, F: Statement of Requirements (SR) for Area Targets and Space Volumes. CG5-78-342, December 13, 1978.

☆ U.S. GOVERNMENT PRINTING OFFICE: 1979—671-014/1609

DISTRIBUTION FOR JSC IN 79-FM-26

JM2/Center Data Management (3)
JM6/Technical Library (2)
CF/M. P. Frank
C. A. Beers
CF3/D. R. Puddy
J. Greene
CF4/C. R. Lewis
G. A. Pennington
CG/J. W. Bilodeau
CG5/T. Holloway
R. Nute
C. Stough
M. Rowles
F. Torres
M. Griffin
FA/H. W. Tindall
L. C. Dunseith
R. G. Rose
FA2/J. P. Mayer
FM/R. L. Berry
J. McPherson
FM2/E. C. Lineberry
A. Lunde
M. D. Jenness
A. A. Menchaca (5)
FM4/M. V. Jenkins
FM6/E. N. McHenry
FM8/E. R. Schiesser
FM14/Report Control Files (25)
A. Wiseman
B. Woodland
FM15/J. Funk
FM17/R. O. Nobles
L. D. Hartley
FR/R. P. Parten
FS/J. C. Stokes
FS47/R. Brown
FS5/L. Hall
T. Price
G. Richardson
L. Kirk
FS15/T. W. Sheehan
CSC/K. Nickerson
O. Dial
M. Bishop (5)
IBM/H. Norman (4)
M. Wagle
H. Norman
T. Carter (4)
M. Bradley

MDAC/W. Hayes (2)